



BRNO UNIVERSITY OF TECHNOLOGY

FACULTY OF INFORMATION TECHNOLOGY

DEPARTMENT OF INTELLIGENT SYSTEMS

**CONNECTION OF ALGORITHMS FOR REMOVAL OF
INFLUENCE OF SKIN DISEASES ON THE PROCESS
FOR FINGERPRINT RECOGNITION**

PH.D. THESIS

AUTHOR

Ing. MONA HEIDARI

SUPERVISOR

Prof. Ing., Dipl.-Ing. MARTIN DRAHANSKY, Ph.D.

BRNO 2023

Abstract

This thesis focuses on data structures, image processing, and computer vision methods for detecting and recognizing diseases in fingerprint images. The number of developed biometric systems and even used biometric characteristics is increasing. It is widely accepted that an individual's fingerprint is unique and remains relatively unchanged throughout life. However, the structure of these ridges can be changed and damaged by skin diseases. As these systems depend heavily on the structure of an individual's fingertip ridge pattern that positively determines their identity, people suffering from skin diseases might be discriminated against as their ridge patterns may be impaired. Likely, fingerprint devices have not been designed to deal with damaged fingerprints; therefore, after scanning the fingerprint, they usually reject it. The influence of skin disease is an important but often neglected factor in biometric fingerprint systems. An individual might be prevented from using specific biometric systems when suffering from a skin disease that affects the fingertips.

Collecting a database of fingerprints influenced by skin diseases is a challenging task. It is expensive and time-consuming, but it also requires the assistance of medical experts and the ability to find willing participants suffering from various skin conditions on fingertips. The raw diseased fingerprint database is first analyzed to provide a solid foundation for future research. Common signs among all fingerprint images affected by the disease are found for every particular disease, and a general description of each disease and its influences is defined. Then we automatically assign the label based on a combination of the known state of the fingerprint image.

The proposed solution is integrated with different algorithms focused on image processing libraries and computer vision methods for object detection. The solution has been evaluated on damaged fingerprint datasets and highlights the state of the art implementations using proposed techniques. The state of the art technique for disease detection implementations uses texture analysis and feature detection by comparing the intensity values of pixels in a small neighborhood in an image. Due to the complexity of each disease pattern, the combination of texture analysis algorithms leads to better detection results. The combination of Gray Level Co-occurrence Matrix (GLCM), Local Binary Pattern (LBP), orientation field, and mathematical morphology can detect damage (artifacts) in fingerprint images. Combining these features makes it possible to identify changes in the texture and shape of the fingerprint flow caused by diseases. These techniques capture different aspects of the texture and shape of the damage in fingerprint images and lead to identifying changes in the texture caused by diseases. In the stages of the detection process, mathematical morphology operations are applied to improve the structural details by removing small irregularities in the image and simplify the shape of objects, making it easier to identify and isolate them expanding the boundaries of objects in an image or filling gaps and connect broken parts of objects, leading to better object detection and recognition. At the end of the detection process, coherence is applied to show the quality evaluation of fingerprint image patches into three types healthy, damaged, and background.

Overall, the proposed solution showcases the effectiveness of integrating multiple image processing and computer vision algorithms for disease detection in fingerprint images. The combination of these algorithms can accurately detect and localize disease patterns in damaged fingerprint datasets, thus providing a reliable solution for disease detection in forensic applications.

Abstrakt

Tato práce se zaměřuje na datové struktury, zpracování obrazu a metody počítačového vidění pro detekci a rozpoznávání nemocí ve snímcích otisků prstů. Počet vyvinutých biometrických systémů a dokonce i používaných biometrických charakteristik se zvyšuje. Všeobecně platí, že otisk prstu jednotlivce je jedinečný a zůstává relativně neměnný po celý život. Struktura papilárních linií se však může měnit nemocemi a může být poškozena kožními chorobami. Vzhledem k tomu, že jsou systémy do značné míry závislé na struktuře papilárních linií jednotlivce, která pozitivně ovlivňuje jejich identitu, lidé trpící kožními nemocemi mohou být diskriminováni, protože jejich papilární linie mohou být narušeny.

Vliv kožních onemocnění je důležitým, ale často opomíjeným faktorem v biometrických systémech založených na otiscích prstů. Jedinec trpící kožním onemocněním, které postihuje konečky prstů nemusí být schopen používat určité biometrické systémy. Shromáždění databáze otisků prstů, ovlivněných kožními nemocemi, je náročný úkol. Je nákladný a časově náročný, vyžaduje také pomoc lékařských odborníků a ochotné účastníky trpící různými kožními nemocemi na bříšcích prstů.

Surová databáze otisků prstů s onemocněním byla nejprve analyzována, aby poskytla pevný základ pro budoucí výzkum. Pro každé konkrétní onemocnění jsou nalezeny společné znaky mezi všemi snímky otisků prstů postižených nemocí a je definován obecný popis každého onemocnění a jeho vlivů. Poté automaticky přiřadíme označení na základě kombinace známého stavu obrazu otisku prstu. Navrhované řešení je integrováno s různými algoritmy zaměřenými na knihovny pro zpracování obrazu a metody počítačového vidění pro detekci objektů. Je vyhodnoceno na poškozených souborech dat otisků prstů a popisuje současný stav implementace pomocí navržených technik. Současný stav techniky pro implementaci detekce onemocnění využívá analýzu textury a detekci prvků porovnáváním hodnot intenzity pixelů v malém okolí v obraze. Vzhledem ke složitosti jednotlivých vzorů nemocí vede kombinace algoritmů analýzy textury k lepším výsledkům detekce. Kombinace Gray Level Co-occurrence Matrix (GLCM), Local Binary Pattern (LBP), pole orientací a matematické morfologie může detekovat poškození v obrazech otisků prstů. Kombinace těchto funkcí umožňuje identifikovat změny v textuře a tvaru toku papilárních linií otisků prstů způsobené nemocemi. Tyto techniky zachycují různé aspekty textury a tvaru poškození v obrazech otisků prstů a vedou k identifikaci změn v textuře způsobených nemocemi. V průběhu detekčního procesu jsou použity matematické morfologické operace pro zlepšení strukturálních detailů tím, že odstraňují malé nesrovnalosti v obraze a zjednodušují tvar objektů, což usnadňuje jejich identifikaci a izolaci, rozšiřováním hranic objektů v obraze nebo vyplněním mezer a propojením rozlomených částí objektů. To vede k lepší detekci a rozpoznání objektů.

Na konci procesu detekce je použita koherence, která ukazuje hodnocení kvality polí obrazu otisku prstu na tři typy: zdravý, poškozený a pozadí.

Keywords

Diseased fingerprint detection; biometrics; computer vision methods; signal processing; pattern recognition; fingerprint database.

Klíčová slova

Detekce onemocnění otisků prstů; biometrie; metody počítačového vidění; zpracování signálu; rozpoznávání vzorů; databáze otisků prstů.

Reference

HEIDARI, Mona. *Connection of algorithms for removal of influence of skin diseases on the process for fingerprint recognition*. Brno, 2023. Ph.D. thesis. Brno University of Technology, Faculty of Information Technology. Supervisor Prof. Ing., Dipl.-Ing. Martin Drahansky, Ph.D.

Connection of algorithms for removal of influence of skin diseases on the process for fingerprint recognition

Declaration

I declare that this dissertation thesis is my original work and that I have written it under the guidance of Prof. Ing., Dipl.-Ing. Martin Drahansky, Ph.D. All sources and literature I have used during my work on the thesis are correctly cited with a complete reference to the respective sources.

.....

Mona Heidari
May 15, 2023

Acknowledgements

Firstly, I would like to express my sincere gratitude to my advisor Prof. Martin Drahansky for the continuous support during my Ph.D., for his patience, encouragement, and immense knowledge. Throughout my research, he has challenged me repeatedly and guided me through the obstacles. I have always appreciated his expertise in the subject matter and how much he has helped me explore its various aspects. I would like to thank my fellow lab mates for their ongoing support. Thank you all for making my experience in the lab a memorable one.

I am forever grateful to my loving parents for all that they have done for me. They have been my constant source of love and support throughout my life, and I cannot thank them enough.

Contents

1	Introduction	8
1.1	Dissertation Focus and Contributions	11
1.2	Structure of the Thesis	12
I	Background	13
2	Fingerprint Recognition	14
2.1	Fingerprint as a Biometric	14
2.2	Fingerprint Acquisition	15
2.2.1	Sensing Technology	16
2.3	Fingerprint Features	18
2.3.1	Local Ridge Orientation and Frequency	19
2.3.2	Singular Points	19
2.4	Fingerprint Matching	20
2.4.1	Quality Assessment	21
2.4.2	Feature Extraction	21
2.4.3	Verification and Identification	21
2.5	Performance Measurements	22
2.6	Fingerprint Recognition System	23
3	Enhancement, Detection, and Localization Methods	25
3.1	Fingerprint Image Preprocessing and Enhancement	25
3.1.1	Segmentation	25
3.1.2	Image Quality Normalization	27
3.1.3	Histogram Equalization	28
3.2	Feature Extraction and Image Descriptors	28
3.2.1	Orientation Field Estimation	29
3.2.2	Fast Fourier Transform	30
3.2.3	Gabor Filters	31
3.2.4	Local Binary Patterns	32
3.2.5	Edge Detectors	33
3.2.6	Gray Level Co-occurrence Matrix	34
3.2.7	Mathematical Morphology	37
3.3	Localization of Damaged Regions	37
3.3.1	Wavelet Transform	38
3.3.2	Coherence	39
3.3.3	Classification	40

3.3.4	Deep Neural Networks	45
II	Proposed Methods	47
4	Diseased Fingerprint Representations	48
4.1	Analysis of Diseased Fingerprint Dataset	48
4.2	Common Features in the Dataset	51
4.3	Related Work	56
4.4	Algorithm Design	57
4.5	Flowchart of Methodologies	58
4.5.1	Detectors	60
4.5.2	Classifier	69
4.6	Implementation	70
5	Conclusions	76
5.1	Future Work	77
	Bibliography	79
	Appendices	89
A	Appendix	90

List of Figures

1.1	The general biometric system contains subsystems for data capturing, signal processing, data storage, comparison, and decision. Different workflows apply for the modes enrolment, verification, and identification [2].	9
1.2	Some of the biometrics are shown: a) fingerprint, b) finger vein, c) hand geometry, d) hand vein, e) face, f) facial thermography, and g) retina.	10
2.1	The ridge pattern of two different fingerprint images using different sensing technology.	14
2.2	Fingerprints of a subject at age 7 (left), age 17 (center), and age 40 (right) [47].	15
2.3	Examples of single-finger live Scanner suprema RealScan-G1 (left), and Ten-print live scanner suprema RealScan-G10 (right).	16
2.4	Recent evolution of fingerprint sensing technology.	17
2.5	Anatomy of skin structure [60].	18
2.6	Ridges and valleys on a fingerprint image.	18
2.7	Various types of ridge characteristics.	19
2.8	Three main fingerprint types.	20
2.9	Block diagram of a fingerprint-based recognition system.	24
3.1	The foreground and the background regions of a fingerprint image.	26
3.2	An example of background extraction from a fingerprint image.	26
3.3	Example of normalization: original fingerprint (left), normalized image (right).	27
3.4	Histogram equalization of a diseased fingerprint image.	28
3.5	The neighborhood of a pixel can have a maximum of 8 pixels.	29
3.6	Computation of orientation estimation based on a gradient. a) Original image, b) orientation field.	30
3.7	Responses of Gabor filtering for parameters $\theta = 0.78, f = 0.08$. Normalized image (left), Gabor wavelet (middle), response (right).	32
3.8	Local neighborhood at different scales of a uniform LBP [4].	33
3.9	Canny edge detection in the diseased fingerprint.	33
3.10	An example of various features of GLCM.	36
3.11	2D-DWT of a fingerprint image in different sub-bands.	38
3.12	Wavelet representation on three resolution levels. These images show the absolute value of the wavelet coefficients (many of the coefficients are near zero (gray)) for each detail image.	39
3.13	Random forest model.	41
3.14	Hyperplane and margin Definition in SVM.	42
3.15	Effect of C parameter on margin size in SVM.	43
3.16	The Concept of maximum margin and maximum margin hyperplane in SVM.	43
3.17	The kernel trick: transforming the input space to a higher-dimensional space.	44

3.18 The architecture of the original convolutional neural network, introduced by Le-Cun et al. (1989).	46
4.1 Examples of estimated fingerprints quality score from the database, using NFIQ 2.	50
4.2 Overall quality estimation based on NFIQ 2 of fingerprint images from the dataset.	50
4.3 Example of fingertip light atopic eczema.	52
4.4 Example of psoriasis influence on fingerprints.	53
4.5 Hyperkeratotic eczema influence on fingerprints.	53
4.6 Fingerprints with dyshidrotic eczema.	54
4.7 Verruca vulgaris influence on fingerprint.	54
4.8 Cut wound influence on fingerprint.	54
4.9 Example of fingerprint images with straight lines or grids.	55
4.10 Examples of papillary lines (ridges) disruptions (left) and “cheetah” spots (right).	55
4.11 Example of fingerprint images with white spots in wart (left) and psoriasis (right).	56
4.12 Example of fingerprint images with large irregular spots in advanced psoriasis.	56
4.13 Structural design diagram of disease detection and recognition algorithms.	59
4.14 Computation of orientation field. a) Original image, b) orientation field based on a Sobel operator, c) orientation field by Fast Fourier Transform filtering, and d) orientation based on Gabor.	60
4.15 Feature detection using LBP in a fingerprint image with eczema.	61
4.16 Feature detection using LBP in a fingerprint image with hyperkeratotic eczema.	61
4.17 Definition of patch and cell in a fingerprint image.	62
4.18 LBP intensity computation on a fingerprint affected by verruca vulgaris.	63
4.19 LBP intensity computation on a fingerprint affected by hyperkeratotic eczema.	63
4.20 Visual steps of an LBP algorithm applied on a diseased fingerprint images with minor (top) and serious damage (bottom).	64
4.21 Examples of GLCM at $d = 1$ and different orientations, $\theta = 0^\circ, 45^\circ$ for (a) homogeneity, (b) dissimilarity and (c) contrast.	67
4.22 Examples of GLCM at $d = 5$ and different orientations, $\theta = 0^\circ, 45^\circ$ for (a) homogeneity, (b) dissimilarity and (c) contrast.	67
4.23 Features detection by applying approximation coefficients for a diseased fingerprint image with 2-level wavelet decomposition.	68
4.24 Example of applying morphological processing on a diseased fingerprint image.	69
4.25 Coherence indicates the damaged parts in a diseased fingerprint image.	69
4.26 Localization of a diseased fingerprint image affected by hyperkeratotic eczema.	71
4.27 Detection of cut wound damage using block orientation field method.	72
4.28 Intermediate steps of detecting white spots.	73
4.29 Intermediate steps of detecting small cheetah spots.	73
4.30 White lines extraction.	74
4.31 ROC curves for diseased fingerprint recognition performance.	75
A.1 Verruca vulgaris detected with 32% damage.	92
A.2 Multiple verruca vulgaris detected with 34% damage.	93
A.3 Eczema detected with 24% damage.	94
A.4 Acrodermatitis detected with 39% damage.	95
A.5 Hyperkeratotic eczema detected with 66% damage.	96
A.6 Running the detection method on an almost ideal fingerprint with 5% damage.	97

List of Tables

4.1	Proportion of diseases in our damaged fingerprint dataset.	49
4.2	Local features of damaged fingerprint images.	51
4.3	Global features of damaged fingerprint images.	52
4.4	Computed dissimilarity values in different directions of images with eczema.	65
4.5	Computed correlation values in different directions of images with eczema.	65
4.6	Computed homogeneity values in different directions of images with eczema.	65
4.7	Computed contrast values in different directions of images with eczema.	66
4.8	Computed ASM values in different directions of images with eczema.	66
4.9	Computed Energy values in different directions of images with eczema.	66
4.10	Classifier accuracy.	74

List of Acronyms

AFIS	Automated Fingerprint Identification System
AI	Artificial Intelligence
ANN	Artificial Neural Networks
ASM	Angular Second Moment
CLAHE	Contrast Limited Adaptive Histogram Equalization
CNN	Convolutional Neural Network
CPU	Central Processing Unit
CWT	Continuous Wavelet Transform
DET	Detection Error Tradeoff
DFT	Discrete Fourier Transform
DL	Deep Learning
DNNs	Deep Neural Networks
DWT	Discrete Wavelet Transform
EER	Equal-Error Rate
FAR	False Accept Rate
FFT	Fast Fourier Transform
FMR	False Match Rate
FNMR	False Non-Match Rate
FRR	False Reject Rate
FTIR	Fourier-Transform Infrared Spectroscopy
GLCM	Gray Level Co-occurrence Matrix
GPU	Graphics Processing Unit
HE	Histogram Equalization

LBP Local Binary Pattern
LSTM Long Short-Term Memory
ML Machine Learning
NFIQ NIST Fingerprint Image Quality
NIST National Institute for Standards and Technology
RGB Red Green Blue
RNN Recurrent Neural Network
ROC Receiver Operating Characteristic
ROI Region Of Interest
SGLDM Spatial Gray Level Dependence Matrix
SVM Support Vector Machine
WT Wavelet Transform

Chapter 1

Introduction

Identifying people by measuring individual anatomy, physiology, or other behavioral characteristics has led to a specific research area called *biometric recognition* [64, 24, 111, 124]. Biometrics deals with identifying or verifying individuals based on their biological or behavioral characteristics [92]. The primary function of a biometric system is to compare two biometric samples and determine whether they pertain to the same or different individuals by generating a match score. Biometric technologies provide a robust mechanism for authentication and are still under continuous development. Their diffusion is mainly supported by governments, forensics, and law enforcement agencies to improve a sense of security; biometric identification does not directly improve security but acts as a deterrent to illegal activities.

Biometrics is utilized widely by governmental and commercial organizations worldwide for purposes such as border control, law enforcement and forensic investigations, voter registration for elections, and national identity management systems. Before automated biometric recognition systems, reliable identification of fellow beings had been a long-standing problem in human society. In early civilizations, people lived in small, connected communities. However, as humankind became more mobile and population increased, we needed to rely on credentials for person recognition. Dating back to ancient Rome, passwords had long been viewed as the ideal method of securing information and gaining access to exclusivity [16]. While passwords may have served their purpose in ancient Rome, in this day and age, passwords, while still in everyday use, are rife with problems. Other knowledge-based authentication schemes such as PINs are also prone to such attacks [8]. To date, significant progress has been made in solidifying the accuracy component of a trustworthy biometric recognition system.

Data collection begins with the measurement of a behavioral/physiological characteristic. Figure 1.1 shows a generic biometric authentication system divided into five subsystems: data collection, transmission, signal processing, decision, and data storage. We will consider these subsystems one at a time.

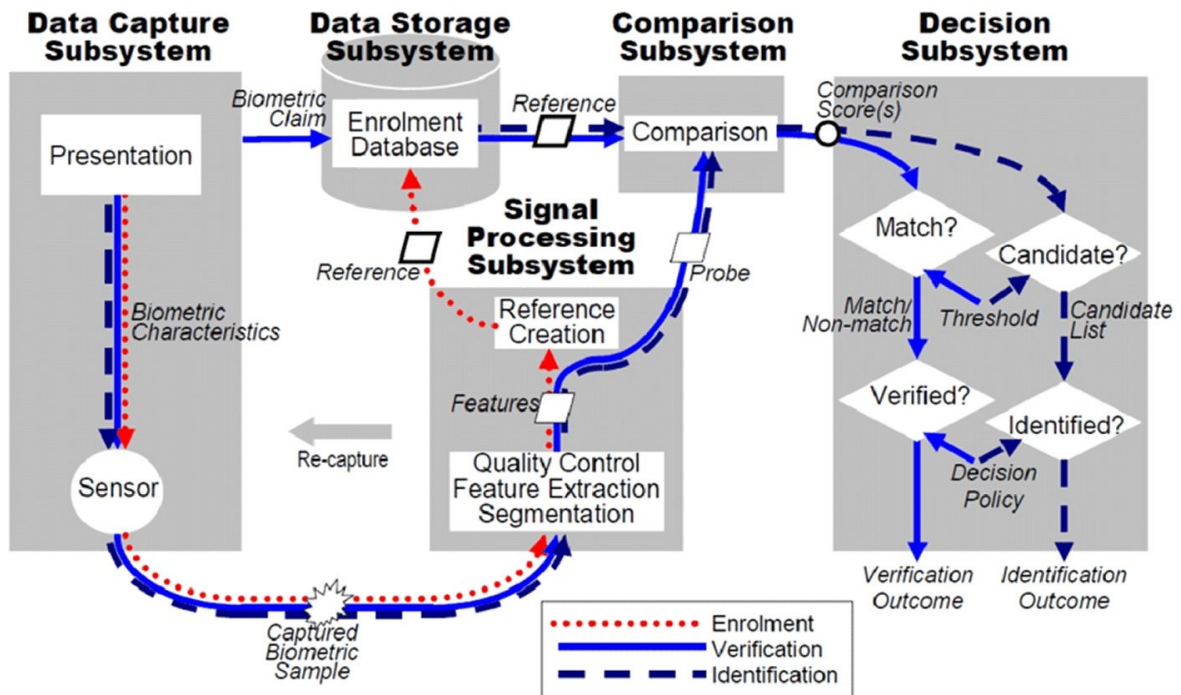


Figure 1.1: The general biometric system contains subsystems for data capturing, signal processing, data storage, comparison, and decision. Different workflows apply for the modes enrolment, verification, and identification [2].

Any human physiological and/or behavioral characteristic can be used as a biometric identifier to recognize a person as long as it satisfies these requirements [8]:

- *universality*, which means that each person should have the biometric;
- *distinctiveness*, which indicates that any two persons should be sufficiently different in terms of their biometric identifiers;
- *permanence*, which means that the biometric should be sufficiently invariant (concerning the matching criterion) over a while;
- *collectability* indicates that the biometric can be measured quantitatively.

However, in a practical biometric system, some other issues should be considered, including [8]:

- *performance*, which refers to the achievable recognition accuracy, speed, robustness, the resource requirements to achieve the desired recognition accuracy and speed, as well as operational or environmental factors that affect the recognition accuracy and speed;
- *acceptability*, which indicates the extent to which people are willing to accept a particular biometric identifier in their daily lives;
- *circumvention* reflects how easy it is to fool the system by fraudulent methods.

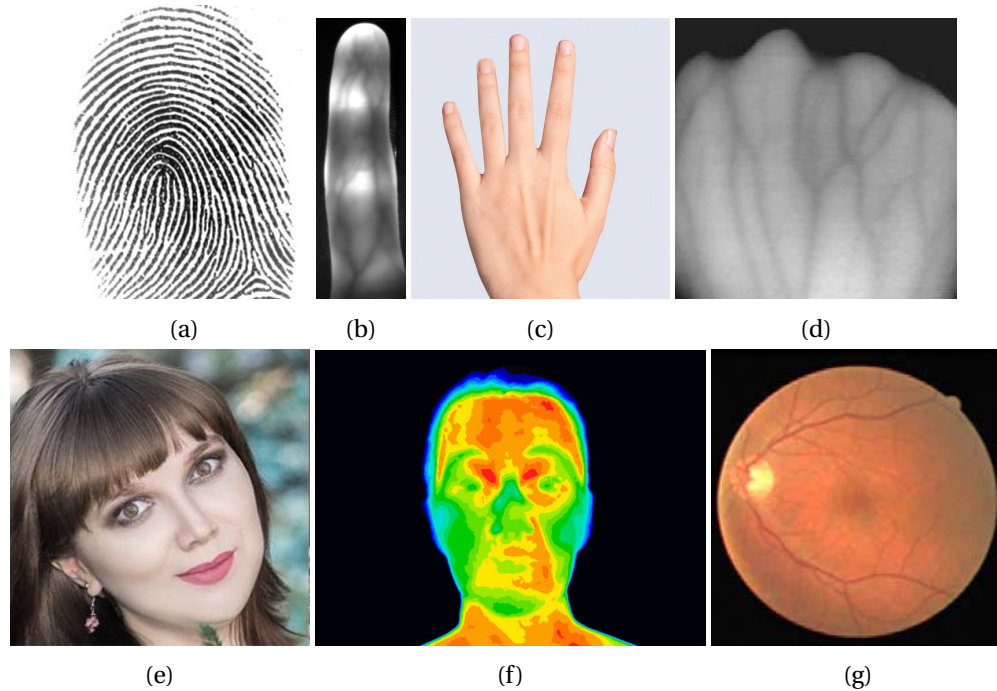


Figure 1.2: Some of the biometrics are shown: a) fingerprint, b) finger vein, c) hand geometry, d) hand vein, e) face, f) facial thermography, and g) retina.

When choosing a biometric for an application, the following issues have to be addressed:

- Does the application need verification or identification? If an application requires identifying a subject from a large database, it needs a scalable and relatively more distinctive biometric (e.g., fingerprint or iris).
- The operational modes of the application, whether the application is attended (semi-automatic) or unattended (fully automatic), and whether the users are habituated (or willing to be habituated) to the given biometrics.
- The storage requirement of the application; for example, an application that performs the recognition at a remote server may require a small template size.
- How stringent are the performance requirements? For example, an application that demands high accuracy needs a more distinctive biometric.
- The types of biometrics acceptable to the users; different biometric characteristics are acceptable in applications deployed in different demographics depending on that society's cultural, ethical, social, religious, and hygienic standards.

1.1 Dissertation Focus and Contributions

Fingerprints are the main biometric characteristic discussed in this thesis. Fingerprints have been routinely used in the forensics community for over one hundred years, and automatic fingerprint identification systems were the first installed almost fifty years back. Law enforcement agencies were the earliest adopters of fingerprint recognition technology; more recently, increasing identity fraud has created a growing need for biometric technology for person recognition in several non-forensic applications [92].

This thesis aims to identify specific approaches and algorithms to detect and recognize various types of diseases in fingerprint images. The analysis and interpretation of medical images represent two of the most responsible and complex tasks and usually consist of multiple processing steps [96]. Such problems can be solved using image processing, computer vision, and machine learning techniques.

In this dissertation, the combination of computer vision methods are presented. The main contributions of my work presented in this thesis are the following:

- **Analysis of the dataset of images distorted by any kind of skin disease:** This dissertation presents an analysis of diseased fingerprint images. Based on this analysis, the primary purpose was to find the infected area of the fingerprint images by skin diseases and classify them into various classes; therefore, the classification of diseased fingerprint images based on their features is reported.
- **Diseased fingerprint images quality estimation:** The clarity of ridges, valleys, and the extractability of the features used for diseased fingerprint detection, such as minutiae, missing regions, blurred and cut parts, etc., are computed. The scar and blurred fingerprint images are low-quality fingerprint images that become a problem in minutiae extraction since broken ridges exist in the images. This was done using the quality assessment algorithms and tools such as NFIQ2 [1] and VeriFinger SDK [99] that quantify specific properties in the fingerprint image, e.g., the ridge sharpness or the number of minutiae. Also, three regions of interest for a digital fingerprint image have been estimated. A well-defined region where ridges and valleys of fingerprint images are differentiated as a first category. The second category is a recoverable corrupted region with scars, smudges, and many more damaged ridges and valleys. However, the ridges and valleys can still be seen, and the neighboring regions can still give sufficient information. The third category is an unrecoverable corrupted region where ridges and valleys are severely damaged up to the ridges structure cannot be seen clearly, and the neighboring does not provide adequate information.
- **New methods for recognition of diseases:** Computer vision algorithms for texture description and object detection are investigated, and efficient methods are proposed to recognize the damages in fingerprint images. The development of algorithms leads to eliminating the adverse influence of skin diseases on the fingerprint recognition process by designing and implementing the detection of particular skin diseases, and a new approach to detect and recognize diseases in fingerprint images with classical algorithms is proposed, which yields segmentation in fingerprint image divided to three parts: low, middle and high quality based on the damages by the dermatological diseases or different types of detriment in the fingerprint.

1.2 Structure of the Thesis

After an introduction to biometrics and fingerprint recognition, this work is organized into three main parts. The next, second chapter serves as a brief introduction to fingerprint acquisition and recognition, along with their characteristics. Chapter 3 gives an overview of the methods and algorithms for fingerprint image processing, localization, detection, and general recognition methods in classical techniques. In the following part of the thesis, chapter 4 describes the datasets and the proposed diseased recognition methods using classical algorithms. Chapter 5 concludes the thesis by summarizing the main results obtained and outlining future research directions. The Appendix A contains some implementation details of the detection methods proposed in the second part.

Part I

Background

Chapter 2

Fingerprint Recognition

2.1 Fingerprint as a Biometric

The modern history of fingerprint identification begins in the late 19th century with the development of identification bureaus charged with keeping accurate records about individuals indexed, not according to name, but according to some physical attribute [23]. Fingerprints are the oldest and the most widely recognized biometric characteristic with one of the highest reliability levels. It is considered legitimate proof of evidence in courts of law worldwide [70]. The graphical flow-like ridges (*papillary lines*) shown in Figure 2.1 present on human fingers are called fingerprints [66].



Figure 2.1: The ridge pattern of two different fingerprint images using different sensing technology.

Fingerprints are fully formed at about seven months of fetus development, and their details are permanent, even if they may temporarily change slightly due to cuts and bruises on the skin or weather conditions [92] (see Figure 2.2). Human beings have always needed a secure world, and with the speed of technology development in recent years, fingerprint recognition is becoming more and more critical.



Figure 2.2: Fingerprints of a subject at age 7 (left), age 17 (center), and age 40 (right) [47].

Biometric technologies are based on recognition of biometric characteristics of individuals, such as the face, speech, or fingerprint, and they represent the most promising way to provide security and represent identity in our growing modern world [92]. Nowadays, fingerprint recognition systems have been applied in various areas [92]. They are used not only in forensics for crime purposes but also as an access method to facilities, computers, mobile phones, or electronic banking; as a data protection method, and for civil identification (passports, driver licenses, national IDs), not to mention applications in government, commercial, financial sector, education or health care [92].

2.2 Fingerprint Acquisition

The term fingerprint refers to an impression left by the friction skin of a finger rather than the anatomical structure itself [7]. The process of capturing the friction ridge details as a fingerprint impression is known as *fingerprint acquisition*. For capturing the digital image of the structure of a person's ridges in the form of a digital image, various sensing mechanisms can be used. In the past, samples were acquired using the so-called *ink-technique*, during which fingertips were covered with black ink and pressed on a paper card. This kind of process is referred to as *off-line* fingerprint acquisition or off-line sensing [92]. A specific case of off-line sensing is the acquisition of a latent fingerprint from a crime scene.

A *latent fingerprint* is a special kind of off-line image that is significant in forensic applications [7]. Latent fingerprint applies the advantage of the contamination of the skin that leaves the ridges structure. These latent prints can be captured (*lifted*) from the surface by employing certain chemical (by means of paper, rhodamine and ninhydrin) and mechanical (powder and brush) techniques. Various chemicals are used to lift the trace of ridges. Latent fingerprint technology is mainly utilized in forensic (criminalistics, or crime scene) analysis, and this technology requires a high degree of specialization to maintain the integrity of fingerprint [126].

Apart, several modern live-scan fingerprint readers allow us to obtain a sample without using ink. The principle of acquiring a fingerprint is reading the finger's ridge pattern; the process can be done using a scanner that reads the finger's ridge pattern, and an A/D converter converts the analog signal to the digital form [92]. An interface module then communicates with external devices such as a computer. *Live-scan acquisition techniques* are now being employed in

the Automated Fingerprint Identification System (AFIS) [87]. Fingerprint scanners can be either single-finger or multi-finger. As the name suggests, only one finger can be scanned at a time using a single-finger scanner, whereas multi-finger scanners usually allow us to scan four fingers at once [92] (see Figure 2.3).



Figure 2.3: Examples of single-finger live Scanner suprema RealScan-G1 (left), and Ten-print live scanner suprema RealScan-G10 (right).

The main parameters characterizing a digital fingerprint image are [92]:

- Resolution, that indicates the number of dots or pixels per inch (dpi);
- Area;
- Number of pixels that can be simply derived by the resolution and the fingerprint area: a scanner working at r area of height(h) \times width(w) $inch^2$ has $r_h \times r_w$ pixels;
- Geometric accuracy;
- Contrast;
- and geometric distortion.

2.2.1 Sensing Technology

The omnipresence use of fingerprint recognition in many applications has led to invent compact, high-resolution, and low-cost fingerprint sensing technologies. Fingerprint sensors have evolved over in years. They have become compact and cheaper, allowing fingerprint sensors to be embedded in devices such as laptops or mobile phones. Some applications still use a large surface area fingerprint sensor (for capturing a whole fingerprint impression resulting in a higher accuracy) and are equipped with several advanced functionalities; the slap sensor is an example that captures multiple fingers' impressions simultaneously [68] (see Figure 2.4). Another example includes 3D FLY by TBS (see Figure 2.4), offering a contactless user experience. This touchless hand scanner captures fingerprints quickly and effectively, delivering unparalleled speed and identification accuracy.

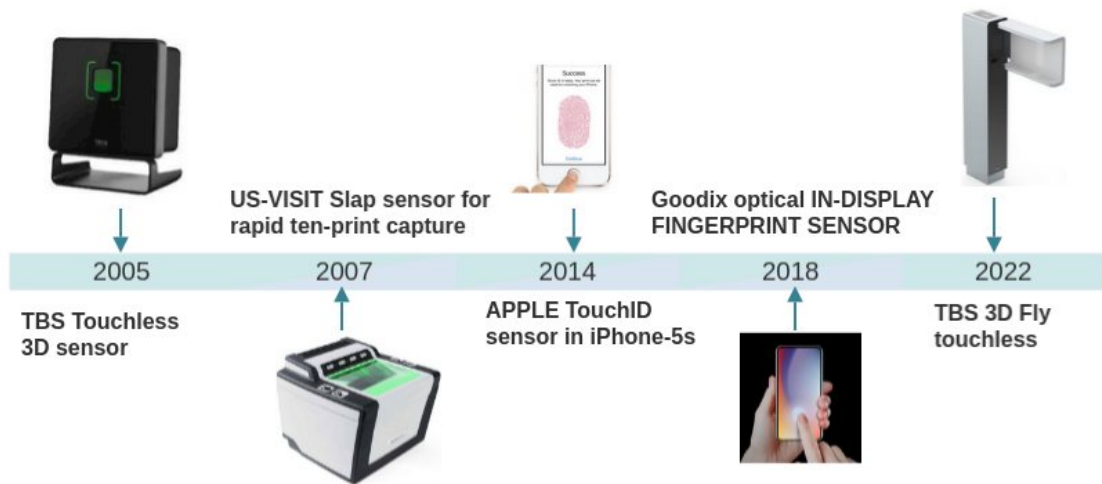


Figure 2.4: Recent evolution of fingerprint sensing technology.

Several live-scan sensing mechanisms (e.g., optical Fourier-Transform Infrared Spectroscopy (FTIR), capacitive, thermal, pressure-based, ultrasound, etc.) can be used to detect the ridges and valleys present in the fingertip.

Optical Technology: Optical scanners have the most extended history; the new solid-state sensors are gaining tremendous popularity because of their compact size and the ease of embedding them into laptop computers, cellular phones, smartpens, and other similar devices [32, 92]. Optical readers either utilize the principle of FTIR or operate in a direct contact view layout. FTIR-based technology works as follows: the finger is placed on the top side of a reader, which is a glass prism, the surface of the finger is illuminated from one side with LEDs, while the other side transmits the image through a lens to a camera that is a CCD (Charge-Coupled Device) or CMOS (Complementary Metal–Oxide–Semiconductor) image sensor, while the ridges enter in contact with the prism surface, the valleys remain at a certain distance [92].

Solid-state: Solid-state sensors were designed to address the drawbacks of optical sensors at the time. Optical sensors were costly and extensive, and the images obtained by them were inferior. Solid-state sensors use a chip or silicon and, therefore, can integrate additional functions onto the chip. These include A/D conversion or integration of a processor core to perform all fingerprint feature extraction and matching on a single chip. Capacitive and temperature are two types of solid-state sensors. The capacitive sensor measures the capacitance difference between ridges and valleys by computing the electric field strength, while temperature-sensitive sensors measure the temperature difference of a finger related to touching ridges versus non-touching valleys [92].

Ultrasound sensors: The ultrasound sensing technology can obtain images using ultrasound, and it is based upon the reflection and transmission coefficients of ultrasound as it propagates through media of varying acoustic impedance [115]. Ultrasound technology is robust to environmental issues, including humidity, extreme temperatures, finger contamination, and other factors that may result in a poor image quality.

2.3 Fingerprint Features

The skin throughout the body comprises three primary layers: epidermis (the outer layer), dermis and the subcutaneous tissue (fat layer) [52] shown in Figure 2.5.

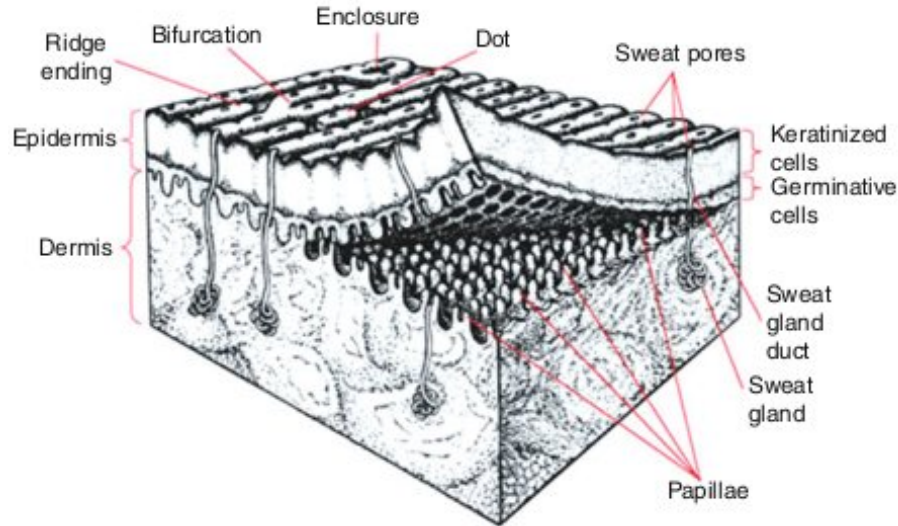


Figure 2.5: Anatomy of skin structure [60].

The epidermis is the outer layer of skin; it prevents water loss through evaporation, acts as a receptor organ, and provides a protective barrier for the underlying tissues against the outside environment. It is constantly being regenerated [60, ?]. The fingerprint is formed by the pattern of ridges (*papillary lines*) and *valleys* (furrows) on the tip of our fingers, see Figure 2.6. Ridges are the patterns that are unique to each individual even they are significant in identical twins [70].



Figure 2.6: Ridges and valleys on a fingerprint image.

The ridges and valleys on the surface of the friction ridge skin are firmly rooted in the dermis by primary ridges (under-the-surface ridges) and the valleys [60]. The layer of connective tissue,

the dermis, supports the epidermis. It is a network of cells, fibers, blood vessels, and gelatinous material that provides structural support and nourishment for the epidermis [60].

2.3.1 Local Ridge Orientation and Frequency

Fingerprints have long been used for forensic identification purposes based on their specific features within their patterns such as *ridge characteristics*, *minutiae*, *pores*, etc. [76]. Ridge characteristics are the points that can be used for recognition purposes. There are many various ridge characteristics shown in Figure 2.7.

Ridge ending and *ridge bifurcation* are the two most prominent ridge characteristics, called *minutiae*. Minutia was introduced by Sir Francis Galton as a feature for fingerprint matching [92]. These features in fingerprints are generally stable and robust to fingerprint impression conditions. Different types of minutiae are shown in Figure 2.7

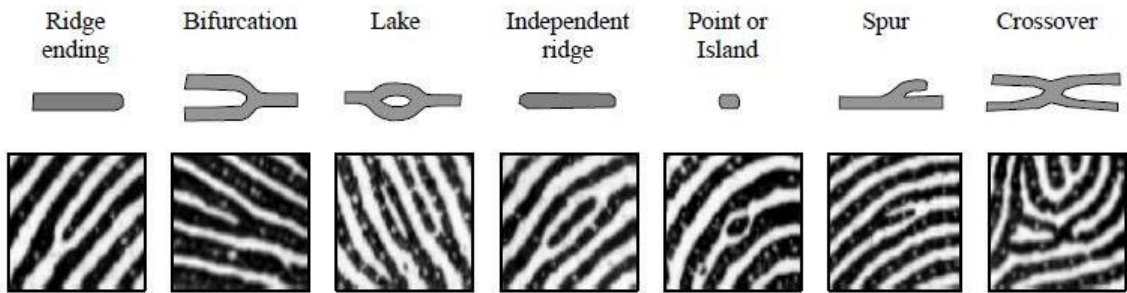


Figure 2.7: Various types of ridge characteristics.

The local ridge orientation is one of the essential characteristics of a fingerprint image. Let $[x, y]$ be a generic pixel in a fingerprint image. The local ridge orientation at $[x, y]$ is the angle θ_{xy} that the fingerprint ridges, crossing through an arbitrarily small neighborhood centered at $[x, y]$, form with the horizontal axis. Because fingerprint ridges are not directed, θ_{xy} is an unoriented direction lying in $[0, \pi]$. The most straightforward and natural approach for extracting local ridge orientation is based on the computation of gradients in the fingerprint image.

The local ridge frequency (density) denotes the number of ridges per unit length along a hypothetical segment centered at $[x, y]$ and orthogonal to the local ridge orientation θ_{xy} . The local ridge frequency varies across different fingers and may also vary across different regions in the same fingerprint.

2.3.2 Singular Points

Fingerprint classification refers to assigning a fingerprint to a class consistently and reliably and is generally based on global features, such as global ridge structure and singularities. One of the effective use of singular points is to classify a fingerprint typically into one of the six categories (left loop, right loop, double loop, arch, tented arch, whorl).

All fingerprints are divided into one of the following three categories:

- no singularity (arch type)
- one core and one delta (left loop, right loop, and tented arch type)
- two cores and two deltas (whorl and twin loop type)

When the ridge lines assume distinctive shapes (characterized by high curvature, frequent termination), the fingerprint pattern exhibits one or more regions called singularities or singular regions classified into three typologies: loop, delta (arc), and whorl. These types are shown in Figure 2.8.

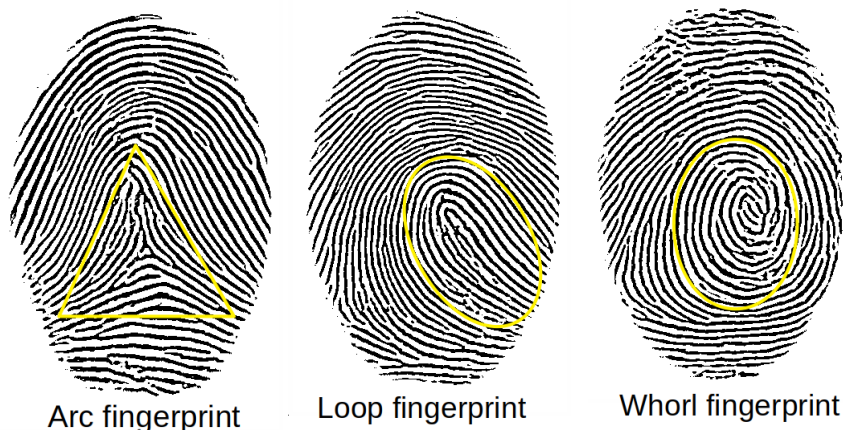


Figure 2.8: Three main fingerprint types.

The Henry classification system [57] is extended now to more specific fingerprint patterns. The patterns are further divided into sub-groups employing the more minor differences between the patterns in the same general group.

Also, singular points can operate as anchors to extract other descriptive features, e.g., the spatial frequency.

2.4 Fingerprint Matching

The *fingerprint matching algorithm* [92] compares two given fingerprint templates and, typically, computes a match (similarity) score, denoted s , between the template fingerprint and a query one. The match score should be high for fingerprints from the same finger and low for those from different fingers. A threshold (t) is set, and any match score above a specified threshold is considered a successful match (leading to a match).

The most fingerprint matching algorithms are based on measuring the similarity in global configurations of two minutiae sets representing the two fingerprint images. The distribution of minutiae points is used to match and establish the similarity between a template fingerprint and a query. Fingerprint matching is considered a complex pattern recognition task due to significant intra-class variations [92] (variations in fingerprint images of the same finger) and considerable inter-class similarity [92] (variations among fingerprint images from different fingers).

The major factors responsible for the intra-class variations are displacement, rotation, partial overlap, non-linear distortion, variable pressure, changing skin condition, noise, and feature extraction errors. Therefore, fingerprints from the same finger may sometimes look quite different; in contrast, fingerprints of different fingers might appear quite similar [92]. Fingerprint matching approaches are mainly based on the minutiae, and a matching system based on the minutiae consists of two stages. In the minutiae extraction stage, the minutiae are extracted from the gray-scale fingerprint, while in the minutiae matching stage, two sets of minutiae are compared to decide whether the fingerprints match [11].

2.4.1 Quality Assessment

Fingerprint image quality [88] is an essential factor in matching accuracy. It is usually defined as a measure of the clarity of ridges and valleys and the extractability of the features used for identification, such as minutiae, core and delta points, etc. Features extracted from poor quality fingerprints are likely to have many spurious or missing minutiae. In the case of low-quality images, such as latent fingerprints, minutiae extraction is challenging. The term quality is somehow related to the *processability* of the fingerprint images [61]. Assessing the quality of captured fingerprints is essential for a fingerprint recognition system. Poor quality fingerprint image causes the fingerprint authentication system to have more severe operation problems such as false acceptance and false rejection, resulting in user-facing difficulties when accessing an identification system.

Methods to evaluate estimation of fingerprint image quality can fall into [5]: the approaches that use local features of the image (i.e., clarity of ridge structure), the techniques that use global features of the image such as continuity of orientation field or energy concentration in the frequency domain over the entire fingerprint region, furthermore, algorithms that address quality assessment as a classification problem [5].

The development of a fingerprint quality metric has been of great interest since the early days of research studies. In response to this, an initiative led by the US National Institute for Standards and Technology (NIST) produced a fingerprint quality metric in 2004. This metric was integrated into the open source tool known as the NIST Fingerprint Image Quality (NFIQ), with the latest version being 2.2.0. Additionally, the Innovatrics IDKit mobile SDK also incorporates the NFIQ for fingerprint quality assessment.

Several factors can affect the quality of fingerprint images: occupation, motivation/collaboration of users, age, temporal or permanent cuts, dryness/wetness conditions, temperature, dirt, residual prints on the sensor surface, and so on [73, 103].

2.4.2 Feature Extraction

Feature extraction [100] refers to extracting a set of distinguishable features such as ridge density and ridge direction from a fingerprint image, and it is a critical task for fingerprint classification. Feature extraction techniques influence the performance of automated fingerprint recognition systems. Feature extraction has an essential role during the enrollment phase; a template that includes the extracted features such as orientation field, singular points, and minutiae from one or more fingerprint images is created and stored in the system along with the images. The features extracted from fingerprint images often have a direct physical counterpart (e.g., singularities or minutiae), but sometimes they are not directly related to any physical characteristics (e.g., local orientation image or filter responses). Features may be used for matching, or their computation may serve as an intermediate step for deriving other features [92]. The fingerprint feature extraction and matching algorithms are usually quite similar for both fingerprint verification and identification problems.

2.4.3 Verification and Identification

A biometric system can be called either a verification system or an identification system [67] - a fingerprint is compared to the unknown fingerprint with the shortlist of candidates in a *verification* system, distinguishing whether it is the correct match. The verification system conducts a one-to-one comparison to distinguish whether the identity claimed by the individual is genuine. The system either rejects or accepts the submitted claim of identity. On the other hand,

an *identification system* recognizes an individual by searching the entire template database for a match. It conducts one-to-many comparisons to establish the identity of the individual. In an identification system, the system establishes a subject's identity (or fails if the subject is not enrolled in the system database) without claiming an identity [107, 92].

A typical biometric verification system commits two types of errors [92]: falsely biometric measurements from two different fingers to be from the same finger (called false match), a false match results in rejecting a genuine request and mistaking two biometric measurements from the same finger to be from two different fingers (called false non-match) which is resulting in falsely accepting an impostor attempt. These two types of errors are also often denoted as false acceptance and false rejection (also see Section 2.5) [43].

2.5 Performance Measurements

In principle, any individual's physiological, behavioral, or anatomical characteristics can be used as a biometric characteristic for personal identification. Aside from iris and face, fingerprint is the most widespread biometric characteristic used for recognition. Fingerprints are assumed to be unique for every finger that makes it an ideal for recognition. Besides, fingerprint recognition has more than a century of tradition in the field of biometric recognition.

Two fundamental dogmas of fingerprints underlie their wide use for recognizing individuals [92]: *uniqueness* and *permanence*. No matter what type of biometric we consider, a general biometric system can be viewed as a pattern recognition system that typically offers a binary decision to a given input.

As a pattern recognition system, a biometric system inevitably makes incorrect decisions, so we need a framework to measure system errors. In a fingerprint recognition system, we define a match score that quantifies the similarity between the input and the database template representations. The match score is a response of a matcher module in a generic biometric recognition system, a decision of the type match/non-match, ranging in the interval $[0,1]$, with a template already stored in a database. The closer the score is to 1, the more certain is the system that the two fingerprints come from the same finger; the closer the score is to 0, the smaller is the system confidence that the two fingerprints come from the same finger. The system decision is regulated by a threshold t : pairs of feature set generating scores higher than or equal to t are inferred as matching pairs, whereas pairs producing scores lower than t are called non-matching pairs. A match (similarity) score is known as a genuine score if it matches two biometric samples of the same user; it is an impostor score if it entails comparing two biometric samples originating from different users. A standard biometric verification system perpetrates two types of errors [104]:

- False match (false acceptance) is when a biometric system incorrectly authenticates an individual or accepts an impostor.
- False non-match (false rejection) is when a biometric system incorrectly declares failure of a match between input sample and matching template, it rejects a genuine user.

In a biometric system, the False Match Rate (FMR) [17] measures the probability that an impostor score exceeds the threshold t ; and the False Non-Match Rate (FNMR) [17] specifies the probability that a genuine score falls below the threshold t .

To evaluate the accuracy of a generic biometric system, one must collect scores produced from several genuine matching (called *genuine distribution*) and scores generated from some impostor matching (called *impostor distribution*) [87].

In general, different systems vary in their behavior concerning the threshold; therefore, it is advisable to report system performance at all operating points (threshold). Detection Error Tradeoff (DET) [92] curves summarize the FMR and FNMR at various values of t , DET curves are independent of any threshold and allow comparison between various systems. Receiver Operating Characteristic (ROC) [92], another significant curve, will be acquired by plotting the FMR against FNMR.

Besides the above distributions and curves, another significant measure is also used to summarize the accuracy of a biometric verification system Equal-Error Rate (EER) [92] that denotes the error rate at the threshold t for which FMR and FNMR are identical. The practical performance requirements of a biometric system are very much application-related. From the viewpoint of system accuracy, a meager false non-match rate may be the primary objective. For example, in some forensic applications, such as criminal identification, it is the false non-match rate that is a primary concern and not the false match rate: that is, we do not want to miss a criminal even at the risk of manually examining a large number of potential matches identified by the biometric system [92]. At the other extreme, a shallow false match rate may be the most critical factor in a highly secure access control application, where the primary objective is not to let in any impostors, although we are concerned with the possible inconvenience to legitimate users to a high false non-match rate [92].

2.6 Fingerprint Recognition System

It has been already explained how to acquire a digital fingerprint image; the acquired raw image is then passed to a quality control module that evaluates whether the fingerprint sample quality is good enough to be automatically processed and extract reliable features. In case of insufficient quality, the system rejects the sample and invites the user to repeat the acquisition; otherwise, the raw image is passed to an image enhancement module, which aims to improve the ridge pattern's clarity, especially in the noisy region, to simplify the subsequent feature extraction. Special digital filtering techniques are usually adopted at this stage; the output enhanced image can still be a gray-scale image or become a black-and-white image [13].

The most widely used technique for fingerprint image enhancement is based on contextual filters [92]. In contextual filtering, the filter characteristics change according to the local context. Usually, a set of filters is pre-computed, and one of them is selected for each image region. In fingerprint enhancement, the context is often defined by the local ridge orientation and local ridge frequency. The sinusoidal-shaped wave of ridges and valleys is mainly defined by a local orientation and frequency that varies slowly across the fingerprint area. An appropriate filter that is tuned to the local ridge frequency and orientation can efficiently remove the undesired noise and preserve the actual ridge and valley structure [92, 32, 77].

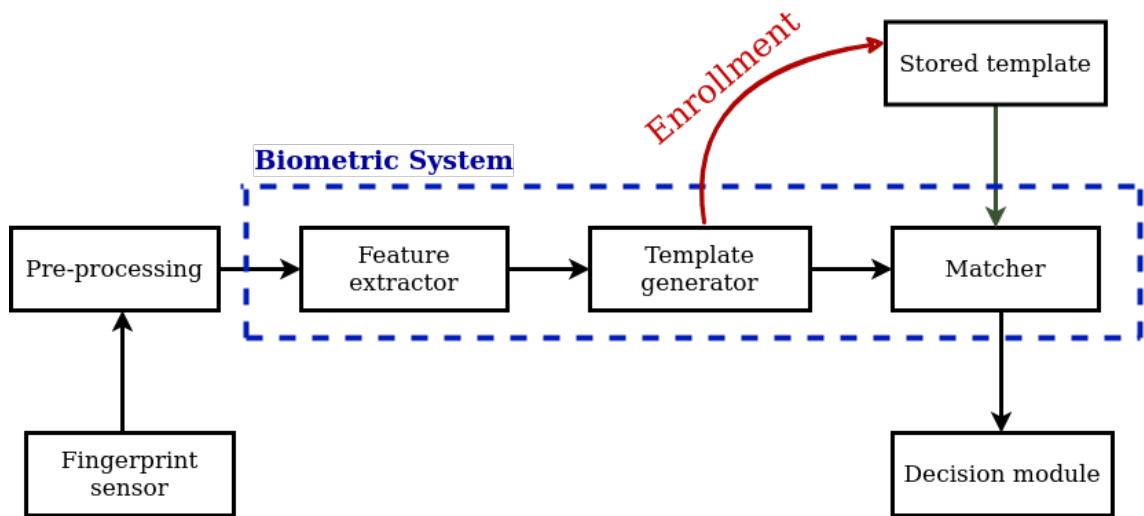


Figure 2.9: Block diagram of a fingerprint-based recognition system.

The feature extraction module further processes the enhanced image and extracts a set of features from it. This feature set often includes minutiae, but, depending on the matching algorithm, other features (e.g., local orientation, local frequency, singularities, ridge shapes, ridge counts, parts of the enhanced image, etc.) can be extracted in conjunction with (or instead of) minutiae. In the end, the fingerprint matching module retrieves from a system database one or more templates and matches the template(s) with the features extracted from the current sample [93]. If the systems operate in verification mode, the user has been required to claim his identity and therefore, just one template is retrieved from the database and matched with the current sample; if the system operates in identification mode, the current sample is matched against all the database templates to check whether one of them is sufficiently similar, see Figure 2.9.

Chapter 3

Enhancement, Detection, and Localization Methods

The following chapters describe the methods and algorithms for fingerprint image preprocessing, localization, detection, and general recognition methods in classical and machine learning techniques. These methods may serve as an intermediate step for deriving other features; for example, some preprocessing and enhancement steps are often performed to simplify the task of minutiae extraction. Finally, post-processing approaches are applied to reduce numbers of false minutiae and pattern analysis to extract classification types.

3.1 Fingerprint Image Preprocessing and Enhancement

Preparatory to fingerprint feature extraction, preprocessing aims at removing noise and other undesirable components. The preprocessing step can range from simple image thresholding to sophisticated gray-level segmentation. There are many preprocessing techniques available in image processing for image enhancement. The choice of which to use will depend on the quality and nature of the image. In the context of the fingerprint image, preprocessing based on minutiae extraction or image-based is an essential step. The performance of a minutiae extraction algorithm relies heavily on the quality of the input fingerprint images. In a high-quality fingerprint image, ridges and valleys alternate and flow in a locally constant direction, and minutiae are anomalies of ridges, i.e., ridge endings and ridge bifurcations which were described in further detail in Section 2.3, therefore, the ridges can be easily detected, and minutiae can be precisely located from the thinned ridges [120]. The general process of preprocessing comprises Red Green Blue (RGB) color model to grayscale image conversion, segmentation, normalization, enhancement, filtering, binarization/thinning and core point detection [22].

3.1.1 Segmentation

Segmentation as a part of preprocessing can be done using color or texture information. A fingerprint image usually consists of two components which are called the foreground (so called the Region Of Interest (ROI)) and the background.



Figure 3.1: The foreground and the background regions of a fingerprint image.

Fingerprint segmentation [10] is an important processing step to separate the fingerprint foreground with the interleaved ridge and valley structure from the image background with non fingerprint patterns to avoid extraction of features in noisy areas of the fingerprint and background. Accurate segmentation of a fingerprint will significantly reduce the computation time of the following processing steps and discard many spurious minutiae [10] [40]. The objective of preprocessing and segmentation is to acquire a binary segmented fingerprint ridge image from an input gray-scale fingerprint image, where the ridges very often have a value 1 (white), and the rest of the image has the value 0, or otherwise. [110].

The ultimate aim of segmentation is to focus only on the foreground regions while the background regions are ignored and to identify the ROI in a fingerprint image. ROI segmentation helps the fingerprint matching system. In the first place, it constraints the area for fingerprint feature extraction only in the foreground. Thus, it prunes the possibility of spurious feature (minutiae) extraction around the boundary of the foreground fingerprint (see Figure 3.2).



Figure 3.2: An example of background extraction from a fingerprint image.

Furthermore, ROI segmentation eliminates the chances of erroneous detection of minutiae due to sensor noise around image boundaries. Secondly, it reduces the computation time for performing matching [72].

Generally, for a given digital fingerprint image, the region of interest can be divided into the following three categories [61]:

- *Well-defined region*, where ridges and valleys are differentiated from each another such that a minutiae extraction algorithm can operate reasonably.
- *Recoverable corrupted region*, where ridges and valleys are corrupted by a small number of creases, smudges, etc. But, they are still visible, and the neighboring regions provide sufficient information about the actual ridge and valley structures.
- *Unrecoverable corrupted region*, where such a harsh noise and distortion corrupt ridges and valleys that no ridges and valleys are visible and the neighboring regions do not provide sufficient information about the actual ridge and valley structures.

3.1.2 Image Quality Normalization

To eliminate the noise in the fingerprint image a *normalization approach* [100] will be applied. The normalization operation makes it possible to increase the contrasts in the image by adjusting the gray levels represented in each pixel without affecting the valuable information included in the fingerprint image. This operation can be done locally on a segmented image according to the computation of the Mean and Variance [61]. A gray-level fingerprint image, I , is defined as an $M \times N$ matrix, where (i, j) represents the intensity of the pixel at the i^{th} row and j^{th} column. The Mean and Variance of a gray-level fingerprint image, I , are defined as [61]:

$$M(I) = \frac{1}{N^2} \sum_{i=0}^{N-1} \sum_{j=0}^{N-1} I(i, j) \quad (3.1)$$

and

$$var(I) = \frac{1}{N^2} \sum_{i=0}^{N-1} \sum_{j=0}^{N-1} (I(i, j) - M(I))^2 \quad (3.2)$$

The normalization of a gray-level image is performed according to the formula [61]:

$$G(i, j) = \begin{cases} M_0 + \sqrt{\frac{var_0(I(i, j) - M)^2}{var}} & \text{if } I(i, j) > M, \\ M_0 - \sqrt{\frac{var_0(I(i, j) - M)^2}{var}} & \text{otherwise} \end{cases} \quad (3.3)$$

where M_0 and Var_0 are the desired mean and variance values.



Figure 3.3: Example of normalization: original fingerprint (left), normalized image (right).

3.1.3 Histogram Equalization

Image enhancement techniques can be divided into two broad categories [108]: *spatial domain* methods that operate directly on pixels and *frequency domain* methods that operate on the Fourier transform of the image. A widely used spatial domain method is *histogram equalization* [100], to reduce the effects of illumination and to separate noise from biometric characteristics. Histogram Equalization (HE) [106] is a commonly used method to convert an image so that it has a uniform histogram, which is considered to produce an optimal overall contrast in the image.

Contrast Limited Adaptive Histogram Equalization (CLAHE) [105] was originally developed for enhancement of low-contrast medical images. It is a technique to overcome the over-amplification of the noise problem. The difference between this method and standard HE is that CLAHE operates on small regions in the image, called blocks, and computes several histograms, each corresponding to a distinct section of the image and redistributing the lightness values of the image [59].

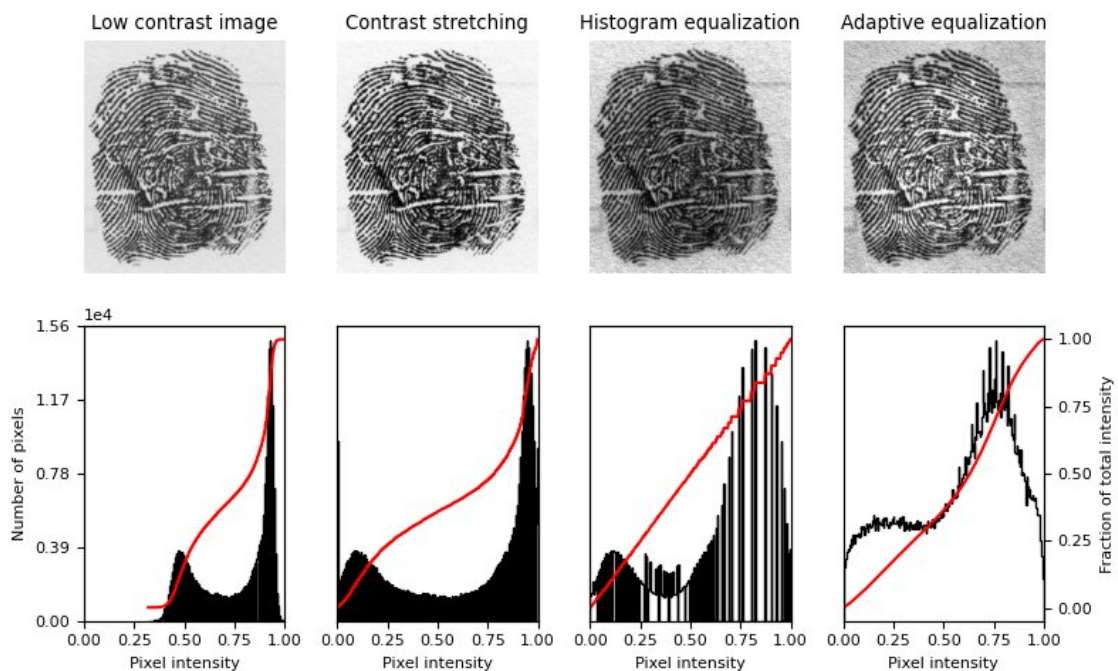


Figure 3.4: Histogram equalization of a diseased fingerprint image.

3.2 Feature Extraction and Image Descriptors

Feature extraction algorithms play a crucial role in identifying meaningful representations of images while minimizing the number of parameters. By extracting relevant features, images can be effectively expressed using fewer parameters, leading to faster and more accurate classification with reduced computational load. Typically, low-level features and high-level features are extracted from images. Low-level features are simpler and incur less computational load, but they may have limited success in classifying complex images. On the other hand, high-level features are more complex and require greater computational resources.

Fingerprint features [87] are parameters in epidermal images of a fingertip that can provide information exclusively specific to a unique person. These parameters can be measured by com-

putational techniques applied to a digital image. Feature extraction approaches help to extract features which might have no obvious relevance for a given task. *Feature selection* [90] selects relevant features and removes noisy ones in the original feature space to improve or not substantially deteriorate the classification accuracy. First of all, features are extracted from input data, and then a decision is made based on the features [87]. The biometric feature extraction process extracts unique features from the biometric samples, e.g., minutiae from fingerprint images [10]. A local feature [87] is an image pattern that differs from its immediate neighborhood. It is usually associated with a change of an image property or several properties simultaneously, though it is not necessarily localized exactly on this change. In local feature extraction, the closest neighboring pixels play an important role. Relationships among neighboring pixels are as important as those between the center pixel and neighboring pixels, see Figure 3.5.

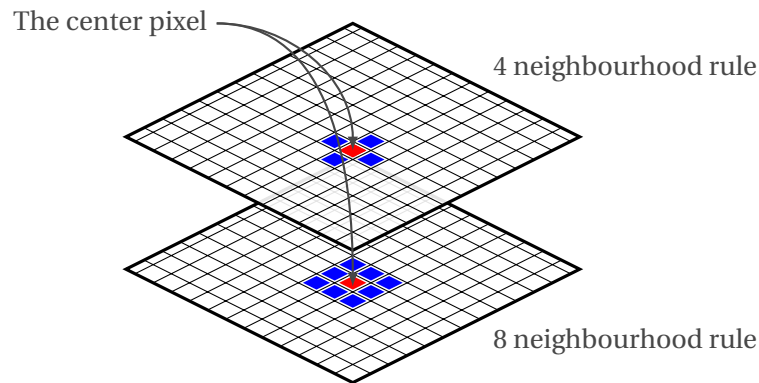


Figure 3.5: The neighborhood of a pixel can have a maximum of 8 pixels.

Fingerprint image enhancement and feature extraction are the most critical stages in fingerprint verification. The system's robustness depends entirely upon its ability to enhance low-quality images and reliably extract minutiae from them. Various feature extractor algorithms extract biometric features differently.

For a robust analysis of biomedical images, the challenge is to retrieve features from ROI that accurately describe image elements, such as texture, intensity, and shape, i.e., properties that can differentiate various features within images. These features are obtained by algorithms commonly called *image descriptors*, which output, a feature vector, describes the salient part of an image [123].

3.2.1 Orientation Field Estimation

The goal of fingerprint orientation extraction [92] is to compute one of the most critical information in fingerprint, the local orientation (explained in Section 2.3.1): a feature denoting the direction of the ridge flow at discrete positions. A good orientation estimation can simplify and improve the subsequent feature extraction steps.

Several methods [110, 79, 46] have been proposed to estimate the *orientation field* of fingerprint images. Developing a reliable fingerprint orientation estimation algorithm is critical. The method is based on a least mean square orientation estimation algorithm. The main steps of the algorithm are as follows [61]:

1. Divide a normalized fingerprint image into blocks of size $w \times w$;
2. Compute the gradients $\partial_x(i, j)$ and $\partial_y(i, j)$ at each pixel (i, j) ;

3. Estimate the local orientation of each block centered at pixel (i, j) based on the following equations:

$$v_x = \sum_{u=i-\frac{w}{2}}^{i+\frac{w}{2}} \sum_{v=j-\frac{w}{2}}^{j+\frac{w}{2}} 2\partial_x(u, v)\partial_y(u, v) \quad (3.4)$$

$$v_y = \sum_{u=i-\frac{w}{2}}^{i+\frac{w}{2}} \sum_{v=j-\frac{w}{2}}^{j+\frac{w}{2}} \partial_x^2(u, v)\partial_y^2(u, v) \quad (3.5)$$

$$\Theta(i, j) = \frac{1}{2} \tan^{-1} \left(\frac{v_y(i, j)}{v_x(i, j)} \right) \quad (3.6)$$

where $\theta(i, j)$ is the least square estimate of the local ridge orientation at the block centered at pixel (i, j) . A gradual change of the grey level indicates the gradient. The ridge is perpendicular to the *gradient*. The orientation field angle gives the orientation field of the fingerprint; see Figure 3.6.

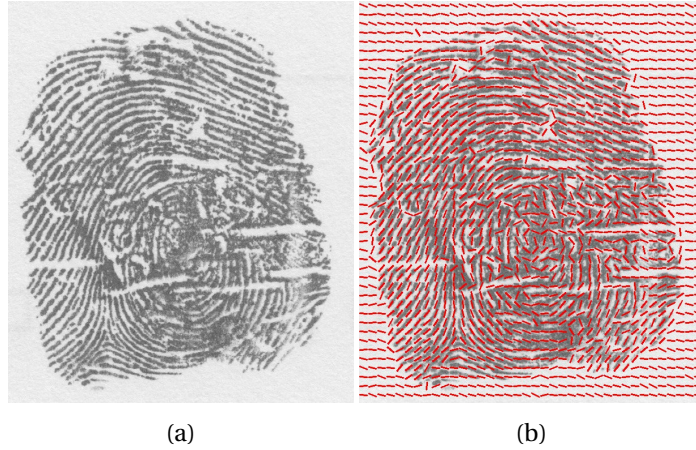


Figure 3.6: Computation of orientation estimation based on a gradient. a) Original image, b) orientation field.

The advantage of this method in forensic applications, is that it is already integrated into the standard fingerprint recognition pipeline, enabling it to be easily implemented into existing methods. Furthermore, it provides a relatively accurate estimate of the fingerprint damage in the sample, which can aid in identifying potential errors in the data. The method's ability to recognize damaged or noisy areas in a fingerprint image also enhances the accuracy and reliability of the fingerprint recognition system.

3.2.2 Fast Fourier Transform

The Fast Fourier Transform (FFT) [101] is an efficient algorithm to calculate the Discrete Fourier Transform (DFT) [101] of a sequence. To bring down the computation, a divide and conquer algorithm recursively breaks the DFT into smaller DFTs. As a result, it successfully reduces the complexity of the DFT from $O(n^2)$ to $O(n \log n)$, where n is the size of the data [82]. This reduction in computation time is significant, especially for data with large n , making FFT widely used in engineering, science, and mathematics [82]. The FFT can only be applied to square images whose size is an integer power of 2 (without special effort).

The calculation involves the separability property of the Fourier transform. Separability means that the Fourier transform is calculated in two stages [100]: the rows are first transformed using a 1D FFT, then this data is transformed in columns, again using a 1D FFT. This process can be achieved since the sinusoidal basis functions are orthogonal.

Let $I(i, j)$ denote the gray level at (i, j) in an $N \times N$ image. The image in the spatial domain is transformed to the frequency domain by the 2D FFT, mathematically a 2D image Fourier transform is [82]:

$$F(k, l) = \sum_{i=0}^{N-1} \sum_{j=0}^{N-1} I(i, j) e^{-i2\pi(\frac{k_i}{N} + \frac{l_j}{N})} \quad (3.7)$$

where:

- $F(k, l)$ represents the value of the Fourier transform of an image at a particular frequency location, denoted by the indices k and l .
- $I(i, j)$ is the image in the spatial domain, and the exponential term is the basis function corresponding to each point $F(k, l)$ in the Fourier space.
- k and l are frequency indices that vary from 0 to $N - 1$, where N is the size of the image. The values of k and l determine the frequency location in the Fourier domain.

The equation can be interpreted as follows: each point $F(k, l)$ value is obtained by multiplying the spatial image with the corresponding base function and summing the result. The basis functions are sine and cosine waves with increasing frequencies ($e^{ix} = \cos(x) + i \sin(x)$).

3.2.3 Gabor Filters

The *Gabor filter*, as described by Nixon [100], is a band-pass filter that is highly selective to both orientation and spatial frequency. It is a powerful tool for detecting local structural patterns from images, and has been extensively used in texture analysis and object recognition. In addition to its versatility and robustness, the Gabor filter shares some important features with the gradient feature. Specifically, both approaches can be applied to binary and gray-scale images, and are highly resilient to image noise [89]. Among various approaches to texture feature extraction, the Gabor filter has emerged as one of the most popular ones. Gabor filter-based feature extractor [74] is a Gabor filter bank defined by its parameters, including frequencies, orientations, and smooth parameters of the Gaussian envelope [74]. Gabor features [75] have been particularly successful in many computer vision and image processing applications. In biometrics, for example, Daugman's iris code [26] is the golden standard for iris recognition, and Gabor features are among the top performers in face recognition, and fingerprint matching [63]. Gabor's original 1D function of time and frequency has been generalized to a 2D function of space and spatial frequency and several forms have been proposed [49, 27].

A common 2D Gabor filter is described by the impulse response [100]:

$$G(x, y: f, \theta) = \exp \left\{ -\frac{1}{2} \left[\frac{x'^2}{\delta_{x'}^2} + \frac{y'^2}{\delta_{y'}^2} \right] \right\} \cos(2\pi f x') \quad (3.8)$$

where $x' = x \sin(\theta) + y \cos(\theta)$, $y' = x \cos(\theta) - y \sin(\theta)$, θ controls the orientation of the function, f is the frequency of sinusoidal plane wave along the direction θ from the x -axis, and $\delta_{x'}$ and $\delta_{y'}$ are the space constants of the Gaussian envelope along x' and y' axes, respectively. Such Gabor filters have been widely used in various applications [65, 38, 13, 26, 69, 85].

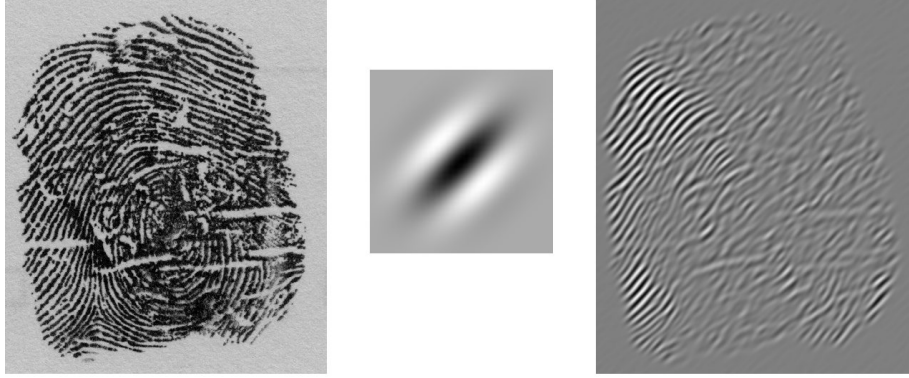


Figure 3.7: Responses of Gabor filtering for parameters $\theta = 0.78, f = 0.08$. Normalized image (left), Gabor wavelet (middle), response (right).

3.2.4 Local Binary Patterns

A very popular and well-known local feature is the family of Local Binary Pattern (LBP) [51]. Since the first basic LBP was introduced in the 1990s, LBP methodology has developed a lot in the past two decades, ranging from extensions and related theories to various new applications [41]. LBP is a theoretically and computationally simple approach that is robust in terms of grayscale variations and which is shown to discriminate an extensive range of rotated textures efficiently [102]. LBP is a powerful texture descriptor used for images, which determines the relationship between neighboring pixels by thresholding them based on the value of the current pixel. It has been widely used in various image processing applications such as object recognition, face recognition, and texture classification.

By applying the LBP operator to an image, each pixel is denoted by an integer label (e.g., 256 different labels in the original LBP with 3×3 neighborhood configuration) which is robust to monotonic illumination change. Each of these labels is called an LBP pattern.

The LBP algorithm works as follows [51]: It is derived for a specific pixel neighborhood radius r by comparing the intensities of M discrete circular sample points to the intensity of the center pixel (clockwise or counterclockwise), starting from a certain angle. The comparison determines whether the corresponding location in the Local Binary Pattern of length M is 1 or 0. A value 1 is assigned if the center pixel intensity is smaller than the sample pixel intensity and 0 otherwise. After the LBP extraction, each pixel in an image is replaced by a binary pattern. The feature vector of an image then consists of a histogram of the pixel LBPs. The initial length of the histogram is 2^M since each possible LBP is assigned a separate bin.

Formally, given a pixel in the image, the resulting LBP can be expressed in the decimal form as [51]:

$$LBP(P, R) = \sum_{p=0}^{p-1} s(g_p - g_c) 2^p \quad \text{where} \quad s(x) = \begin{cases} 0 & \text{if } x < 0 \\ 1 & \text{if } x \geq 0 \end{cases} \quad (3.9)$$

where g_c is the gray value of the central pixel, g_p is the value of its neighbors, P is the total number of involved neighbors, and R is the radius of the neighborhood.

An LBP is called uniform if the binary pattern contains at most two bitwise transitions from 0 to 1 or vice versa when the bit pattern is considered circular. For example, patterns 00111000, 11111111, 00000000, and 11011111 are uniform, and patterns 01010000, 01001110, or 10101100 are non-uniform. Choosing only uniform patterns contributes to both reducing the length of

the feature vector (LBP histogram) and improving the performance of classifiers using the LBP features [4, 102, 116].

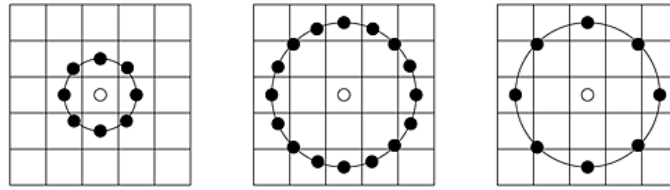


Figure 3.8: Local neighborhood at different scales of a uniform LBP [4].

In general the LBP feature extraction algorithm is a robust method that effectively handles variations in lighting conditions. The LBP process involves traversing a window with a specified neighborhood value over the image and assigning labels to the center pixels. During this process, a threshold is applied based on the pixel values surrounding the center pixel. The LBP matrix is then calculated, taking into account the local neighborhood values in a clockwise or counter-clockwise direction. This mathematical calculation yields a statistical and structural model of the textural pattern. The key advantages of the LBP algorithm include its resistance to gray level changes and computational simplicity, making it suitable for real-time applications [50].

3.2.5 Edge Detectors

In image processing, edges are significant local changes (discontinuities) in the intensity of the image and are important features for extracting valuable information from the image [100]. An edge [117] can be characterized by an abrupt change in intensity, indicating the boundary between two regions of an image. Therefore edge detection is equal to extracting the high-frequency components from an image, see Figure 3.9.

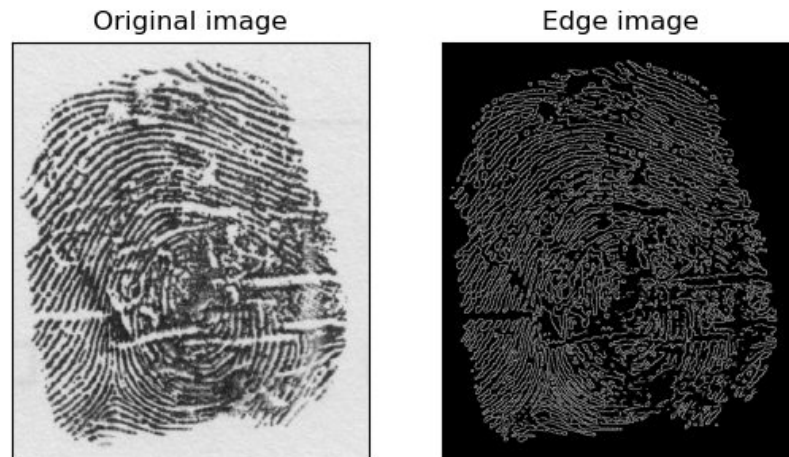


Figure 3.9: Canny edge detection in the diseased fingerprint.

The Laplacian operator [100] is a second derivative operator, and as such, it is sensitive only to changes in intensity gradient. In 2D its standard (mathematical) definition is given by [100]:

$$\Delta f = \frac{\partial^2 f}{\partial x^2} + \frac{\partial^2 f}{\partial y^2} \quad (3.10)$$

where x and y are the standard Cartesian coordinates of the xy -plane. A Laplacian edge detector is devised to tackle both vertical and horizontal edges. It is described in the following matrix [100]:

$$\begin{bmatrix} 0 & 1 & 0 \\ 1 & -4 & 1 \\ 0 & 1 & 0 \end{bmatrix} \quad (3.11)$$

Compared with the first derivative-based edge detectors, such as the Sobel operator [100], it may yield better results in edge localization. The Sobel operator is the magnitude of the gradient computed by [100]:

$$M = \sqrt{s_x^2 + s_y^2} \quad (3.12)$$

where s_x and s_y can be implemented using convolution masks [28]:

$$s_x = \begin{bmatrix} -1 & 0 & 1 \\ -2 & 0 & 2 \\ -1 & 0 & 1 \end{bmatrix}, \quad s_y = \begin{bmatrix} 1 & 2 & 1 \\ 0 & 0 & 0 \\ -1 & -2 & -1 \end{bmatrix} \quad (3.13)$$

These operators are more sensitive to noise due to the second derivative. Canny edge operator [100] comes in this category. It provides good detection, localization, and much clear response. A more sophisticated filter for edge detection is *Laplacian of Gaussian* [100] which is a combined Gaussian lowpass filter, and Laplacian derivative operator (highpass filter). The filter smoothes the image to suppress noise using the lowpass Gaussian filter, then uses the Laplacian derivative operation for edge detection since the noisy image is very sensitive to the Laplacian derivative operation.

3.2.6 Gray Level Co-occurrence Matrix

The co-occurrence matrix, also called the Spatial Gray Level Dependence Matrix (SGLDM) [53], is a technique that allows for the extraction of statistical information from the image regarding the distribution of pairs of pixels. The Gray Level Co-occurrence Matrix (GLCM) [53] characterizes the texture of an image by calculating how often pairs of pixels with specific values and in a specified spatial relationship co-occur in an image [53].

Typically, the GLCM operates on pairs of pixels within the image. By examining the frequency of combinations of pixel brightness values, the GLCM constructs a matrix that represents the occurrence patterns of pixel pairs. This matrix has the same number of rows and columns as the number of gray values in the image. The matrix elements reflect the probabilities of specific pixel pairs based on their gray values, which can vary depending on their local neighborhood. When the intensity values are extensive, the resulting GLCM matrix can become large, leading to increased computational load and longer processing times. Principally, the GLCM measures how often different combinations of pixel brightness values occur in an image. It is a two-dimensional square matrix computed by defining a direction θ and a distance d , and pairs of pixels separated by this distance, computed across the defined direction, are analyzed. The spatial relationship, also called *offset*, defines the direction and distance between the pixel of interest and its neighbor. For the right immediate neighbor, the direction corresponds to 0 and the distance to 1, which corresponds to an offset vector of (0, 1). A count is then made of the number of pairs of pixels that possess a given distribution of grey-level values. Each entry of the matrix thus corresponds to one such grey-level distribution [18].

Let $f : N_y \times M_x \rightarrow I$ be an image with dimensions, $N_y = (0, 1, 2, \dots, I_y - 1)$ and $M_x = (0, 1, 2, \dots, I_x)$ having a set of quantized gray-tones $G = (0, 1, 2, \dots, L - 1)$.

The coordinates of this image $N_y \times M_x$ represent the resolution cells containing the gray levels for each pixel. The texture is assessed by the four closely related measures called angular nearest neighbor gray tone spatial dependence matrices. The spatial measurement, for a 2D image at different angles with the distance d in four different directions (0° , 45° , 90° and 135°) is defined as [53, 39, 118]:

$$C(i, j, d, 0^\circ) = \#\{(k, l), (m, n) : k - m = 0, |l - n| = d\} \quad (3.14)$$

$$C(i, j, d, 45^\circ) = \#\{(k, l), (m, n) : k - m = d, l - n = -d\} \\ \text{or} \quad (3.15)$$

$$C(i, j, d, 45^\circ) = \#\{(k, l), (m, n) : k - m = -d, l - n = d\}$$

$$C(i, j, d, 90^\circ) = \#\{(k, l), (m, n) : |k - m| = d, l - n = 0\} \quad (3.16)$$

$$C(i, j, d, 135^\circ) = \#\{(k, l), (m, n) : k - m = d, l - n = d\} \\ \text{or} \quad (3.17)$$

$$C(i, j, d, 135^\circ) = \#\{(k, l), (m, n) : k - m = -d, l - n = -d\}$$

where # represents the count of pixel pairs with the same intensity level.

Haralick [53] proposed 14 statistical features extracted from textural features of the co-occurrence matrix to estimate the similarity among different GLCMs. Only some of these features are used in my research to reduce the computational complexity.

Contrast [53], also known as variance, is a measure of intensity variations between a pixel and its neighbor over the whole image. The higher the contrast, the more the entries of the normalized GLCM move away from the matrix diagonal. The minimum value is 0, which is obtained for a constant image. The contrast function of an image is defined as follows [53]:

$$Contrast = \sum_{i,j} p(i, j) |i - j|^2 \quad (3.18)$$

Correlation [53] is a measure of how correlated a pixel is to its neighbor over the whole image. The range is $[-1, 1]$, where 1 equals a perfectly positive correlation and -1 equals a perfectly negative correlation. The correlation feature of an image is defined as follows [53]:

$$Correlation = \sum_{i,j} p(i, j) \frac{(i - \mu_x)(j - \mu_y)}{\sigma_x \sigma_y} \quad (3.19)$$

where μ_x is a mean value of the partial probability function in x -direction (column); σ_x is standard deviation of the partial probability function in x -direction (column); for symmetric GLCMs: $\mu_x = \mu_y$ and $\sigma_x = \sigma_y$ [53].

Energy [53], also known as uniformity or angular second moment, is a measure of texture roughness. When pixels have similar intensity, the energy is high. The range is $[0, 1]$. The energy of a constant image equals 1 and is defined as follows [53]:

$$Energy = \sum_i \sum_j p(i, j)^2 \quad (3.20)$$

where $p(i, j)$ represents the probability of two neighboring pixels having gray levels i and j , respectively.

Dissimilarity [53] is a measure of distance between pairs of objects (pixels) in the region of interest and is defined as follows [53]:

$$Dissimilarity = \sum_{i,j=0}^{N-1} p_{i,j} |i - j| \quad (3.21)$$

Homogeneity [53] is a measure of how close the elements of the normalized GLCM are to its diagonal. Typically, homogeneity increases with decreasing contrast. Homogeneity has a range of [0, 1]. For a diagonal GLCM, the homogeneity equals 1. The homogeneity feature of an image is defined as follows [53]:

$$Homogeneity = \sum_{i,j=0}^{N-1} \frac{p_{i,j}}{1 + (i - j)^2} \quad (3.22)$$

The second group of features emphasizes orderliness. That is, how regularly an arbitrary pair of neighbor pixels occurs. Among them, the Angular Second Moment (ASM), *energy* and *entropy* are as follows [53]:

$$ASM = \sum_{i,j=0}^{N-1} p^2(i, j) \quad (3.23)$$

$$Energy = \sqrt{ASM} \quad (3.24)$$

$$Entropy = \sum_{i,j=0}^{N-1} p_{i,j} (\log(p_{i,j})) \quad (3.25)$$

The effect of applying these features on an image is shown in Figure 3.10.

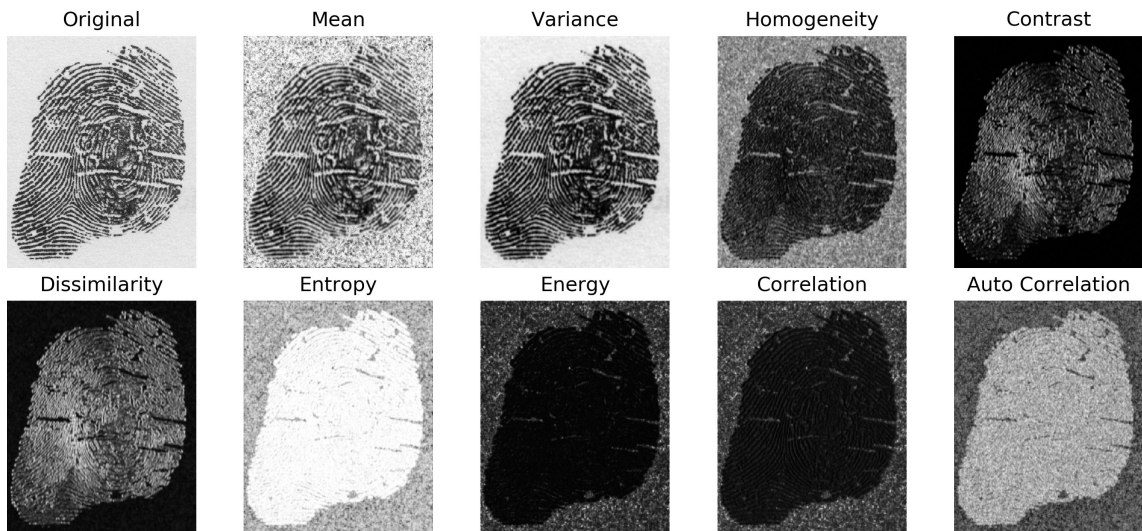


Figure 3.10: An example of various features of GLCM.

3.2.7 Mathematical Morphology

Binary images may contain numerous imperfections. In particular, the binary regions produced by simple thresholding are distorted by noise and texture [112]. The morphological operators are defined in terms of simple logical operations on local groups of pixels, which deals with an image's form and shape. *Dilation* and *erosion* [31] are the two basic morphological operators, where dilation selects the brightest value in the neighborhood of the structuring element and erosion selects the darkest value in the neighborhood. Many operations are derived from these operators, such as *opening* and *closing* [31]. Opening an image refers to erosion followed by dilation, whereas closing refers to dilation followed by erosion [12]. Some mathematical morphological operators are [31]:

- *Erosion*: shrinking the foreground;
- *Dilation*: expanding the foreground;
- *Closing*: removing holes in the foreground;
- *Opening*: removing stray foreground pixels in background.

Let A be the set of points representing the binary pixels of the original binary image and B be the set of points representing the binary pixels of a structuring element. The dilation of A by B , denoted $A \oplus B$, is defined by [86]:

$$A \oplus B = \bigcup_{a \in A} \{b + a \mid b \in B\} \quad (3.26)$$

and the erosion of A by B , denoted $A \ominus B$, is defined by:

$$A \ominus B = \{p \mid B + p \subseteq A\} \quad (3.27)$$

The difference between a binary image and a dilated (or eroded) version of it is one effective way of detecting object boundaries.

3.3 Localization of Damaged Regions

Image object recognition has been a significant research direction in computer vision. Its goal is two-fold: deciding *what* objects are in an image (classification) and *where* they are in the image (localization). Intuitively, if we know which objects are present, determining their location should be easier; alternatively, if we know where to look, recognizing the objects should be more accessible. Thus, it is natural to think of these two tasks jointly [20, 25, 55, 98, 130]. Object localization refers to identifying the location of one or more objects in an image and involves drawing a bounding box around the objects. In the case of diseases in fingerprint, it refers to locating the presence of each disease in an image. It can be defined as obtaining a single 2D coordinate corresponding to the location of each object. It's not desirable to use the boundary boxes around the diseases in fingerprint images; therefore, we decided to show it by heatmap or wavelet transform. An alternative approach to object localization would be to use image representation methods. An ideal heatmap can be regarded as a filter that approximates the existence of the damages by blocking irrelevant features in a diseased fingerprint image.

3.3.1 Wavelet Transform

The Wavelet Transform (WT) [100] is a good technique for signal compression and noise reduction. The wavelet transform can present a signal with a good time resolution, or a good frequency resolution [100]. There are two types of wavelet transforms the Continuous Wavelet Transform (CWT) and the Discrete Wavelet Transform (DWT) [100]. The most remarkable applications of WT in biomedical imaging are [96]:

- ability of the WT to make visible simple objects in a noisy background, which were previously considered to be invisible to a human viewer;
- demonstrated the superiority of the WT over existing techniques for unsharp mask enhancement and median filtering;
- enhancing the visibility of clinically important features.

WT represents the image as a sum of wavelets on various resolution levels. The power of WT is that it offers high temporal localization for high frequencies while attempting good frequency resolution for low frequencies. Thus, WT is a proper tool to extract the local features of the image. There is a mother wavelet in wavelet analysis, and then there are wavelet coefficients derived from this mother wavelet. These coefficients are independent, and they create a set of features of the actual fingerprint image at different resolutions [121, 62]. DWT is a multiresolution image decomposition tool representing image features through various frequency subbands, one low frequency subband (LL) and three high frequency subbands (HL , LH and HH) [100]. Therefore, this tool has the well-known advantage of multiscale analysis (see Figure 3.11). The LL -subband contains an approximation of the original image while the other subbands contain the missing details. The LL -subband output from any stage can be decomposed further.

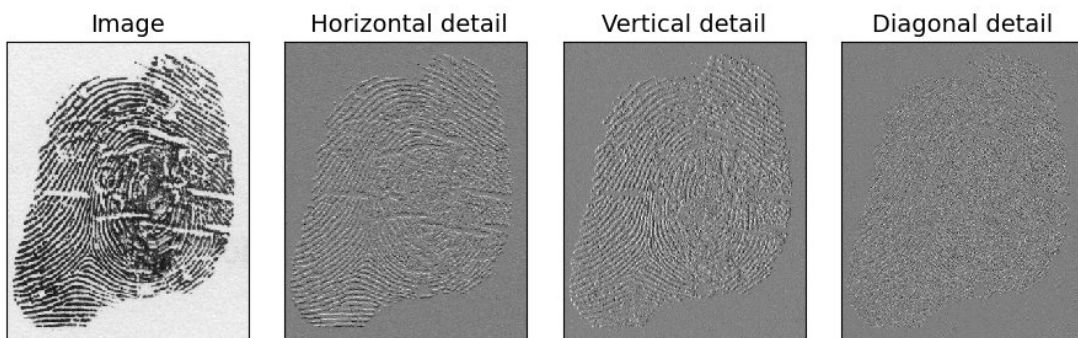


Figure 3.11: 2D-DWT of a fingerprint image in different sub-bands.

WT is commonly used in fingerprint applications for enhancement, detection, and ridge reconstruction [62]. The fingerprint image is decomposed into several spatial frequency subbands using a DWT. Multiresolution representations are effective for analyzing the information content of images. A multiresolution decomposition enables us to have a scale-invariant interpretation of the image. The most common approach to the multilevel discrete wavelet transform involves further decomposition of only the approximation subband at each subsequent level. At different resolutions, the details of an image generally characterize different physical structures of the scene. At a coarse resolution, these details correspond to the larger structures which provide the image context. It is, therefore, natural to analyze first the image details at a coarse

resolution and then gradually increase the resolution. Such a coarse-to-fine strategy is useful for pattern recognition algorithms [91]. In 2D, the discrete wavelet transform produces four sets of coefficients corresponding to the four possible combinations of the wavelet decomposition filters over the two separate axes. The wavelet coefficients have a high amplitude around the edges of the image and in the textured areas within a given spatial orientation, see Figure 3.12. The presented images showcase the absolute values of wavelet coefficients at three different resolution levels. These coefficients are mostly zero, resulting in gray pixels in the images, and represent each detail image. The wavelet representation technique is a powerful tool for signal processing and image analysis, providing an efficient method to decompose a signal into distinct frequency bands. This technique enables the identification of patterns and features that may not be readily apparent in the original image, making it a valuable tool for a range of applications.

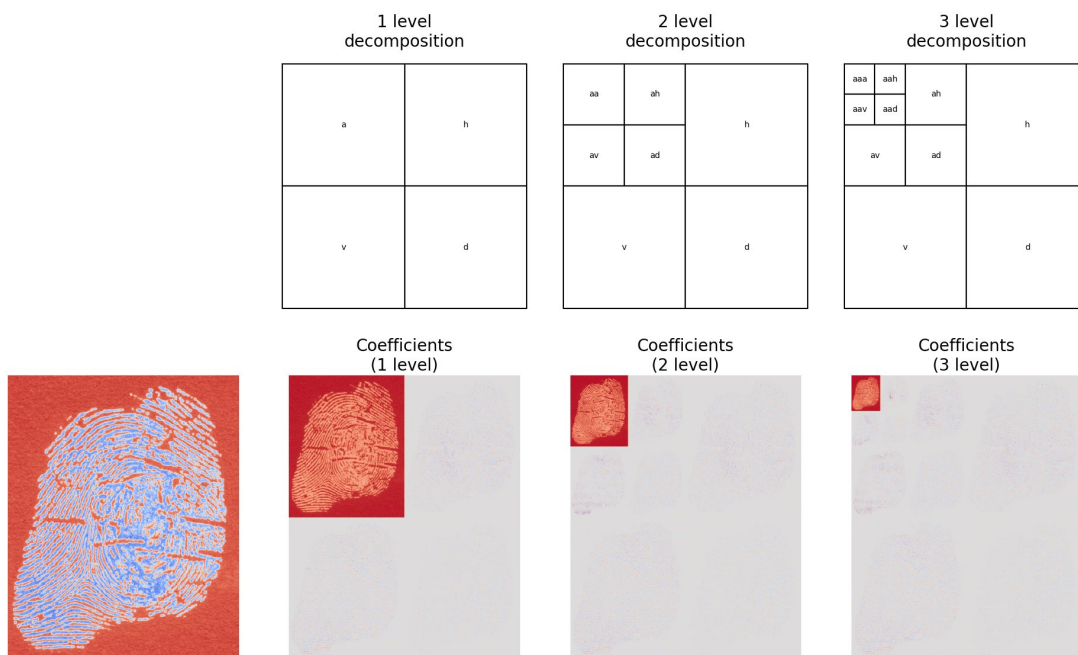


Figure 3.12: Wavelet representation on three resolution levels. These images show the absolute value of the wavelet coefficients (many of the coefficients are near zero (gray)) for each detail image.

3.3.2 Coherence

A *coherence feature* represents the strength of local gradients centered at the target pixel, which has a dominant representation [10]. Kass and Witkin [78] first proposed coherence, defined as the norm of the sum of orientation vectors divided by the sum of their norms; this scalar always lies in the range of [0, 1].

Generally, the coherence is higher in the foreground, where the grey-level values are much smoother along the ridge direction. On the contrary, the coherence is comparatively lower in the region where many spikes exist, emanating from noises such as stains and smudges. The coherence is promising to be used as a single feature to segment the foreground; however, more is needed for robust segmentation. Therefore, a systematic combination of several features is necessary [129, 125].

The coherence function is used in applications such as time delay estimation, and signal-to-noise ratio measurements [122]. Segmentation-based quality of the fingerprint can be done using the gradient coherence approach, which Zhang and Yan [127] adopt to detect the noise regions in the foreground.

Generally, gradient coherence describes the variation of grey-level values in an image. It can also be applied to investigate how each pixel block behaves in terms of its gradient value concerning fingerprint ridge flows.

For a given normalized fingerprint image, defined as $W \times H$ gradient coherence $coh(i, j)$ of each block at pixel (i, j) is calculated as follows [113]: Let $G_x(u, v)$ and $G_y(u, v)$ denote the gradient in x and y directions of the pixel at u^{th} row and v^{th} column in the $B \times B$ block. The coherence of the averaging method is given by [113]:

$$coh(i, j) = \frac{\sqrt{V_x(i, j)^2 + V_y(i, j)^2}}{V_z(i, j)} \quad (3.28)$$

where

$$\begin{aligned} V_x(i, j) &= \sum_{u=i}^{i+B-1} \sum_{v=j}^{j+B-1} (G_x^2(u, v) - G_y^2(u, v)) \\ V_y(i, j) &= \sum_{u=i}^{i+B-1} \sum_{v=j}^{j+B-1} 2(G_x(u, v)G_y(u, v)) \\ V_z(i, j) &= \sum_{u=i}^{i+B-1} \sum_{v=j}^{j+B-1} (G_x^2(u, v) + G_y^2(u, v)) \end{aligned}$$

where $i = 0, 16, 32, \dots, W - B$, and $j = 0, 16, 32, \dots, H - B$, and $V(i, j)$ is a local variance value of the gradient magnitude.

3.3.3 Classification

Choosing an appropriate classification algorithm for a particular problem requires practice and experience. In practice, it is always recommended to compare the performance of at least a handful of different learning algorithms to select the best model for the particular problem; these may differ in the number of features or examples, the amount of noise in a dataset, and whether the classes are linearly separable [95].

The *decision tree* [109] is one of the learning models used in the classification problem. In the decision tree, internal nodes represent a test on the characteristics, the branch portrays the outcome, and leaves are the decisions generated after subsequent processing.

Decision tree algorithms can be applied and used in various fields. It can be used as a replacement for statistical procedures as they are more accurate and highlight some important attributes we may overlook to find data, extract text, find missing data in a class, improve search engines, and find various applications in medical fields [95].

Machine Learning (ML) [83] usage is growing vastly in the medical diagnosis industry, where manual error can be reduced with computer analysis, and accuracy is improved. The diagnosis of a disease is highly reliable with machine learning techniques. Classification algorithms such as decision tree, naive Bayes [114], and Support Vector Machine (SVM) [19] are available; similarly, regression algorithms, namely Random forest [15], lasso, and logistic regressions [37], were used in the medical industry.

Random Forest is another classification technique, an ensemble learning approach based on a decision tree; it is a collection of tree predictors. Each tree independently depends on a vector's values, with the same distribution over all trees in the forest. *Ensemble learning* [131] is a machine learning scheme to boost accuracy by integrating multiple models to solve the same problem. In particular, multiple classifiers participate in ensemble classification to obtain more accurate results than a single classifier [15]. Each tree casts a unit vote for the most popular class to classify an input vector. Error with generalization converges as the number of trees in the forest increases. The error associated with a model of this classifier primarily depends on the strength of the individual trees in the forest and the correlation between the trees [95]. Next, a voting scenario is designed to assign a label to unlabeled samples. The commonly used voting approach is majority voting, which assigns the label with the maximum number of votes from various classifiers to each unlabeled sample [44], see Figure 3.13.

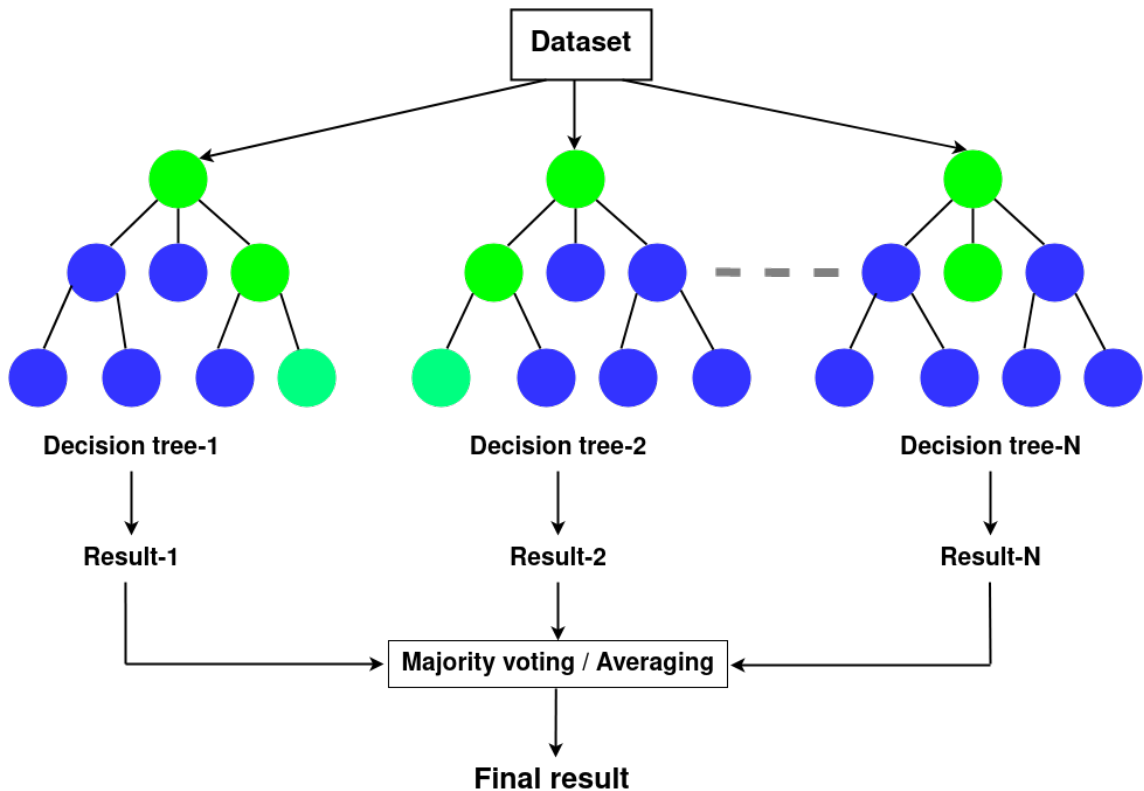


Figure 3.13: Random forest model.

The SVM algorithm, a linear binary classifier, is one of the most widely used kernel-based learning algorithms in various machine learning applications, primarily image classification [97]. In SVMs, the main goal is to solve a convex quadratic optimization problem to obtain a globally optimal solution, in theory, thus overcoming the local extremum dilemma of other machine learning techniques. SVM belongs to non-parametric supervised techniques, insensitive to underlying data distribution. This is one of the advantages of SVMs compared to other statistical techniques, such as ML, wherein data distribution should be known in advance [97]. SVMs are a type of machine learning algorithm commonly used for linear classification tasks. In addition to their proficiency in linear classification, SVMs can effectively perform non-linear classification by utilizing the kernel trick. This enables the algorithm to implicitly map inputs into

high-dimensional feature spaces, allowing for more complex decision boundaries and improved accuracy. Some common SVM terminologies are listed below:

- **Hyperplane:** is a decision boundary that separates a given set of data points with different class labels. SVM classifiers utilize this concept to separate data points using a hyperplane with the maximum margin, which is referred to as the maximum margin hyperplane. The linear classifier defined by the maximum margin hyperplane is known as the maximum margin classifier, see Figure 3.14.
- **Support Vectors:** are the data points that lie closest to the maximum margin hyperplane and determine its position.
- **Kernel:** a kernel function is used to transform the original input data into a higher dimensional space where a hyperplane can be used to separate the classes.
- **C:** the C parameter determines the trade-off between maximizing the margin and minimizing the classification error.
- **Gamma:** the gamma parameter defines how far the influence of a single training example reaches.
- **Soft Margin:** allows for some misclassifications in order to achieve a larger margin.
- **Hard Margin:** does not allow for any misclassifications and aims to find a maximum margin hyperplane that perfectly separates the data points.

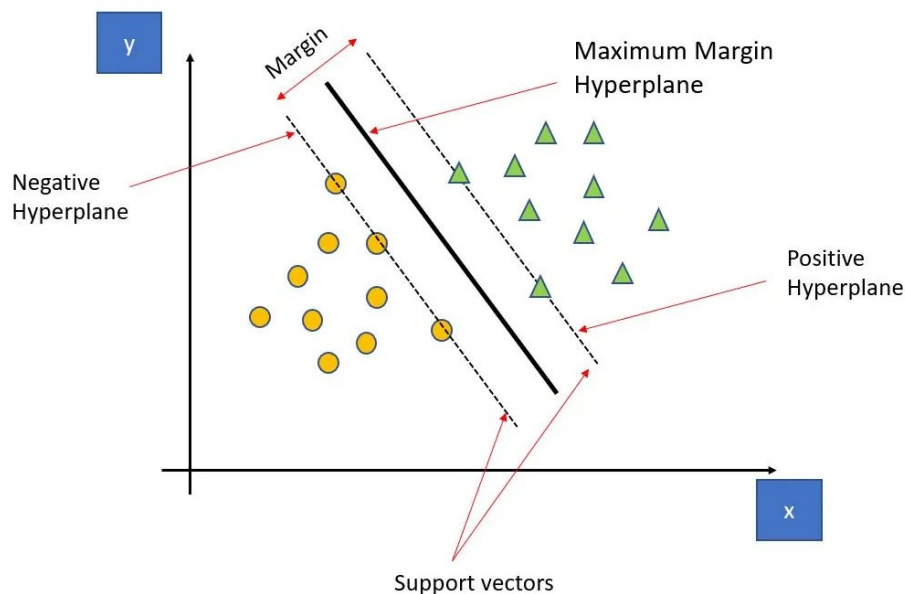


Figure 3.14: Hyperplane and margin Definition in SVM.

The C parameter in SVM is inversely related to the margin size. A larger value of C corresponds to a smaller margin, while a smaller value of C results in a larger margin. The C parameter, which can be used with any kernel, determines the algorithm's emphasis on avoiding misclassification of each training sample and is also referred to as regularization, see Figure 3.15.

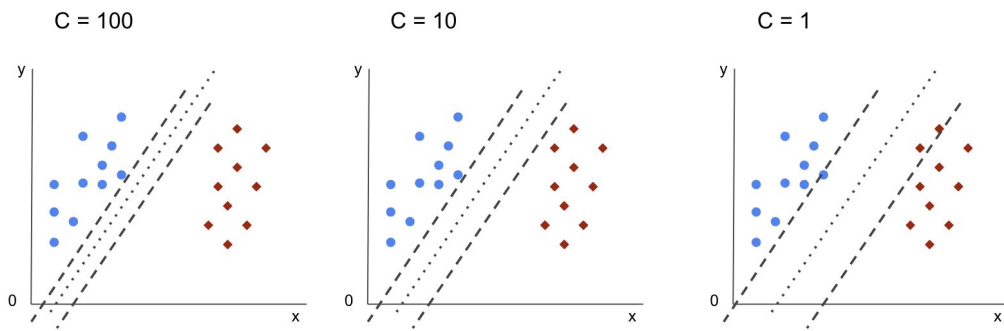


Figure 3.15: Effect of C parameter on margin size in SVM.

In SVMs, the primary objective is to select a hyperplane that maximizes the margin between support vectors in the given dataset. The process of finding the maximum margin hyperplane involves the following two steps:

- Generating hyperplanes that effectively separate the classes. There are multiple hyperplanes that can classify the data.
- Choosing the hyperplane that offers the largest margin between the classes that the distance from it to the support vectors on each side is maximized. If a hyperplane exists that satisfies this condition, it is referred to as the maximum margin hyperplane, and the linear classifier it defines is known as a maximum margin classifier (Figure 3.16).

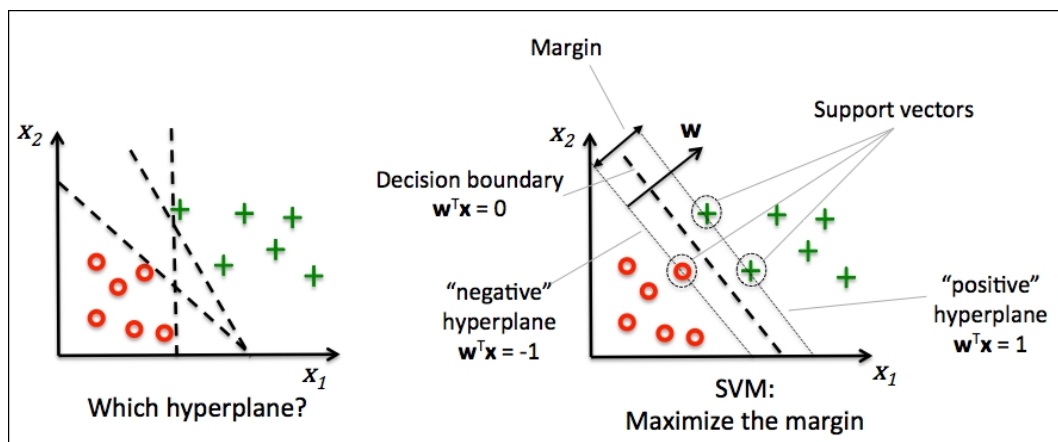


Figure 3.16: The Concept of maximum margin and maximum margin hyperplane in SVM.

In certain cases, the distribution of sample data points may be so scattered that it becomes infeasible to separate them using a linear hyperplane. To address this, SVMs employ a technique known as the kernel trick. This technique involves transforming the input space to a higher-dimensional space, as depicted in the diagram below, see Figure 3.17. By applying a mapping function, the original 2-dimensional input space is transformed into a 3-dimensional input space. Consequently, the data points can be effectively segregated using linear separation techniques.

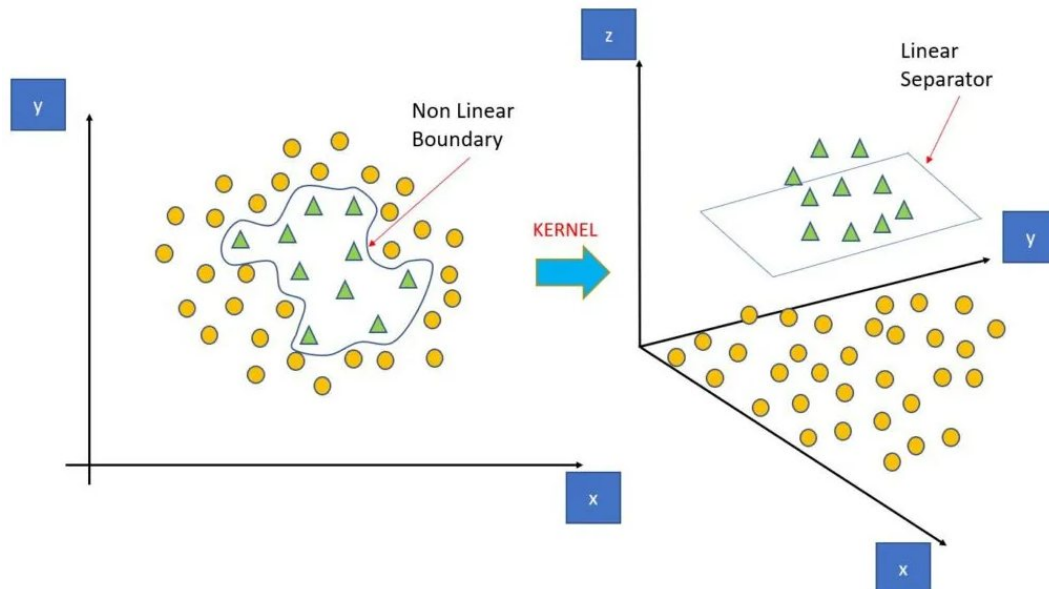


Figure 3.17: The kernel trick: transforming the input space to a higher-dimensional space.

These methods offer several advantages as a powerful classification technique:

- Compact models: SVMs depend on a relatively small number of support vectors, making them highly memory-efficient.
- Fast prediction: once the model is trained, the prediction phase is computationally efficient.
- Handling high-dimensional data: SVMs perform well with high-dimensional data, even when the number of dimensions exceeds the number of samples.
- Versatility with kernel methods: SVMs integrate well with kernel methods, allowing them to adapt to various types of data.

However, SVMs also have some drawbacks:

- Computational cost: the computational complexity of SVMs scales with the number of samples N . For large datasets, this can become computationally prohibitive.
- Parameter selection: the choice of the softening parameter C significantly impacts the results and needs to be carefully selected using techniques such as cross-validation, which can be time-consuming for large datasets.
- Lack of direct probabilistic interpretation: SVM results do not have a direct probabilistic interpretation. Estimating probabilities requires additional computation, such as internal cross-validation, which adds to the overall cost.

Another method for solving classification and object detection problems focusing on the algorithms are the existing implementations of ML. ML is a paradigm that may refer to learning from experience, which is previous data to improve future performance. The sole focus of this field is automatic learning methods. Learning refers to automatically modifying or improving algorithms based on past experiences without any external assistance from humans. The ability

to learn is one of the central features of intelligence, which makes it an important concern for both cognitive physiology and Artificial Intelligence (AI) [6]. ML, which crosses this discipline, studies the computational process that underlines learning in both humans and machines.

At the very fundamental level, ML is a category of Artificial Intelligence (AI) that enables computers to think and learn independently. It is about making computers modify their actions to acquire more accuracy, where accuracy is measured in the number of times the chosen decisions result in the correct ones. Machine learning is a multi-disciplinary field having a wide range of research domains reinforcing its existence. Real-world problems have high complexity, which makes them excellent candidates for the application of ML.

ML is required to make the computers sophisticatedly perform the task without any intervention of human beings based on learning and constantly increasing experience to understand the problem complexity and need for adaptability. Thus depending on the type of problem, such as *classification problem* [6], *anomaly detection problem* [21], and *reinforcement problem* [6], an appropriate machine learning approach can be applied. Several successful machine learning techniques for previously mentioned problems exist and have been used in object detection and recognition applications.

3.3.4 Deep Neural Networks

Deep Learning (DL) [29] or deep neural network refers to Artificial Neural Networks (ANN) with multi-layers, see Figure 3.18. DL has recently shown outstanding performance on image classification tasks. DL is a machine learning algorithm that automatically learns important features from raw data. Like classical neural networks, the Deep Neural Networks (DNNs) also consist of artificial neurons arranged as input, hidden, and output layers [58, 3]. Contrary to traditional neural networks, the number of hidden layers in deep networks is usually more than one. The hierarchical nature of deep neural networks allows them to learn features at multiple levels where each level corresponds to a particular level of abstraction [84].

Neural networks usually involve large and numerous buffers of parameters, activation values, and gradient values, each of which must be updated entirely during every training step. These buffers are large enough to fall outside the cache of a traditional computer, so the system's memory bandwidth often becomes the rate-limiting factor. Graphics Processing Unit (GPU) offers a compelling advantage over Central Processing Unit (CPU) because of their high memory bandwidth. Neural network training algorithms typically do not involve much branching or sophisticated control, so they are appropriate for GPU hardware. Since neural networks can be divided into multiple individual neurons that can be processed independently from the other neurons in the same layer, neural networks easily benefit from the parallelism of GPU computing. The most important reasons for the popularity of deep learning are the highly improved parallel processing abilities of hardware, especially the general-purpose GPUs, the substantially increased amount of data available for training, and the recent advances in ML algorithms [48].

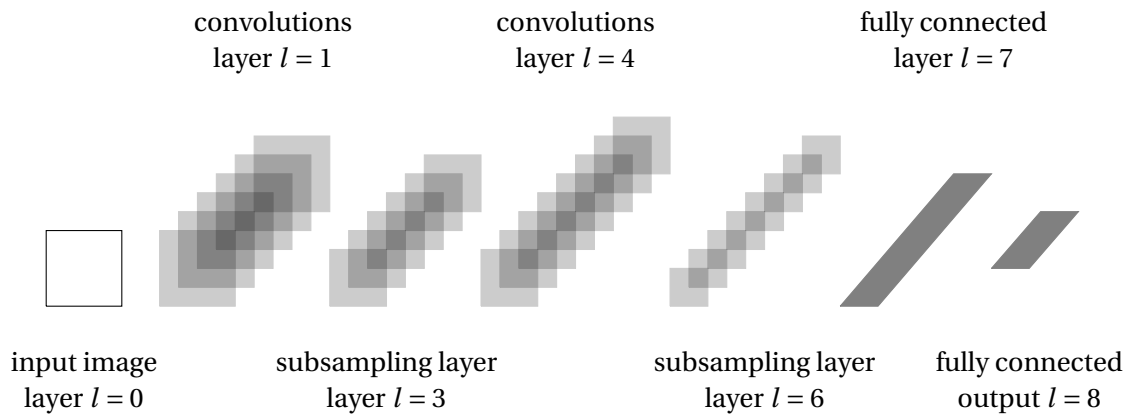


Figure 3.18: The architecture of the original convolutional neural network, introduced by LeCun et al. (1989).

Part II

Proposed Methods

Chapter 4

Diseased Fingerprint Representations

This part introduces a detailed description of the acquisition and analysis of a diseased fingerprint database, as well as the characteristics of each skin disease from the database and characteristics of the specific influence they have on the resulting fingerprint images. Efficient implementation of computer vision methods is also proposed for detecting and recognizing damaged parts in fingerprint images.

4.1 Analysis of Diseased Fingerprint Dataset

Skin diseases represent a critical but often neglected factor of fingerprint acquirement. In general medical practice, about 20 – 25% of patients with skin disorders are referred. When discussing whether fingerprint recognition technology is a perfect solution to all our security problems, we should always consider those potential users who suffer from some skin disease. Many skin diseases can affect palms and fingers. We find plenty of skin diseases, including a description of their influence on the structure and color of the skin, in specialized medical literature, e.g. [71]. These diseases may cause problems for most types of sensors because the color of the skin and the structure of the epidermis and dermis are influenced. In the following, we describe several skin diseases, which attack the hand, palms, and fingertips, with photographs. These clearly show that these diseases may cause many problems in automatic biometric systems [36, 30, 35, 33].

The first group of skin diseases represents those ones causing *histopathological changes* [35] in the epidermis and dermis. These diseases usually cause problems for all kinds of fingerprint scanners because they can influence the skin's color or internal structure. The most typical representatives of this group are [71]: *hand* and *fingertip eczema*, *dyshidrosis*, or *Raynaud's phenomenon* [36].

The second group represents diseases causing *skin discoloration* [35]. These diseases may cause problems for optical fingerprint sensors and sensors that use a fingerprint anti-spoof detection [81, 94, 80] check based on the color or spectral analysis of the human skin. Typical representatives are [71]: *Raynaud's phenomenon* or *hereditary hemorrhagic telangiectasia* [35].

The last group represents diseases causing *histopathological changes* at the junction of the epidermis and dermis. These diseases could cause structural changes underneath the skin at the junction between the dermis and epidermis. Typical representatives include [71]: *hand eczema*, which encompasses *atopic eczema* and *hyperkeratotic dermatitis*, *verruca vulgaris (warts)*, and *psoriasis* [36].

These diseases are classified into three categories according to the seriousness of the damage:

1. **Minor damage:** *verruca vulgaris, Raynaud's phenomenon, cut wound, scleroderma.*
2. **Medium damage:** a mild form of *fingertip eczema*, a mild form of *dyshidrotic eczema*, *hyperkeratotic eczema*, *effusion of fingers*, *collagenosis.*
3. **Major damage (unrecoverable):** *acrodermatitis*, every form of *fingertip eczema*, severe form of *dyshidrotic eczema*, *psoriasis.*

Acquired databases contain over 2,000 fingerprint images from patients suffering from various types of skin diseases. In total, 12 particular skin diseases were obtained [36]. The raw diseased fingerprint database was thoroughly analyzed to find any common features in the damage caused by the diseases. For every particular disease, common signs are found among all fingerprint images affected by this disease, and a general description of each disease and its influences is defined. Based on these descriptions and sets of common signs and their frequencies, the diseased fingerprint images are classified into five categories that are later used for the disease detection task.

Most of the fingerprint images come from a dactyloscopic card. The database of diseased fingerprint images shown in Table 4.1, containing 2,165 fingerprints from 44 patients affected by various skin diseases, was collected with the help of medical experts and dermatologists.

Table 4.1: Proportion of diseases in our damaged fingerprint dataset.

Disease	No. of fingerprints	Percentages [%]	No. of patients
Fingertip eczema	72	24.650	17
Psoriasis	326	15.058	9
Dyshidrotic eczema	247	11.409	4
Hyperkeratotic eczema	118	5.450	2
Verruca vulgaris	96	4.434	4
Scleroderma	50	2.310	1
Acrodermatitis continua	40	1.848	1
Colagenosis	36	1.663	1
Raynaud's phenomenon	9	0.416	1
Effusion of fingers	35	1.617	1
Cut wound	18	0.831	2
Unknown disease	83	3.834	1
Total	2,165	-	44

The quality values of all the images in the database were extracted using the publicly available NIST software [119], NFIQ 2.1.0 [1]. This algorithm exhibits increased reliability and accuracy in terms of determining which fingerprint sample is going to fail in the recognition stage, concerning its previous version. An example of five different quality scores of the various diseased fingerprint images from the database is given in Figure 4.1.

According to the NFIQ 2 algorithm, fingerprint quality is grouped into three relevant classes: excellent, good, and, finally, bad quality fingerprints. Some results for the quality estimation are shown in Figure 4.2.

4.2 Common Features in the Dataset

By observing and comparing the fingerprint images, 12 common features are defined. 7 of them are local features (see Table 4.2):

- straight lines (SL);
- a grid (G);
- small papillary lines (ridges) disruptions (PLD);
- small “cheetah” spots (CS);
- larger round/oblong spots (ROS);
- large irregular spots (IS) and
- dark places (DP).

Table 4.2: Local features of damaged fingerprint images.

Disease	Percentages of particular features [%]							Sum
	SL	G	PLD	CS	ROS	IS	DP	
Fingertip eczema	72.03	24.65	15.91	12.24	32.34	16.61	15.73	572
Psoriasis	40.37	6.42	2.75	12.84	48.17	32.57	62.84	218
Dyshidrotic eczema	63.11	7.38	14.75	18.03	78.69	29.51	32.79	122
Hyperkeratotic eczema	3.92	0.00	66.67	15.69	74.51	3.92	5.88	51
Verruca vulgaris	3.17	0.00	14.29	12.70	74.60	0.00	25.40	63
Scleroderma	0.00	0.00	0.00	0.00	0.00	0.00	30.43	23
Acrodermatitis continua	14.29	0.00	0.00	85.71	60.00	14.29	65.71	35
Colagenosis	100.00	78.13	0.00	0.00	15.63	0.00	25.00	32
Raynaud's phenomenon	0.00	0.00	100.00	0.00	0.00	0.00	0.00	8
Effusion of fingers	10.00	0.00	73.33	43.33	63.33	6.67	13.33	30
Cut wound	93.75	0.00	0.00	0.00	18.75	0.00	12.50	16
Unknown disease	100.00	86.67	0.00	0.00	76.67	30.00	73.33	30

The other five are global image patterns (see Table 4.3):

- blurriness of (parts of) the image (B);
- a significantly high contrast of the image (HC);
- the entire fingerprint area affected (EA);
- total deformation of the fingerprint image (TD) and
- a significantly high quality and healthy fingerprint (HQ).

Table 4.3: Global features of damaged fingerprint images.

Disease	Percentages of particular features [%]					Sum
	B	HC	EA	TD	HQ	
Fingertip eczema	18.01	21.50	40.38	36.36	29.02	572
Psoriasis	34.86	27.06	61.93	58.72	18.35	218
Dyshidrotic eczema	30.33	30.33	31.97	29.51	9.84	122
Hyperkeratotic eczema	31.37	29.41	9.80	0.00	37.25	51
Verruca vulgaris	19.05	80.95	7.94	7.94	76.19	63
Scleroderma	0.00	0.00	0.00	0.00	100.00	23
Acrodermatitis continua	48.57	25.71	100.00	100.00	0.00	35
Colagenosis	9.38	40.63	0.00	0.00	25.00	32
Raynaud's phenomenon	0.00	0.00	0.00	0.00	100.00	8
Effusion of fingers	23.33	16.67	40.00	16.67	3.33	30
Cut wound	37.50	68.75	0.00	0.00	50.00	16
Unknown disease	30.00	20.00	90.00	83.33	0.00	30

Local and global features for every disease and the proportion of the diseased images recognized by these features in the dataset are counted and shown in Tables 4.2 and 4.3.

The dataset's most common and typical diseases are light atopic eczema, advanced atopic eczema, verruca vulgaris, psoriasis, and cut wound. The cut wound does not belong to dermatologic diseases; it is related to them because it can negatively affect the fingerprint recognition process. In the following text, several samples of acquired fingerprints are presented, followed by a detailed description of the influence of the disease on the fingerprints.

Fingertip eczema [34]: is a very dry, inflammatory, non-infectious disease which occurs on the palmar surface or the fingertips. The skin becomes cracked and scaly and usually starts peeling off, which results in an exposition of red and tender skin surfaces, see Figure 4.3 for an example of fingertip eczema.



Figure 4.3: Example of fingertip light atopic eczema.

As the number of fingerprints with fingertip eczema in the database is large, a wide range of typical features was observed. There are two groups of these fingerprints: (i) less and (ii) more severely damaged. In the first group of fingerprints, thin lines of different directions are typical. These lines often connect or cross each other. In some cases, small round white spots are present; in others, occasional dark areas make the ridges partially unreadable. However, ridges of fingerprints of the first group are generally very well readable, and it is possible to remove the influence of the disease from the fingerprint.

Psoriasis [34]: is a common, chronic, inflammatory disease of the skin that is often indistinguishable from a severe form of hand eczema. It is characterized by dry and scaling plaques covered with dry scales that peel in layers, see Figure 4.4.



Figure 4.4: Example of psoriasis influence on fingerprints.

The vast majority of fingerprints affected by psoriasis are wholly damaged. Ridges are mostly unreadable. The most frequent feature is a large irregular dark spot bounded by a white border. Apart from this feature, larger dark areas or thick lines are also common, as well as round and oblong spots.

Hyperkeratotic eczema [34]: a chronic form of hand eczema characterized by the occurrence of orange and brown scales with cracks between them. Only one-third to one-half of the fingerprint area is usually affected. Sometimes, only the Ridges are multiply disrupted. In other cases, however, ridges are distorted, making their direction challenging to determine. Small to medium round spots are likely to be present, see Figure 4.5.



Figure 4.5: Hyperkeratotic eczema influence on fingerprints.

Dyshidrotic eczema [34]: also known as *pompholyx*, this disease is a variant of hand and foot dermatitis that makes skin extremely dry. Its typical features are itching vesicles and scales on the palms and sides of fingers. Fingerprint images damaged by dyshidrotic eczema are generally covered with irregular blurred shapes with no specific form. Another typical feature is a thick line. These fingerprints are divided into two groups according to the damage's severity, see Figure 4.6.

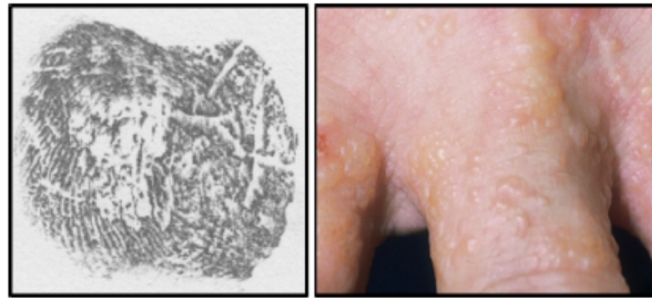


Figure 4.6: Fingerprints with dyshidrotic eczema.

In the first group of less severely affected fingerprints, the entire area of a fingerprint is often covered, but ridges remain visible. Ridges are usually disrupted at multiple places, and irregular, blurred white spots may appear. Fingerprints in the second group are seriously damaged and cannot be repaired. Thicker lines and large blurred white spots typically cover the image area. Ridges are not sufficiently visible.

Verruca vulgaris (warts) [34]: is a prevalent skin disease characterized by the presence of stiff elevated bumps on the skin surface, see Figure 4.7. They grow about 5mm in size but may reach up to more than 1cm. On their surface, tiny black dots may appear. Large widespread warts occur in immunodeficient patients as well in patients with atopic eczema. The aggressive surgical therapy may result in scarring. The lesions can affect all fingers of both hands. Typically, 1 to 4 round white spots occur, sometimes with black dots in their center.

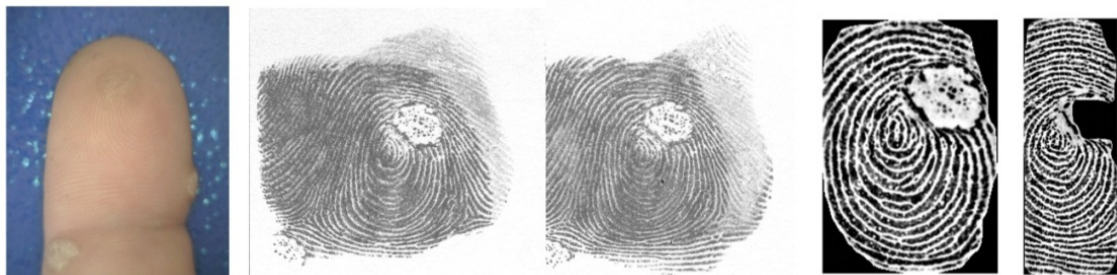


Figure 4.7: Verruca vulgaris influence on fingerprint.

Cut wounds [34]: a cut wound typically causes a straight line in a fingerprint image or a more blurred white area. The damage is minor and should not be difficult to remove. An example of cut wound on fingerprint image is shown in Figure 4.8.



Figure 4.8: Cut wound influence on fingerprint.

Based on the dataset analysis, the diseased fingerprint images were classified into five basic feature classes. Such classification is supposed to help access each type of damage individually and facilitate the detection process. For each detector of the disease, a different combination of features to detect is chosen, which helps differentiate between signs of particular diseases and correctly determine the type of disease present in the fingerprint image.

Straight lines and grids: Fingertip eczema, cut wound, collagenosis, dyshidrotic eczema, “unknown” disease. An example is shown in Figure 4.9.

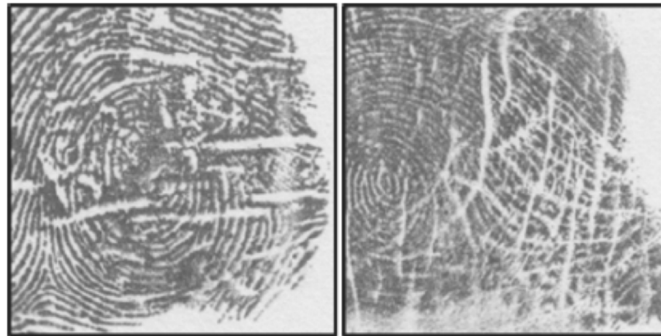


Figure 4.9: Example of fingerprint images with straight lines or grids.

Small papillary lines (ridges) disruptions: In this case, papillary lines (ridges) are disrupted at multiple places, but no significant damage is present. Representatives are: dyshidrotic eczema, hyperkeratotic eczema, effusion of fingers, and fingertip eczema, see Figure 4.10.

Small “cheetah” spots: The only representative of this group is acrodermatitis, see Figure 4.10.

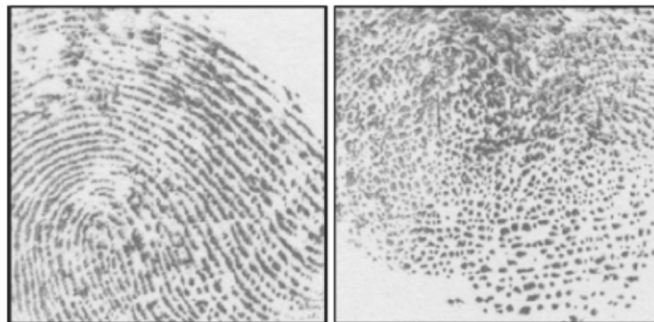


Figure 4.10: Examples of papillary lines (ridges) disruptions (left) and “cheetah” spots (right).

Round/Oblong spots: Although round or oblong spots occur in most diseases, typical representatives with a significant amount of them are: verruca vulgaris, effusion of fingers, and psoriasis. The examples of this type of disease is shown in Figure 4.11.



Figure 4.11: Example of fingerprint images with white spots in wart (left) and psoriasis (right).

Large irregular spots: Psoriasis and severe form of fingertip eczema often cause extreme damage to the fingerprint, and one of their features is also large spots of irregular shapes, see Figure 4.12.

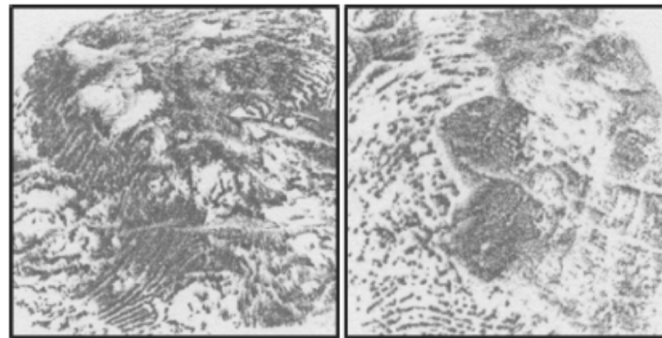


Figure 4.12: Example of fingerprint images with large irregular spots in advanced psoriasis.

4.3 Related Work

Unlike fingerprint recognition, which is very well-researched and widely understood, diseased fingerprint recognition [56, 9] is much more challenging. This section discusses the specific algorithms used in disease detection and recognition, their pros and cons, and the core methods essential for detection functionality. The work of [9] discusses the challenges of designing and implementing the detector. Three major algorithms are used for the detection: block orientation field, histogram analysis, and flood fill. Their combination provides valuable information about the fingerprint quality and character of the possible disease.

All three of these methods detect different kinds of damage in the image, and only flood fill provides logically structured results that can be used in classification [9].

Due to the need for more data on diseased fingerprints, there is more research on damaged fingerprints than on diseased ones.

The work of Feng et al. [45] considers the problem of automatic detection of alterations that result in distorted (unnatural) fingerprints. Detection of altered fingerprints based on analyzing the ridge orientation field is proposed based on decomposing the original orientation field into two components: singular and continuous. The continuous orientation field of the original fingerprint is indeed continuous (i.e., no singularity), but the continuous component of the ori-

entation field of the altered fingerprint is not continuous. The continuous orientation field of the original fingerprint is indeed continuous (i.e., no singularity), but the continuous component of the orientation field of the altered fingerprint is not continuous! The high-level features from the continuous orientation field are further extracted, and an SVM is used to classify a fingerprint as natural or altered.

Yoon et.al [128] further refined the work of Feng. The main objective of their work is to develop a technique to automatically detect altered fingerprints, *obliteration*, *distortion*, and *imitation* based on analyzing orientation field and minutiae distribution. The work of Fattahi [42] explores a deep learning model to assist in recognizing damaged fingerprints. Obliteration, by various means such as burning, abrasion, application of solid chemicals, and skin transplantation, causes an alteration of the morphology of the fingertips' surface from an intense and damaging action on the skin cells, a *Z-cut*, a lesion in the shape of the letter Z, and a central rotation that removes a slice of the skin from a finger and plants it in a different position on the finger's tip in a rotated way were considered as damages to be recognized in fingerprint images. The paper focuses on recognizing damaged fingerprints by Convolutional Long Short-Term Memory (LSTM) [42] networks and considers the alterations that can muddle most fingerprint verification software. The proposed technique also uses a well-known orientation field algorithm to compute ridge discontinuities and direction.

4.4 Algorithm Design

In computer vision and machine learning, feature extraction refers to a primary set of data that is measured and constructs features anticipated to be non-redundant and informative, simplifying the succeeding learning process, which leads to enhanced human understanding and interpretations. Feature extraction is a dimensionality reduction technique in which a set of raw variables is reduced to adaptable groups of features for further processing keeping the original data set as it is.

Most fingerprint recognition and classification algorithms require a feature extraction stage for identifying salient features. The features extracted from fingerprint images often have a direct physical counterpart (e.g., singularities or minutiae), but sometimes they are not directly related to any physical traits (e.g., local orientation image or filter responses). Features computation may serve as an intermediate step for deriving other features. In this work, some preprocessing and enhancement steps are often performed to simplify the feature extraction task. Features are extracted from the dataset with multiple feature extraction methods to give data for the classifier. Because the main objective of this work is to detect and recognize diseases in fingerprint images, the primary function of the method is the ability to classify an image according to the specific features found during the detection process. The program recommends a disease that most likely matches the input image's characteristics and, therefore, could be related to the disease the patient might suffer from it.

Apart from the apparent main emphasis of the program, the application possesses other sub-goals that logically follow the major one:

- To extract all damaged areas from the fingerprint sample.
- To distinguish between healthy, partially damaged, and unrecoverable fingerprints.
- To visualize the whole detection process.
- To recognize the disease in a fingerprint image.

4.5 Flowchart of Methodologies

The algorithm framework is illustrated in the Figure 4.13, which is divided into three parts. The flowchart depicts a multi-stage object detection model consisting of multiple modules. The input image is subjected to preprocessing and enhancement algorithms that are customized to the specific requirements of the system. A detailed description of enhancement and preprocessing algorithms can be found in Chapter 3. The post-processed image is then passed to the next module for detecting damage and artifacts. The detectors, which have a uniform design, serve the dual purpose of identifying diseases, as well as extracting features for the subsequent classifier component. Additionally, a sequence of dilation, erosion, closing, and opening operators are employed, followed by thresholding for the detection module. The visualization step is based on the detection module. The extracted features consist of vectors generated through various detection processes, aiding the classifier in disease identification. The classifier utilizes the features extracted by the detection module to classify the fingerprint image into one of five categories based on the size, shape, and number of features: Acrodermatitis, Hyperkeratotic eczema, Psoriasis, Verruca vulgaris, or a healthy image. To establish decision rules for the classifier, a script was developed to count the number and type of detected features for each disease in the entire database. The medians and standard deviations of these numerical values were utilized to aid the classifier in making its decision.

To establish decision rules for the classifier, a script was developed to count the number and type of detected features for each disease in the entire database. If the number of detected features in an input image was less than the counted number for a specific disease, the classifier would reject the image as that disease. The medians and standard deviations of these numerical values were used to assist the classifier in making its decision. According to the normal probability distribution, it is anticipated that a vast majority of values will cluster around the median and fall within one standard deviation from it. Additionally, a considerable proportion of values will lie within two standard deviations of the median, while there will be almost no values that deviate beyond that range. These statistical properties are utilized to approximate the probability that a particular set of features is associated with a particular disease.

The calculation of damage percentage in fingerprint images is accomplished by utilizing a coherence map. By analyzing the number of regions within the fingerprint that have been damaged in comparison to the total area of the fingerprint, the percentage of damage is determined. In the context of analyzing damage in fingerprint images, the damage is quantified based on a scale from the least to the most damaged blocks. The least damaged blocks are assigned a value of 0, while the most damaged blocks are assigned a value of 1. Additionally, the background is considered in the analysis.

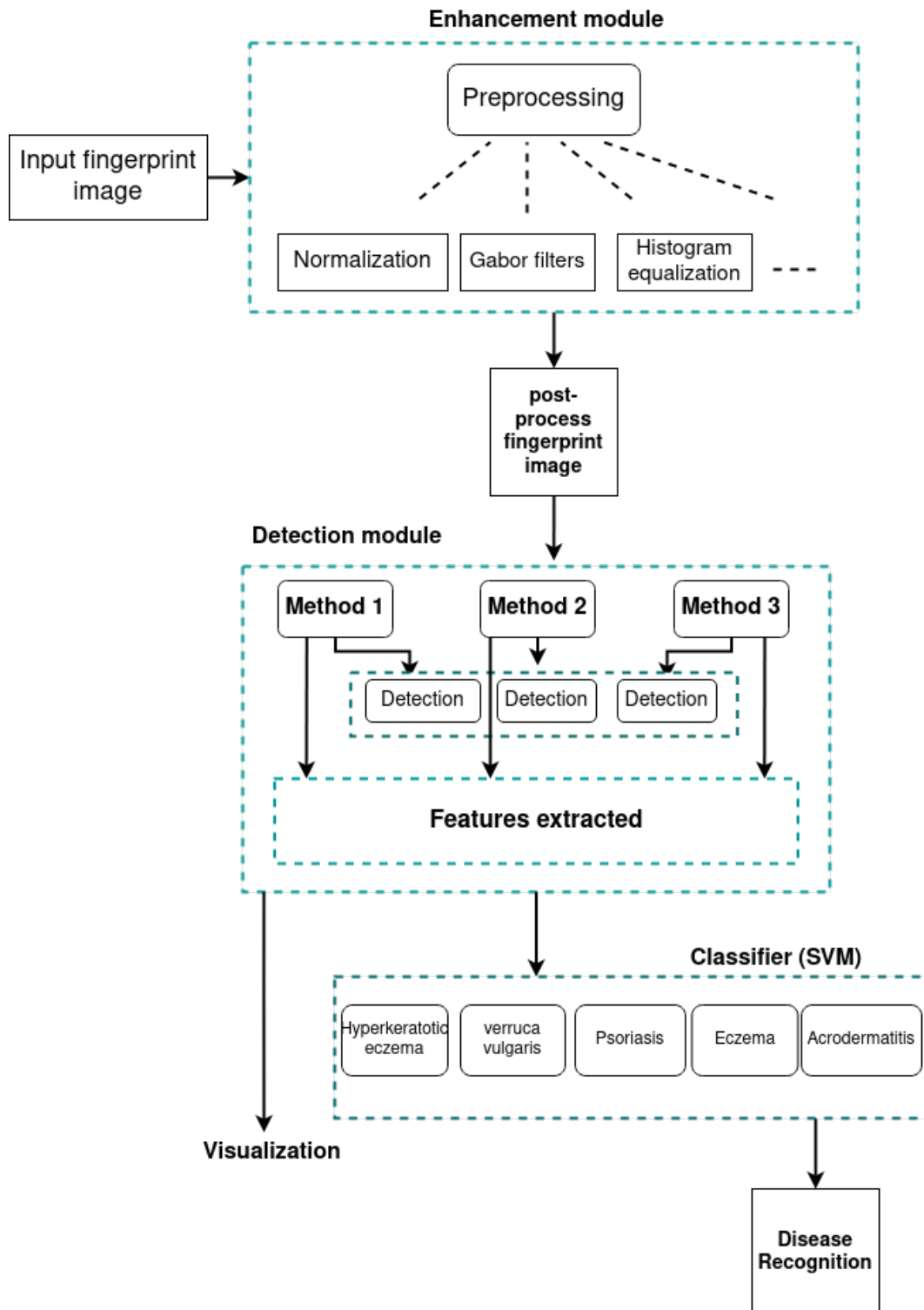


Figure 4.13: Structural design diagram of disease detection and recognition algorithms.

4.5.1 Detectors

The task of the *detector* is to extract the damaged image areas, record their properties, such as size, shape, and location, and assign their type, if possible. Since a wide range of possible types of damage could occur in a fingerprint image, the detector consists of several sub-detectors, each for a different type of damage.

- Orientatin Field Discontinuity Detector;
- Lines Detector;
- White Spots Detector;
- Papillary Lines Disruptions Detector;
- Cheetah Spots Detector.

Each of them includes a preprocessing part and a feature extraction part. The feature extraction is based on the block orientation field, LBP, and GLCM. The detector outputs a list of extracted features and their properties, which are later used in the classification process. The computation of block orientation field is commonly used in the fingerprint recognition process to estimate the ridges' direction and classify the fingerprint image into one of the several fingerprint classes. Because a typical fingerprint pattern consists of alternating dark and white lines, this information can be easily processed by a gradient operator that estimates the image gradient for each pixel. This low-level information is gathered and averaged for each $w \times w$ block in the image. For a healthy image, the transformation can result in a relatively smooth and continual image of the ridges' direction estimates.

Fingerprints are flow-like patterns that consist of locally parallel ridges and valleys. They have well-defined local frequency and local orientation. A set of bandpass filters can efficiently remove the undesired noise and preserve the accurate ridge/valley structures. The ridge extraction algorithm is applied for each image, and the corresponding ridge map is extracted from the image. An FFT is then performed on the resulting computed orientation field images to remove the noise and make the ridges smoother. Applying FFT on a set of pixels from a small image patch allows reconnection of broken ridges following the same FFT orientation. Also, the Gabor filter is performed afterward on the output of FFT image orientation for some very noisy images (see Figure 4.14).

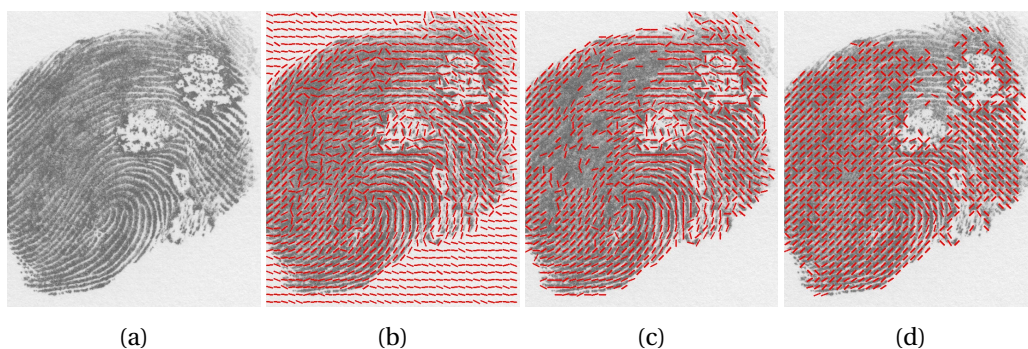


Figure 4.14: Computation of orientation field. a) Original image, b) orientation field based on a Sobel operator, c) orientation field by Fast Fourier Transform filtering, and d) orientation based on Gabor.

Since texture is a spatial property, a simple one-dimensional histogram does not help characterize texture, e.g., an image in which pixels alternate from black to white will have the same histogram as an image in which the top half is black and the bottom half is white. In order to capture the spatial dependence of gray-level values in diseased fingerprint images that contribute to the perception of texture, a two-dimensional dependence matrix known as a gray-level co-occurrence matrix is used. At the same time, the LBP is used for damage detection by analyzing the texture of the fingerprint ridges and to compare the results for the classification step. See Figures 4.15 and 4.16 for examples of LBP feature detection in diseased fingerprint images.

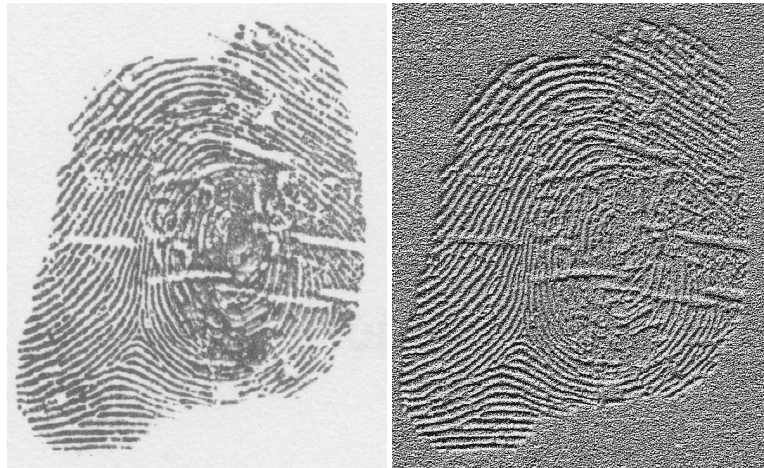


Figure 4.15: Feature detection using LBP in a fingerprint image with eczema.

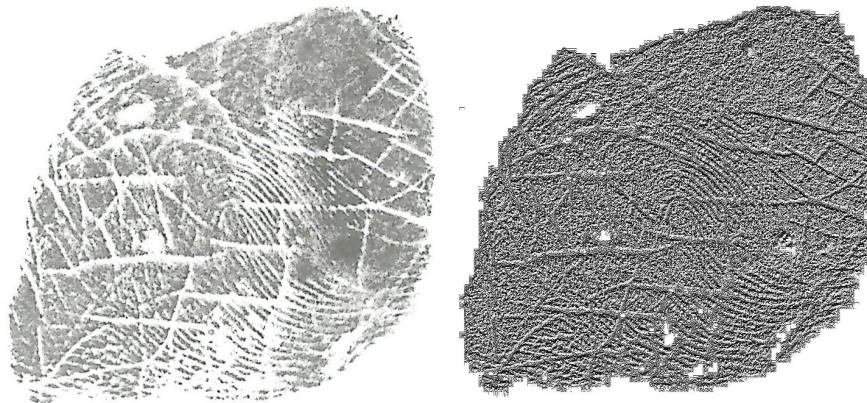


Figure 4.16: Feature detection using LBP in a fingerprint image with hyperkeratotic eczema.

The pixels in the image are represented by a feature vector that is defined based on their neighborhood. In this case, a basic LBP approach has been used, considering an 8-neighborhood. Each pixel in the image is labeled by thresholding its neighborhood, converting the results to binary numbers, and storing them in a vector. The input image is divided into cells 16×16 pixels for each cell (see Figure 4.17 for the schematic image of the definition of patch and cell in a fingerprint image).

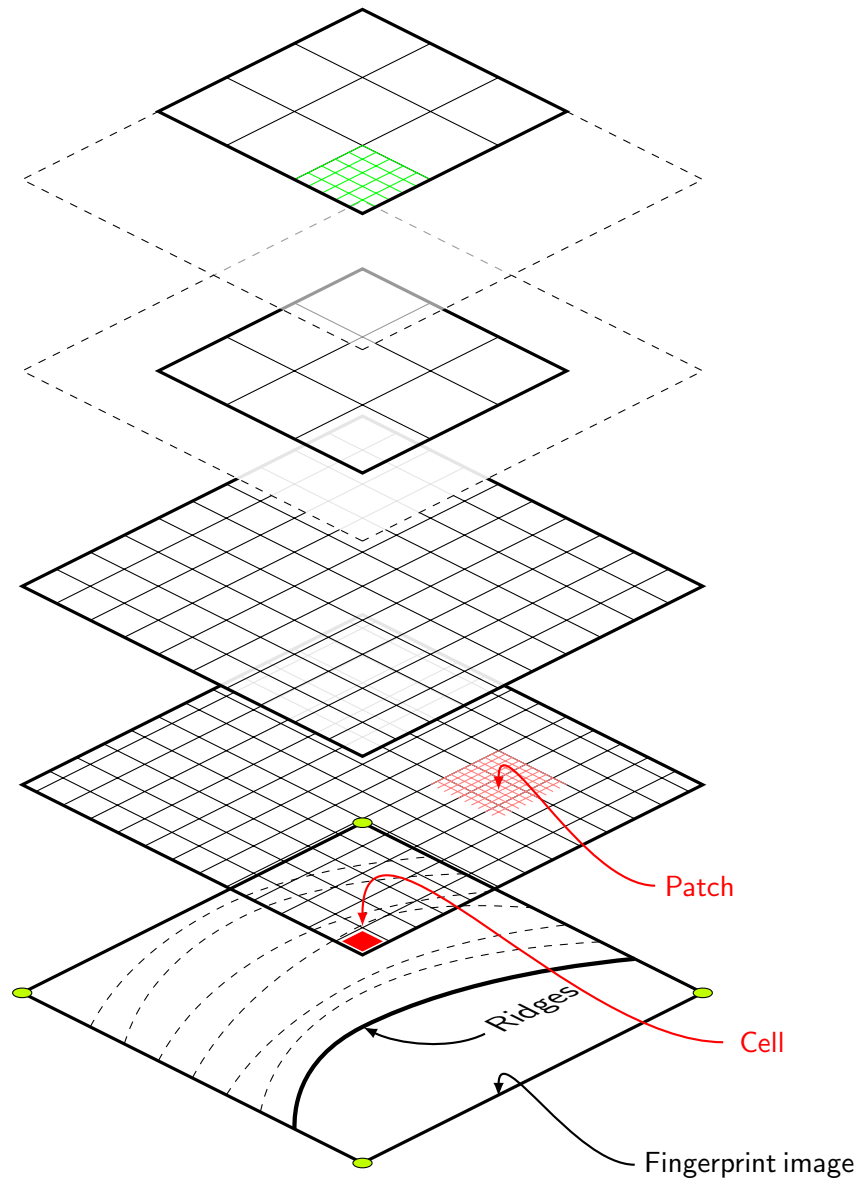


Figure 4.17: Definition of patch and cell in a fingerprint image.

The *objective patterns* are extracted in a circularly symmetric neighborhood by comparing each image pixel with its neighborhood (Algorithm 1).

Algorithm 1: Detection steps using LBP algorithm.

- 1: Convert the fingerprint image into a grayscale.
 - 2: Divide the fingerprint image into small regions or blocks.
 - 3: Apply the LBP operator to each block to generate an LBP histogram.
 - 4: Concatenate the LBP histograms of all the blocks to form a feature vector.
-

The LBP operator compares the intensity of pixels (see Figures 4.18 and 4.19 with less and more severe damage, respectively) in a small neighborhood around a central pixel and

encodes the result into a binary pattern. The resulting binary patterns can be used to identify the texture of the fingerprint ridges.

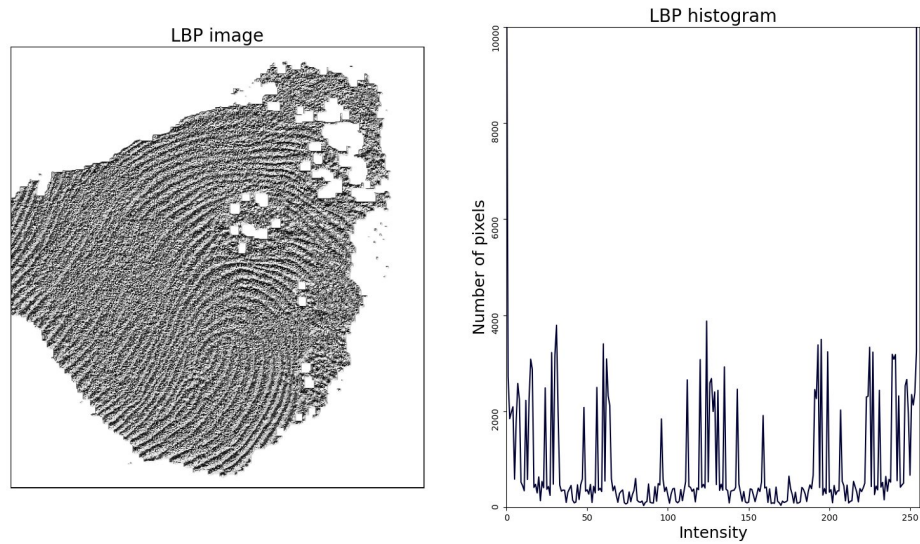


Figure 4.18: LBP intensity computation on a fingerprint affected by verruca vulgaris.

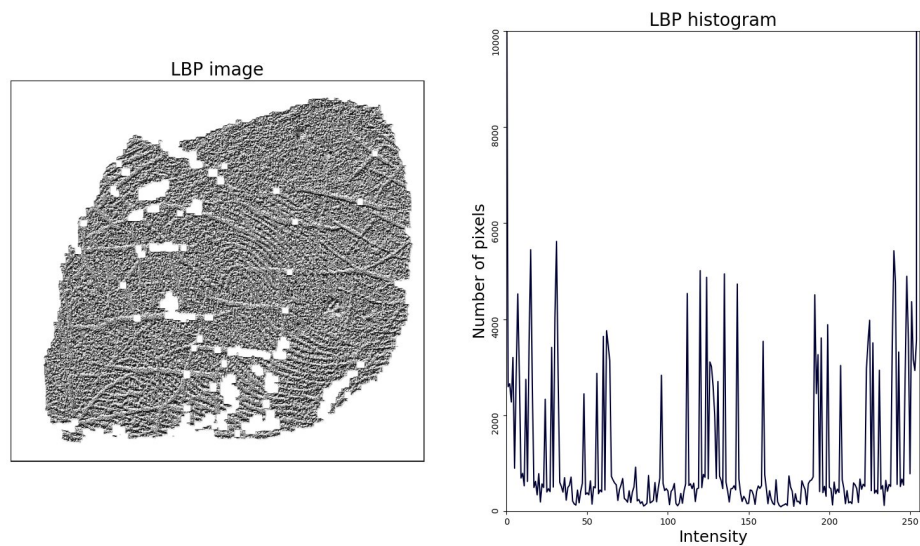


Figure 4.19: LBP intensity computation on a fingerprint affected by hyperkeratotic eczema.

In a diseased fingerprint, the ridges' texture is distorted, resulting in a different LBP histogram than a typical fingerprint. By analyzing the LBP histograms of different blocks of the fingerprint image, it is possible to identify the damaged regions of the fingerprint, see Figure 4.20.

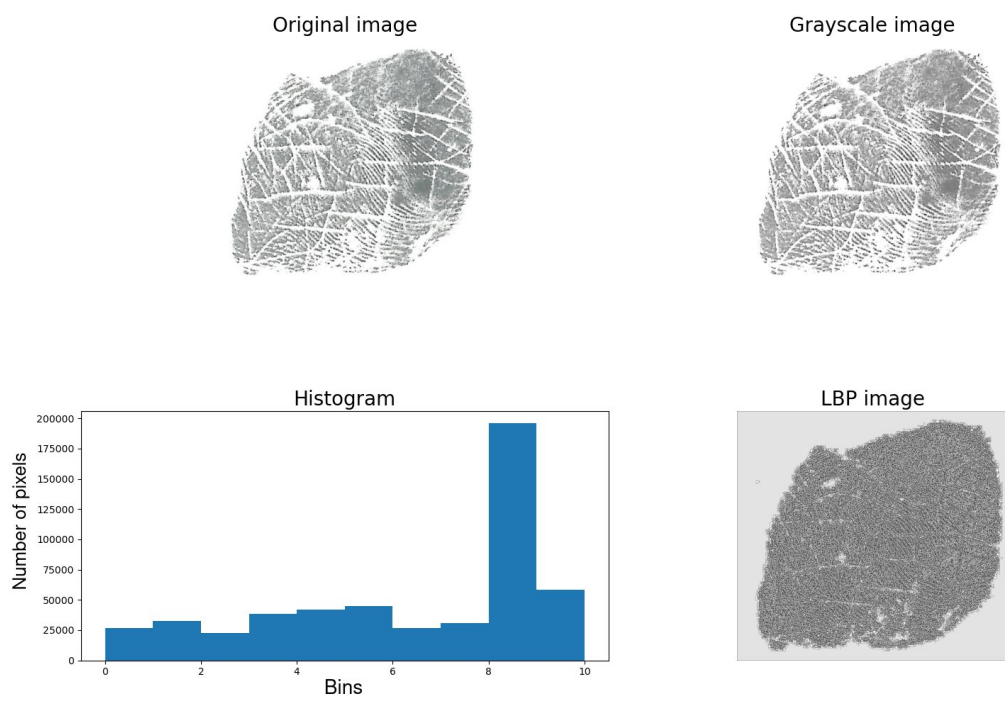
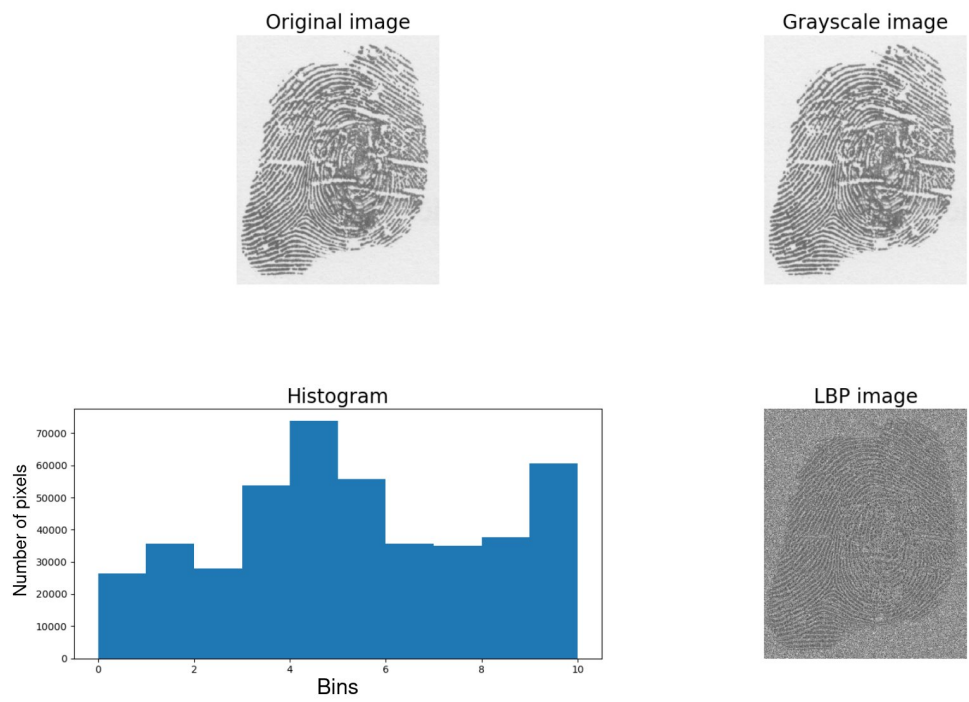


Figure 4.20: Visual steps of an LBP algorithm applied on a diseased fingerprint images with minor (top) and serious damage (bottom).

GLCM is another algorithm to detect damage in fingerprint images. By analyzing the statistical properties of the image texture, specifically by calculating the occurrence of pairs of pixel intensity values at a given distance and direction. The GLCM as it is defined in Subsection 3.2.6 and is based on the estimation of the second-order joint conditional probability density functions, $P(i, j, d, a)$. A distance pair, the offset between the center and its neighboring pixel, is computed regarding their spatial distance and relative gray level values.

Multiple GLCMs is computed for various offsets, which determine the relationships between pixels in different directions and distances, Tables 4.4, 4.5, 4.6, 4.7, 4.8 and 4.9 represent the GLCM values for a particular set of features in different direction for some images with eczema in the dataset. The spatial relationships of pixels with defined offsets for different angles, such as 0° , 45° , 90° , and 135° , and a fixed distance that is any integer between 1 and the image size. Although other angles such as 180° , 225° , 270° , and 315° computed, they would produce the same results. Therefore, only the four angles mentioned earlier are considered.

Table 4.4: Computed dissimilarity values in different directions of images with eczema.

Image	Dissimilarity 0°	Dissimilarity 45°	Dissimilarity 90°	Dissimilarity 135°
1	14.365565	14.464557	14.130311	14.652256
2	17.370465	16.398673	16.766219	17.788139
3	18.105816	18.322853	17.198894	18.684004
4	11.005523	10.951884	10.471292	10.777871
5	22.259734	24.432881	23.669832	24.518891

Table 4.5: Computed correlation values in different directions of images with eczema.

Image	Correlation 0°	Correlation 45°	Correlation 90°	Correlation 135°
1	0.558776	0.560176	0.575717	0.552342
2	0.443192	0.493385	0.484862	0.434934
3	0.855047	0.850790	0.869555	0.847417
4	0.505797	0.517556	0.555226	0.538482
5	0.733247	0.686855	0.703133	0.683913

Table 4.6: Computed homogeneity values in different directions of images with eczema.

Image	Homogeneity 0°	Homogeneity 45°	Homogeneity 90°	Homogeneity 135°
1	0.713150	0.710478	0.712945	0.710171
2	0.714464	0.712702	0.714613	0.711649
3	0.102358	0.099776	0.101683	0.097518
4	0.779748	0.777912	0.780307	0.777981
5	0.100327	0.093590	0.094579	0.092414

Table 4.7: Computed contrast values in different directions of images with eczema.

Image	Contrast 0°	Contrast 45°	Contrast 90°	Contrast 135°
1	1260.692430	1259.489659	1210.702496	1281.924315
2	1797.882365	1639.514972	1661.005529	1828.673681
3	741.170350	760.166644	665.129211	777.354575
4	993.690016	972.713892	893.396349	930.522593
5	1119.434099	1314.729731	1246.207535	1327.092575

Table 4.8: Computed ASM values in different directions of images with eczema.

Image	ASM 0°	ASM 45°	ASM 90°	ASM 135°
1	0.489223	0.486578	0.489715	0.486498
2	0.493735	0.491079	0.494315	0.491102
3	0.000541	0.000518	0.000528	0.000512
4	0.590625	0.588803	0.591762	0.588255
5	0.000591	0.000569	0.000590	0.000566

Table 4.9: Computed Energy values in different directions of images with eczema.

Image	Energy 0°	Energy 45°	Energy 90°	Energy 135°
1	0.699445	0.697552	0.699796	0.697494
2	0.702663	0.700770	0.703075	0.700787
3	0.023252	0.022756	0.022982	0.022634
4	0.768521	0.767335	0.769260	0.766978
5	0.024306	0.023853	0.024298	0.023785

Then different combinations of the occurrence of gray-level pairs in an image based on the distance and orientation between the pixels are estimated. The distance pair in GLCM helps for detection by capturing the spatial relationships between neighboring pixels in an image and providing a measure of the texture or pattern of the image. Analyzing the texture features extracted from GLCM computed at different distance pairs and orientations makes it possible to identify the most informative features and use them for detection and classification tasks.

By varying the distance pair and other parameters in the GLCM computation, it is possible to extract different texture features in damage detection in the fingerprint image. When detecting damage in fingerprint images, a GLCM is computed using a specific distance pair and orientation, such as a horizontal offset of 1 pixel and a vertical offset of 0 pixels, to capture the texture information in the horizontal direction, see Figures 4.21 and 4.22.

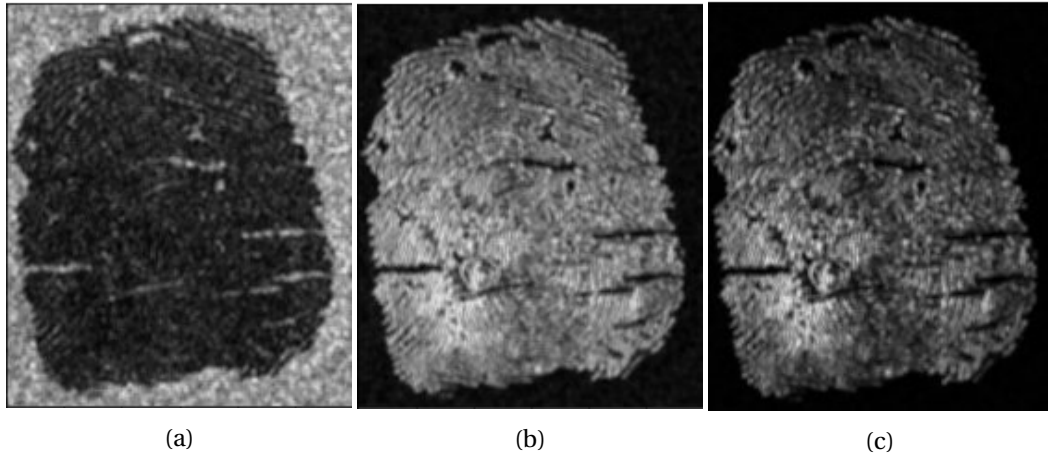


Figure 4.21: Examples of GLCM at $d = 1$ and different orientations, $\theta = 0^\circ, 45^\circ$ for (a) homogeneity, (b) dissimilarity and (c) contrast.

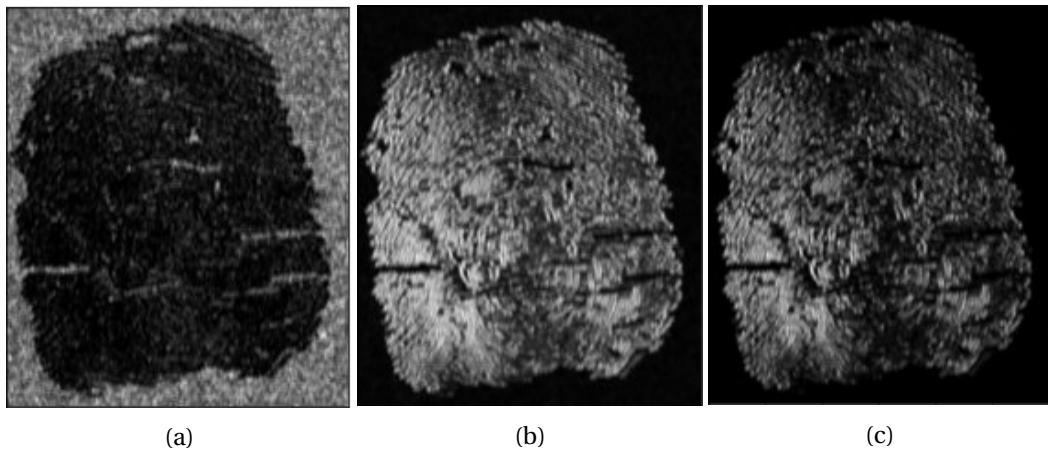


Figure 4.22: Examples of GLCM at $d = 5$ and different orientations, $\theta = 0^\circ, 45^\circ$ for (a) homogeneity, (b) dissimilarity and (c) contrast.

The resulting GLCM is then used to extract texture features such as contrast, homogeneity, and entropy, which can help to differentiate between healthy and damaged regions in the fingerprint image. The GLCM captures the spatial relationship between pixel intensity values in an image that is used to identify changes in texture caused by disease. By examining the GLCM of different blocks of the fingerprint image, it is possible to identify the damaged regions of the fingerprint. The blocks of the diseased fingerprint image are thoroughly examined, and the damaged parts are identified, see Algorithm 2 steps.

Algorithm 2: Detection steps using GLCM algorithm.

- 1: Convert the fingerprint image into a grayscale.
 - 2: Divide the fingerprint image into blocks.
 - 3: Calculate the GLCM for each block by counting the occurrence of pairs of pixel intensity values at a given distance and direction.
 - 4: Compute statistical features from the GLCM, such as homogeneity, contrast, dissimilarity, entropy and auto correlation.
 - 5: Concatenate the statistical features of all the blocks to form a feature vector.
-

The sorting process of HL and LH wavelet features in each level is considered an essential operation, which in turn increases the performance of the detection process because HL features represent the horizontal details of the transformed image while LH features represent the vertical details of the transformed image. Also the HH features, which contain information about the diagonal details, are eliminated since they did not provide accurate feature detection. Combining GLCM feature extraction with wavelet decomposition is another powerful method to image damage detection in diseased fingerprint images. The wavelet decomposition separates an image into different frequency bands. Several texture features of GLCM are applied on each frequency band to extract texture features. The high-frequency coefficients from the decomposed image are extracted, and a GLCM analysis is applied to each frequency band to extract texture features. The texture features extracted from different frequency bands are combined to obtain a comprehensive feature vector for each image.

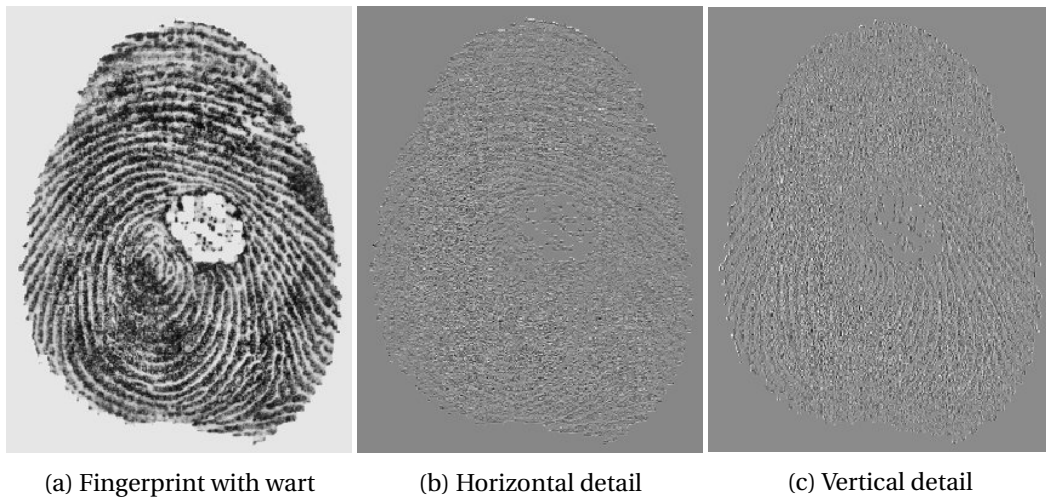


Figure 4.23: Features detection by applying approximation coefficients for a diseased fingerprint image with 2-level wavelet decomposition.

The morphological filters, such as dilation and erosion, are applied to connect or remove small groups of pixels, hence enhancing the detection method's structural details. Also, closing and opening are applied to remove small noisy regions and fill gaps to smooth out the overall shape of damage in the diseased fingerprint image. Figure 4.24 shows the morphological operations for detection and connecting pixels in a fingerprint image to improve the accuracy and robustness of detection algorithms.

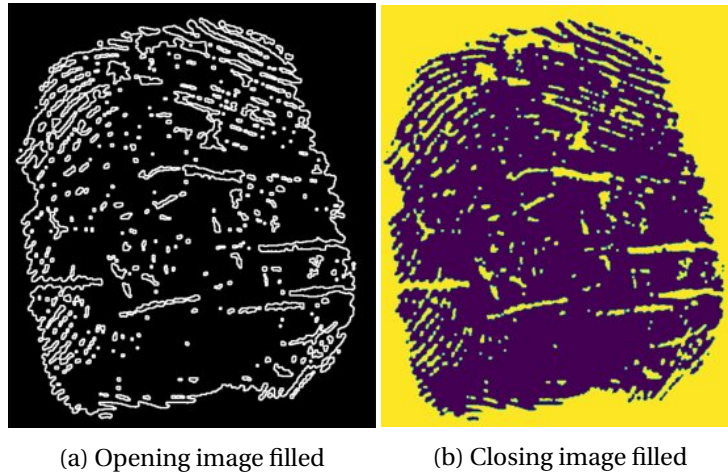


Figure 4.24: Example of applying morphological processing on a diseased fingerprint image.

Coherence is applied to measure the linear correlation between two signals at different spatial locations or frequencies and to investigate how each pixel block behaves regarding its gradient value concerning fingerprint ridge flows, indicating healthy and unhealthy patches in a diseased fingerprint image defined in Subsection 3.3.2 and Equation 3.28. In the context of damage indications in diseased fingerprint images, coherence analysis can identify regions of an image affected by damage, as these regions exhibit changes in coherence compared to entire regions, see Figure 4.25.

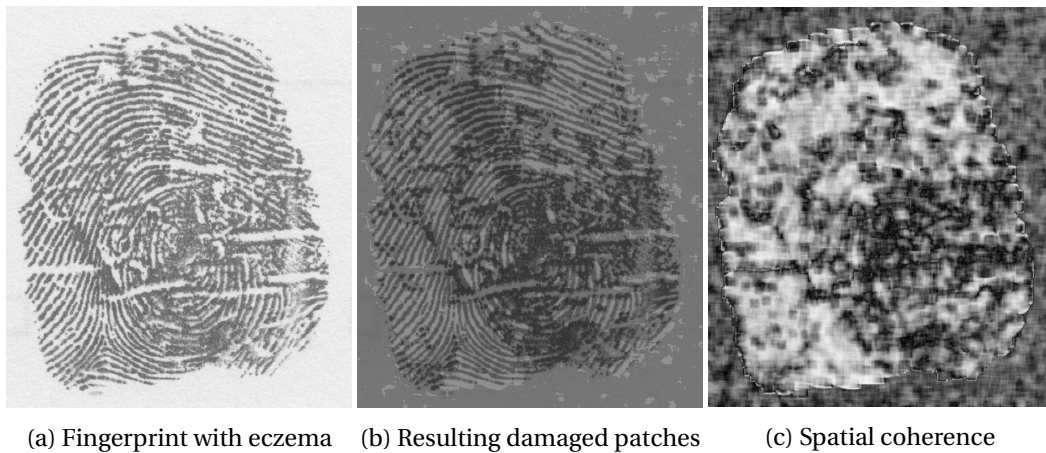


Figure 4.25: Coherence indicates the damaged parts in a diseased fingerprint image.

4.5.2 Classifier

Defining a classifier for detected features involves using machine learning algorithms to train a model to accurately classify the detected features into different classes of diseased fingerprints. The feature vectors should be normalized to ensure each feature has the same scale. This step is important for the SVM to work correctly.

As mentioned in Section 4.4, the method consists of the detectors and the classifier. Both use many smaller supporting parts of the program, for instance, algorithms for image preprocessing and normalizing the fingerprint sample.

The classifier is a single class that implements the decision rules. It requires a vector of features extracted by the detection methods and outputs the resulting disease. The detectors require a normalized fingerprint image as an input and output vector of detected features. The extracted features go into the classifier that output is the suggested disease. The classifier's classification goal depends on the number and types of disease features provided by the detector.

4.6 Implementation

The proposed methods is implemented in Python, using computer vision, image processing, OpenCV [14], and NumPy [54] libraries. Some unique data structures are used. One is NumPy, a library for the Python programming language, which adds support for large, multi-dimensional arrays and matrices, along with an extensive collection of high-level mathematical functions to operate on these arrays.

A data structure is used to visualize the extent of damage in the fingerprint. It consists of an $n \times m$ matrix that indicates the number of columns and the number of rows, respectively. It is essential to consider that n and m are always smaller than the width and height of the input image so that the visualization can capture the global extent of damage in $w \times w$ sub-regions of the image; the values of this matrix range from -1 and 1 . In this representation, negative values are used to indicate the background, while zero represents a healthy area and positive values are indicative of damage.

$$Q = \begin{cases} \textit{background} & \text{if Coh} \in \langle -1, 0 \rangle \\ \textit{healthy} & \text{if Coh} = 0 \\ \textit{damaged} & \text{if Coh} \in (0, 1) \end{cases} \quad (4.1)$$

In this section, the specific algorithms used for detection will be discussed. The challenge involved combining three output matrices to form a data structure that provides an overview of the damage state for every block of pixels with dimensions $w \times w$. All pixel values from the three methods were constrained to non-negative to ensure proper merging. Information about the background was extracted using the background extractor method, which marks pixels as either -1 (background) or 1 (fingerprint area) and generates a fourth matrix with pixel values. Another crucial data structure for storing disease indicators extracted from the image includes a feature type (if it is a diseased/damaged pixel), location of the first pixel, size, and particular pixels belonging to that specific area. This structure serves the purpose of visualizing localization results, see Figure 4.26.

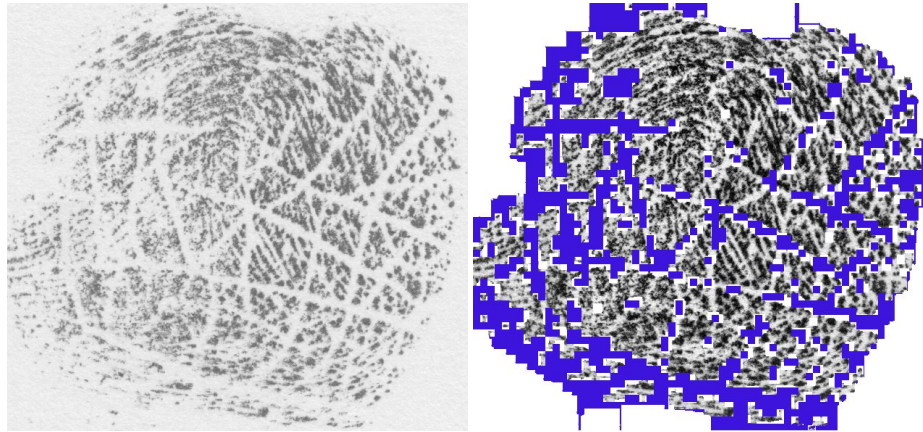


Figure 4.26: Localization of a diseased fingerprint image affected by hyperkeratotic eczema.

The preprocessing steps include contrast and brightness adjustment, dilations, erosions, closing and opening operators, fingerprint area detection, Gaussian blur, thresholding and foreground-background separation. The first step of background subtraction are analyzed using Algorithm 3.

Algorithm 3: Background separation algorithm.

- 1: Get the height and width of the image.
 - 2: Create a data structure to hold a zero mask.
 - 3: Define a rectangular region using a tuple to represent the top-left corner and bottom-right corner coordinates of the rectangle.
 - 4: Extract the object using the defined rectangle.
 - 5: Set the mask values to either 0 or 1.
 - 6: Multiply the mask with the input image and save it as a new image with the new axis.
 - 7: Get the difference between the input image and the mask image.
 - 8: Change all non-black pixels in the background to white.
 - 9: Add the background and the image using $\text{final} = \text{background} + \text{new image}$.
 - 10: Smoothen the edges.
-

The major algorithms for detecting diseases in fingerprint images are block orientation field, GLCM, and LBP. The different features extracted from these algorithms and their combination provide valuable information about the disease in fingerprint detection and recognition. The orientation field algorithm has a significant advantage over the other algorithms, a fingerprint recognition benchmark that provides a relatively accurate estimate of the fingerprint damage in the sample. However, it is not always able to detect local damages, such as spots or lines. A combination of algorithms and morphological operations is used to solve this problem. Sometimes, the method detects single discontinuities that may be erroneous, but on the other hand (under different circumstances), one unmarked block may appear amid discontinuous blocks. In order to make the algorithm as accurate as possible, although mistakes never disappear entirely, these cases are taken into account. The algorithm handles them by copying the properties of their neighboring blocks (marking the single ones as all right or as a discontinuity, depending on the neighborhood). The resulting block orientation field is analyzed using the Algorithm 4 to detect any possible discontinuities. The analysis uses a row-wise and column-wise scanning approach that reveals areas of possible damage in the fingerprint, see Figure 4.27.

Algorithm 4: Detection based on orientation computation for discontinuities.

- 1: Compute the block orientation field for every $w \times w$ block of pixels using the Equations 3.4, 3.5, and 3.6.
 - 2: Row-wise and column-wise approach to detect possible damage.
 - 3: **if** $pixel == -1$ **then**
 - 4: assign it as a background.
 - 5: **end if**
 - 6: Compare neighboring blocks' directions.
 - 7: **if** $|\theta(i, j) - \theta(i, j + 1)| > 45^\circ$ **then**
 - 8: mark block as a discontinuity.
 - 9: **end if**
-

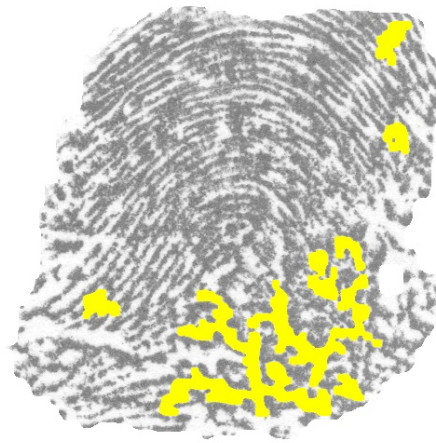


Figure 4.27: Detection of cut wound damage using block orientation field method.

The strenuous step is to detect large white spots, thick white lines, small “cheetah” spots, and papillary lines (ridges) disruptions that are managed by using morphological functions combined with connecting components and thresholding. The strenuous step is to detect large white spots, thick white lines, small “cheetah” spots, and papillary lines (ridges) disruptions that are managed by using morphological functions combined with connecting components and thresholding. It extracts damages, such as the absence of ridge lines and discoloration, based on the thresholding level, in the form of a binary map, see Figures 4.28, 4.29 and 4.30.



(a) Input image

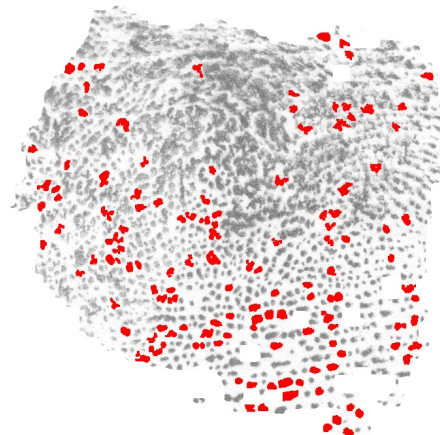


(b) White spots detection.

Figure 4.28: Intermediate steps of detecting white spots.



(a) Input image



(b) Cheetah spots detection.

Figure 4.29: Intermediate steps of detecting small cheetah spots.

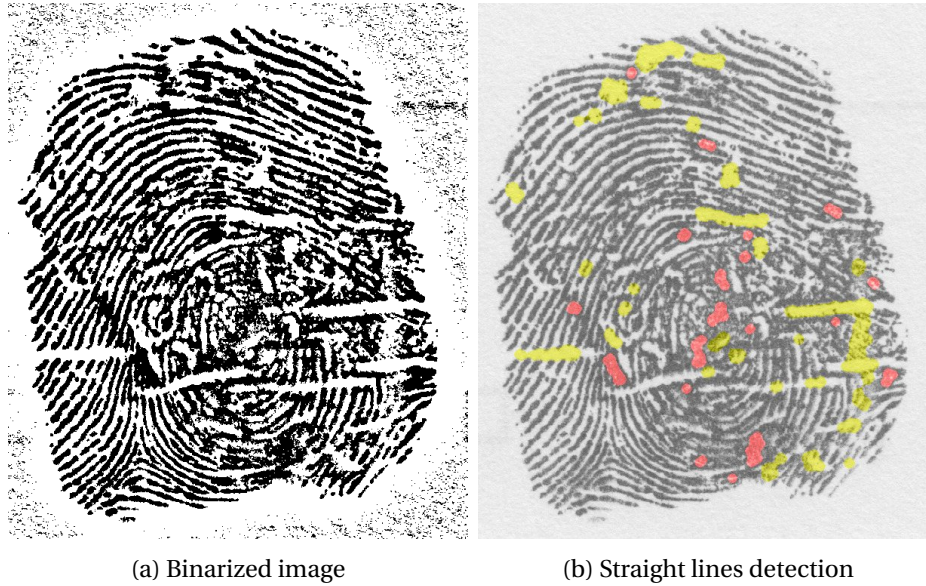


Figure 4.30: White lines extraction.

All the methods mentioned above detect different kinds of damage in the image. At the end, it is necessary to apply a machine learning classifier to the feature vector to determine whether the fingerprint is damaged. The classifier decides based on features extracted by the GLCM for several specific distance and orientation parameters, LBP and morphological features algorithms and classifies the fingerprint image, according to the features' numbers and shapes, into one of these seven categories: eczema, hyperkeratotic eczema, psoriasis, verruca vulgaris, acrodermatitis, unknown disease or healthy.

In reference to the SVM model, it should be noted that 804 fingerprint images from the database were utilized. The accuracy metrics for the classifier were determined based on the detection results. These metrics comprise the False Accept Rate (FAR) and False Reject Rate (FRR), as well as accuracy and F1 score, which are listed in Table 4.10.

Table 4.10: Classifier accuracy.

	FAR	FRR	F1-score	ACC
Eczema	0.17	0.62	0.39	0.61
Hyperkeratotic eczema	0.15	0.56	0.33	0.69
Acrodermatitis	0.11	0.50	0.11	0.89
Psoriasis	0.26	0.57	0.18	0.71
Verruca vulgaris	0.12	0.31	0.10	0.86

Additionally, the ROC curves in Image 4.31 depict the performance of the classifier across different operating points. In a binary classification task, it displays the trade-off between sensitivity (true positive rate) and specificity (true negative rate) as the discrimination threshold is varied. The classifier produces a score for each instance, which is then used to make a binary decision: classifying the instance as either positive or negative.

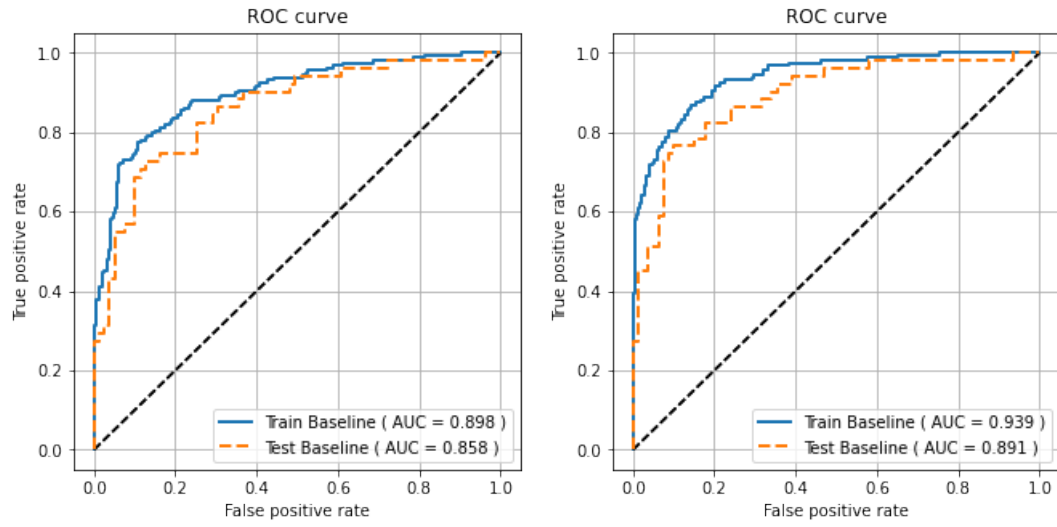


Figure 4.31: ROC curves for diseased fingerprint recognition performance.

Chapter 5

Conclusions

The main focus of this dissertation was to conduct a comprehensive analysis of fingerprint images affected by skin diseases, with the aim of identifying the infected regions and categorizing them into distinct classes based on their features. As a result, the thesis achieved the successful classification of diseased fingerprint images based on their unique characteristics.

Specifically, the thesis addressed the challenge of detecting skin diseases from fingerprint images by designing and developing methods to locate the damaged areas in the fingerprint image and determine the specific type of disease present based on its distinctive characteristics. The objective was successfully achieved, and a classifier was developed for several types of skin diseases, including eczema, hyperkeratotic eczema, acrodermatitis, psoriasis, and verruca vulgaris.

Additionally, the dissertation estimated three distinct regions of interest for digital fingerprint images. The first category includes a well-defined region where ridges and valleys can be easily differentiated. The second category included a recoverable corrupted region with scars, smudges, and other forms of damage to ridges and valleys. However, they can still be discerned, and neighboring regions can provide adequate information. Lastly, the third category was an unrecoverable corrupted region where the ridges and valleys were severely damaged, so the ridge structure could not be clearly seen, and neighboring regions needed to provide more information. To summarize, the main contributions of the work presented in this thesis are:

New method for detecting disease in fingerprint images: A novel approach for detecting diseases in fingerprint images was developed, which involved defining the scope of damages and determining the types of damages that needed to be detected. Several methods were explored in both the spatial and frequency domains to enhance the quality of fingerprint images. Specifically, the orientation image, which is a matrix representing the local ridge orientation, was used in combination with local binary patterns and grey-level co-occurrence matrices to detect diseases in fingerprint images. Additionally, frequency domain approaches such as the FFT were also considered.

Damage localization in diseased fingerprint images: to identify specific areas in diseased fingerprint images affected by damage or disease, various features and characteristics, such as ridges, valleys, and minutiae, were analyzed to detect any abnormalities or deviations from the typical pattern. The ultimate goal was to accurately locate and isolate damaged areas for further analysis and classification based on the type of damage or disease present. Computer vision algorithms, including image segmentation, feature extraction, and classification techniques, were utilized to achieve this goal. GLCM, LBP, and block orientation field were the most significant algorithms in this work. Additionally, intermediate steps such as morphological approaches to

detect white lines and round oblong white spots were employed to improve the accuracy of the detection process. In addition to the previously mentioned methods, the application of background subtraction and masking of the entire background proved useful in locating diseases in fingerprint images. This was achieved by assigning negative values to the background pixels at the end of the detection process.

Classification and disease recognition: to identify diseases in fingerprint images based on their symptoms or other relevant features which was done using SVM. Features were categorized and labeled based on GLCM, LBP features, and morphological operations. The SVM algorithm was trained on a labeled dataset that helped it distinguish between different types of diseases in fingerprint images based on their unique features, including LBP, GLCM, and orientation field features. These features were first extracted from the images and used to train the SVM classifier on a labeled dataset.

Each detection method mentioned above separately provided interesting outputs, but their connection made the result noticeable. The techniques explored and presented in this thesis lay a strong groundwork for future investigations and hold significant potential for further expansion to address real-world use cases. Detecting skin diseases using image recognition algorithms is a challenging task, especially considering the novelty and uniqueness of this project, which means there currently needs to be established methods for detection.

5.1 Future Work

The method has the potential for enhancement in several areas, including:

Damage removal: the methods used in this work could be applied to develop a program that automatically removes damaged areas in fingerprints, leaving only the healthy regions.

Damaged fingerprint reconstruction: in some cases, it may be possible to repair damaged areas, such as by connecting disrupted ridges caused by minor eczema or cut wound in the skin.

Signal processing algorithms: overall, computing ridges and valleys in diseased fingerprint images is important in analyzing fingerprint images for disease detection and classification.

Image processing methods: the challenging task is to detect straight lines affected by cut wounds or eczema; one approach is to use the inpainting method combined with the Gabor filter and the set of morphological operators.

Optimization: the damage localization algorithms could be optimized for faster processing.

Generating realistic synthetic diseased fingerprint: as there is currently a shortage of datasets containing diseased fingerprints, creating synthetic diseased fingerprints may aid in utilizing deep learning techniques for analysis.

Machine Learning (ML) algorithms are also investigated, and efficient methods are proposed using the Attention-Based Recurrent Neural Network approach, a deep learning model to detect diseases in fingerprint images. A new technique is proposed based on a Recurrent Neural Network (RNN) to locate infected regions and extract relevant disease classification features automatically.

A new sequential image classification model is proposed to detect diseases by combining RNN and Convolutional Neural Network (CNN) inspired by the previous works, a combination of an RNN attention mechanism with Long Short-Term Memory (LSTM) is developed to dynamically push salient fingerprint disease characteristics to the forefront to strengthen the model in identifying disease characteristics.

Bibliography

- [1] *NFIQ 2.0, National Institute of Standards and Technology. NIST.* Accessed: 2022-December-8. Available at: <https://www.nist.gov/services-resources/software/nfiq-2>.
- [2] *ISO: Text of standing document 11 (sd 11), part 1 overview standards harmonization document.* Standard, International Organization for Standardization, August 2010.
- [3] AHMAD, J., FARMAN, H. and JAN, Z. Deep Learning Methods and Applications. In: *Deep Learning: Convergence to Big Data Analytics*. Singapore: Springer Singapore, 2019, p. 31–42. Available at: https://doi.org/10.1007/978-981-13-3459-7_3. ISBN 978-981-13-3459-7.
- [4] AHONEN, T., HADID, A. and PIETIKAINEN, M. Face Description with Local Binary Patterns: Application to Face Recognition. *IEEE Transactions on Pattern Analysis and Machine Intelligence*. 2006, vol. 28, no. 12, p. 2037–2041.
- [5] ALONSO-FERNANDEZ, F., FIERREZ, J., ORTEGA-GARCIA, J., GONZALEZ-RODRIGUEZ, J., FRONTHALER, H. et al. A Comparative Study of Fingerprint Image-Quality Estimation Methods. *IEEE Transactions on Information Forensics and Security*. 2007, vol. 2, no. 4, p. 734–743.
- [6] ALPAYDIN, E. *Machine learning: the new AI*. MIT press, 2016.
- [7] ASHBAUGH, D. R. Quantitative-Qualitative Friction Ridge Analysis: An Introduction to Basic and Advanced Ridgeology. In: . 1999.
- [8] AVIV, A. J., GIBSON, K., MOSSOP, E., BLAZE, M. and SMITH, J. M. Smudge Attacks on Smartphone Touch Screens. In: *Proceedings of the 4th USENIX Conference on Offensive Technologies*. USA: USENIX Association, 2010, p. 1–7. WOOT'10.
- [9] BAROTOVA, S. Detector of skin diseases by fingerprint technology. Bachelor's thesis FIT BUT. 2017, p. 50.
- [10] BAZEN, A. and GEREZ, S. Segmentation of fingerprint images. December 2001, vol. 12.
- [11] BAZEN, A. M. and GEREZ, S. H. Fingerprint matching by thin-plate spline modelling of elastic deformations. *Pattern Recognition*. 2003, vol. 36, no. 8, p. 1859–1867. Available at: <https://www.sciencedirect.com/science/article/pii/S0031320303000360>. ISSN 0031-3203.
- [12] BOVIK, A. C. Chapter 4 - Basic Binary Image Processing. In: BOVIK, A., ed. *The Essential Guide to Image Processing*. Boston: Academic Press, 2009, p. 69–96. Available at: <https://www.sciencedirect.com/science/article/pii/B9780123744579000044>. ISBN 978-0-12-374457-9.

- [13] BOVIK, A. C., CLARK, M. and GEISLER, W. S. Multichannel texture analysis using localized spatial filters. *IEEE transactions on pattern analysis and machine intelligence*. IEEE. 1990, vol. 12, no. 1, p. 55–73.
- [14] BRADSKI, G. The OpenCV Library. *Dr. Dobb's Journal of Software Tools*. 2000.
- [15] BREIMAN, L. Random forests. *Machine learning*. Springer. 2001, vol. 45, no. 1, p. 5–32.
- [16] BRICE, L. L. A HISTORY OF ROME - T.R. Martin Ancient Rome. From Romulus to Justinian. Pp xii 237, ills, maps. New Haven and London: Yale University Press, 2012. Cased, US\$35(Paper, US\$16). ISBN 978-0-300-16004-8 (978-0-300-19831-7 pbk). *The Classical Review*. Cambridge University Press. 2015, vol. 65, no. 2, p. 519–520.
- [17] BUSCH, C. Standards for biometric presentation attack detection. In: *Handbook of Biometric Anti-Spoofing*. Springer, 2019, p. 503–514. ISBN 978-981-19-5288-3.
- [18] CASTELLANO, G., BONILHA, L., LI, L. and CENDES, F. Texture analysis of medical images. *Clinical Radiology*. 2004, vol. 59, no. 12, p. 1061–1069. Available at: <https://www.sciencedirect.com/science/article/pii/S000992600400265X>. ISSN 0009-9260.
- [19] CERVANTES, J., GARCIA LAMONT, F., RODRÍGUEZ MAZAHUA, L. and LOPEZ, A. A comprehensive survey on support vector machine classification: Applications, challenges and trends. *Neurocomputing*. Elsevier. 2020, vol. 408, p. 189–215.
- [20] CHAI, Y., LEMPITSKY, V. and ZISSERMAN, A. BiCoS: A Bi-level co-segmentation method for image classification. In: *2011 International Conference on Computer Vision*. 2011, p. 2579–2586.
- [21] CHANDOLA, V., BANERJEE, A. and KUMAR, V. Anomaly detection: A survey. *ACM computing surveys (CSUR)*. ACM New York, NY, USA. 2009, vol. 41, no. 3, p. 1–58.
- [22] CHIKKERUR, S., WU, C. and GOVINDARAJU, V. A Systematic Approach for Feature Extraction in Fingerprint Images. In: ZHANG, D. and JAIN, A. K., ed. *Biometric Authentication*. Berlin, Heidelberg: Springer Berlin Heidelberg, 2004, p. 344–350. ISBN 978-3-540-25948-0.
- [23] COLE, S. A. History of Fingerprint Pattern Recognition. In: RATHA, N. and BOLLE, R., ed. *Automatic Fingerprint Recognition Systems*. Springer New York, 2004, p. 1–25. ISBN 978-0-387-21685-0.
- [24] COUNCIL, N. R., COMMITTEE, W. B. et al. Biometric recognition: Challenges and opportunities. National Academies Press. 2010.
- [25] CRANDALL, D. J. and HUTTENLOCHER, D. P. Weakly Supervised Learning of Part-Based Spatial Models for Visual Object Recognition. In: LEONARDIS, A., BISCHOF, H. and PINZ, A., ed. *Computer Vision – ECCV 2006*. Springer Berlin Heidelberg, 2006, p. 16–29. ISBN 978-3-540-33833-8.
- [26] DAUGMAN, J. High confidence visual recognition of persons by a test of statistical independence. *IEEE Transactions on Pattern Analysis and Machine Intelligence*. 1993, vol. 15, no. 11, p. 1148–1161.

- [27] DAUGMAN, J. G. Uncertainty relation for resolution in space, spatial frequency, and orientation optimized by two-dimensional visual cortical filters. *JOSA A*. Optical Society of America. 1985, vol. 2, no. 7, p. 1160–1169. Available at: <https://opg.optica.org/josaa/abstract.cfm?URI=josaa-2-7-1160>.
- [28] DAVIES, E. CHAPTER 5 - Edge Detection. In: DAVIES, E., ed. *Machine Vision (Third Edition)*. Third Editionth ed. Burlington: Morgan Kaufmann, 2005, p. 131–157. Signal Processing and its Applications. Available at: <https://www.sciencedirect.com/science/article/pii/B9780122060939500083>. ISBN 978-0-12-206093-9.
- [29] DENG, L., YU, D. et al. Deep learning: methods and applications. *Foundations and trends® in signal processing*. Now Publishers, Inc. 2014, vol. 7, 3–4, p. 197–387.
- [30] DOLEZEL, M., DRAHANSKY, M., URBANEK, J., BREZINOVA, E. and KIM, T. hoon. Influence of Skin Diseases on Fingerprint Quality and Recognition. In: YANG, J. and XIE, S. J., ed. *New Trends and Developments in Biometrics*. Rijeka: IntechOpen, 2012, chap. 12. Available at: <https://doi.org/10.5772/51992>.
- [31] DOUGHERTY, E. *Mathematical morphology in image processing*. CRC press, 2018. ISBN 9780824787240.
- [32] DRAHANSKÝ, M. Fingerprint Recognition Technology - Related Topics. In: Lambert Academic Publishing, 2011, p. 172. Available at: <https://www.fit.vut.cz/research/publication/9636>. ISBN 978-3-8443-3007-6.
- [33] DRAHANSKÝ, M., BŘEZINOVÁ, E., ORSÁG, F. and LODROVÁ, D. Classification of skin diseases and their impact on fingerprint recognition. *BIOSIG 2009: biometrics and electronic signatures*. Gesellschaft für Informatik eV. 2009.
- [34] DRAHANSKÝ, M., BŘEZINOVÁ, E., LODROVÁ, D. and ORSÁG, F. Fingerprint Recognition Influenced by Skin Diseases. *International Journal of Bio-Science and Bio-Technology*. 2010, vol. 3, no. 4, p. 11–22. Available at: <https://www.fit.vut.cz/research/publication/9446>. ISSN 1976-118X.
- [35] DRAHANSKY, M., DOLEZEL, M., URBANEK, J., BREZINOVA, E. and KIM, T.-h. Influence of skin diseases on fingerprint recognition. *Journal of Biomedicine and Biotechnology*. Hindawi. 2012, vol. 2012.
- [36] DRAHANSKÝ, M., KANICH, O. and BŘEZINOVÁ, E. *Challenges for Fingerprint Recognition—Spoofing, Skin Diseases, and Environmental Effects*. Cham: Springer International Publishing, 2017. 63–83 p. Available at: https://doi.org/10.1007/978-3-319-50673-9_4. ISBN 978-3-319-50673-9.
- [37] DREISEITL, S. and OHNO MACHADO, L. Logistic regression and artificial neural network classification models: a methodology review. *Journal of biomedical informatics*. Elsevier. 2002, vol. 35, 5-6, p. 352–359.
- [38] DUNN, D. and HIGGINS, W. E. Optimal Gabor filters for texture segmentation. *IEEE Transactions on image processing*. IEEE. 1995, vol. 4, no. 7, p. 947–964.
- [39] EICHKITZ, C. G., AMTMANN, J. and SCHREILECHNER, M. G. Calculation of grey level co-occurrence matrix-based seismic attributes in three dimensions. *Computers & Geosciences*. 2013, vol. 60, p. 176–183. Available at: <https://www.sciencedirect.com/science/article/pii/S0098300413001957>. ISSN 0098-3004.

- [40] FAHMY, M. F and THABET, M. A. A fingerprint segmentation technique based on Morphological processing. In: *IEEE International Symposium on Signal Processing and Information Technology*. 2013, p. 000215–000220.
- [41] FAN, B., WANG, Z. and WU, F. Classical Local Descriptors. In: *Local Image Descriptor: Modern Approaches*. Springer Berlin Heidelberg, 2015, p. 5–24. Available at: https://doi.org/10.1007/978-3-662-49173-7_2. ISBN 978-3-662-49173-7.
- [42] FATTAHI, J. and MEJRI, M. Damaged Fingerprint Recognition by Convolutional Long Short-Term Memory Networks for Forensic Purposes. In: IEEE. *2021 IEEE 5th International Conference on Cryptography, Security and Privacy (CSP)*. 2021, p. 193–199.
- [43] FAUNDEZ ZANUY, M. Data fusion in biometrics. *IEEE Aerospace and Electronic Systems Magazine*. IEEE. 2005, vol. 20, no. 1, p. 34–38.
- [44] FAWAGREH, K., GABER, M. M. and ELYAN, E. Random forests: from early developments to recent advancements. *Systems Science & Control Engineering: An Open Access Journal*. Taylor & Francis. 2014, vol. 2, no. 1, p. 602–609.
- [45] FENG, J., JAIN, A. K. and ROSS, A. Detecting altered fingerprints. In: IEEE. *2010 20th International Conference on Pattern Recognition*. 2010, p. 1622–1625.
- [46] FENG, J., ZHOU, J. and JAIN, A. K. Orientation field estimation for latent fingerprint enhancement. *IEEE transactions on pattern analysis and machine intelligence*. IEEE. 2012, vol. 35, no. 4, p. 925–940.
- [47] GALTON, F. *Finger Prints*. Macmillan and Company, 1892. 19th-century legal treatises. Available at: <https://books.google.cz/books?id=ZfDUAAAAMAAJ>. ISBN 9781646797158.
- [48] GOODFELLOW, I., BENGIO, Y. and COURVILLE, A. *Deep Learning*. MIT Press, 2016. <http://www.deeplearningbook.org>.
- [49] GRANLUND, G. H. In search of a general picture processing operator. *Computer Graphics and Image Processing*. 1978, vol. 8, no. 2, p. 155–173. Available at: <https://www.sciencedirect.com/science/article/pii/0146664X78900473>. ISSN 0146-664X.
- [50] GUNAY, A. and NABIYEV, V. V. Automatic age classification with LBP. In: IEEE. *2008 23rd international symposium on computer and information sciences*. 2008, p. 1–4.
- [51] GUO, Z., ZHANG, L. and ZHANG, D. A Completed Modeling of Local Binary Pattern Operator for Texture Classification. *IEEE Transactions on Image Processing*. 2010, vol. 19, no. 6, p. 1657–1663.
- [52] HABIF, T. *Clinical Dermatology E-Book*. Elsevier Health Sciences, 2015. ISBN 9780323266079.
- [53] HARALICK, R. M., SHANMUGAM, K. and DINSTEN, I. Textural Features for Image Classification. *IEEE Transactions on Systems, Man, and Cybernetics*. 1973, SMC-3, no. 6, p. 610–621.
- [54] HARRIS, C. R., MILLMAN, K. J., WALT, S. J. van der, GOMMERS, R., VIRTANEN, P. et al. Array programming with NumPy. *Nature*. Springer Science and Business Media LLC. september 2020, vol. 585, no. 7825, p. 357–362. Available at: <https://doi.org/10.1038/s41586-020-2649-2>.

- [55] HARZALLAH, H., JURIE, F. and SCHMID, C. Combining efficient object localization and image classification. In: *2009 IEEE 12th International Conference on Computer Vision*. 2009, p. 237–244.
- [56] HEIDARI, M., KANICH, O. and DRAHANSKÝ, M. Processing of fingerprints influenced by skin diseases. In: *Hand-Based Biometrics: Methods and Technology*. The Institution of Engineering and Technology, 2018, p. 135–168. IET Book Series on Advances in Biometrics. Available at: <https://www.fit.vut.cz/research/publication/11693>. ISBN 978-1-78561-224-4.
- [57] HENRY, E. R. *Classification and uses of finger prints*. HM Stationery Office [printed by Harrison and sons, Limited], 1922.
- [58] HINTON, G., DENG, L., YU, D., DAHL, G. E., MOHAMED, A.-r. et al. Deep Neural Networks for Acoustic Modeling in Speech Recognition: The Shared Views of Four Research Groups. *IEEE Signal Processing Magazine*. 2012, vol. 29, no. 6, p. 82–97.
- [59] HITAM, M. S., AWALLUDIN, E. A., JAWAHIR HJ WAN YUSSOF, W. N. and BACHOK, Z. Mixture contrast limited adaptive histogram equalization for underwater image enhancement. In: *2013 International Conference on Computer Applications Technology (ICCAT)*. 2013, p. 1–5.
- [60] HOLDER, E. H., ROBINSON, L. O. and LAUB, J. H. *The Fingerprint Sourcebook*. Washington, DC: U.S. Department. of Justice, Office of Justice Programs, National Institute of Justice: [b.n.], 2011.
- [61] HONG, L., WAN, Y. and JAIN, A. Fingerprint image enhancement: algorithm and performance evaluation. *IEEE Transactions on Pattern Analysis and Machine Intelligence*. 1998, vol. 20, no. 8, p. 777–789.
- [62] HSIEH, C.-T., LAI, E. and WANG, Y.-C. An effective algorithm for fingerprint image enhancement based on wavelet transform. *Pattern Recognition*. Elsevier. 2003, vol. 36, no. 2, p. 303–312. Available at: <https://www.sciencedirect.com/science/article/pii/S0031320302000328>. ISSN 0031-3203.
- [63] JAIN, A., CHEN, Y. and DEMIRKUS, M. Pores and Ridges: Fingerprint Matching Using Level 3 Features. In: *18th International Conference on Pattern Recognition (ICPR'06)*. 2006, p. 477–480. ISBN 0-7695-2521-0.
- [64] JAIN, A., ROSS, A. and PRABHAKAR, S. An introduction to biometric recognition. *IEEE Transactions on Circuits and Systems for Video Technology*. 2004, vol. 14, no. 1, p. 4–20.
- [65] JAIN, A. and HEALEY, G. A multiscale representation including opponent color features for texture recognition. *IEEE Transactions on Image Processing*. IEEE. 1998, vol. 7, no. 1, p. 124–128.
- [66] JAIN, A., BOLLE, R. and PANKANTI, S. Introduction to Biometrics. In: JAIN, A. K., BOLLE, R. and PANKANTI, S., ed. *Biometrics: Personal Identification in Networked Society*. Boston, MA: Springer US, 1996, p. 1–41. Available at: https://doi.org/10.1007/0-306-47044-6_1. ISBN 978-0-306-47044-8.
- [67] JAIN, A. K., FLYNN, P. and ROSS, A. A. *Handbook of biometrics*. Springer Science & Business Media, 2007.

- [68] JAIN, A. K., NANDAKUMAR, K. and ROSS, A. 50 years of biometric research: Accomplishments, challenges, and opportunities. *Pattern Recognition Letters*. 2016, vol. 79, p. 80–105. ISSN 0167-8655.
- [69] JAIN, A. K., PRABHAKAR, S., HONG, L. and PANKANTI, S. Filterbank-based fingerprint matching. *IEEE Transactions on Image Processing*. IEEE. 2000, vol. 9, no. 5, p. 846–859.
- [70] JAIN, A. K., PRABHAKAR, S. and PANKANTI, S. On the similarity of identical twin fingerprints. *Pattern Recognition*. 2002, vol. 35, no. 11, p. 2653–2663.
- [71] JAMES, W., ELSTON, D., TREAT, J. and ROSENBAACH, M. *Andrews' Diseases of the Skin: Clinical Dermatology*. Elsevier Health Sciences, 2019. Available at: <https://books.google.cz/books?id=UEaEDwAAQBAJ>. ISBN 9780323551885.
- [72] JOSHI, I., KOTHARI, R., UTKARSH, A., KURMI, V. K., DANTCHEVA, A. et al. Explainable Fingerprint ROI Segmentation Using Monte Carlo Dropout. In: *2021 IEEE Winter Conference on Applications of Computer Vision Workshops (WACVW)*. 2021, p. 60–69. ISBN 978-1-6654-1967-3.
- [73] JOUN, S., KIM, H., CHUNG, Y. and AHN, D. An Experimental Study on Measuring Image Quality of Infant Fingerprints. In: PALADE, V., HOWLETT, R. J. and JAIN, L., ed. *Knowledge-Based Intelligent Information and Engineering Systems*. Springer Berlin Heidelberg, 2003, p. 1261–1269. ISBN 978-3-540-40804-8.
- [74] KAMARAINEN, J.-K., KYRKI, V. and KALVIAINEN, H. Invariance properties of Gabor filter-based features-overview and applications. *IEEE Transactions on image processing*. IEEE. 2006, vol. 15, no. 5, p. 1088–1099.
- [75] KAMARAINEN, J.-K. Gabor features in image analysis. In: IEEE. *2012 3rd international conference on image processing theory, tools and applications (IPTA)*. 2012, p. 13–14. ISBN 978-1-4673-2585-1.
- [76] KAMIJO, M. Classifying fingerprint images using neural network: deriving the classification state. In: *IEEE International Conference on Neural Networks*. 1993, p. 1932–1937. ISBN 0-7803-0999-5.
- [77] KANICH, O. and DRAHANSKÝ, M. State of the Art in Fingerprint Recognition. In: *Hand-based Biometrics: Methods and Technologies*. IET, 2018, p. p. 28. ISBN 978-1-78561-224-4.
- [78] KASS, M. and WITKIN, A. Analyzing oriented patterns. *Computer vision, graphics, and image processing*. Elsevier. 1987, vol. 37, no. 3, p. 362–385.
- [79] KEKRE, H. and BHARADI, V. Fingerprint orientation field estimation algorithm based on optimized neighborhood averaging. In: *2009 Second International Conference on Emerging Trends in Engineering & Technology*. 2009, p. 228–234. ISBN 978-1-4244-5250-7.
- [80] KOLBERG, J., GLÄSNER, D., BREITHAUPT, R., GOMEZ BARRERO, M., REINHOLD, J. et al. On the Effectiveness of Impedance-Based Fingerprint Presentation Attack Detection. *Sensors*. 2021, vol. 21, no. 17. Available at: <https://www.mdpi.com/1424-8220/21/17/5686>. ISSN 1424-8220.

- [81] KOLBERG, J., GOMEZ BARRERO, M., VENKATESH, S., RAMACHANDRA, R. and BUSCH, C. Presentation Attack Detection for Finger Recognition. In: UHL, A., BUSCH, C., MARCEL, S. and VELDHUIS, R., ed. *Handbook of Vascular Biometrics*. Cham: Springer International Publishing, 2020, p. 435–463. Available at: https://doi.org/10.1007/978-3-030-27731-4_14. ISBN 978-3-030-27731-4.
- [82] KONG, Q., SIAUW, T. and BAYEN, A. M. Chapter 24 - Fourier Transform. In: KONG, Q., SIAUW, T. and BAYEN, A. M., ed. *Python Programming and Numerical Methods*. Academic Press, 2021, p. 415–443. Available at: <https://www.sciencedirect.com/science/article/pii/B9780128195499000348>. ISBN 978-0-12-819549-9.
- [83] KOUROU, K., EXARCHOS, T. P., EXARCHOS, K. P., KARAMOUZIS, M. V. and FOTIADIS, D. I. Machine learning applications in cancer prognosis and prediction. *Computational and Structural Biotechnology Journal*. 2015, vol. 13, p. 8–17. Available at: <https://www.sciencedirect.com/science/article/pii/S2001037014000464>. ISSN 2001-0370.
- [84] LECUN, Y., BENGIO, Y. and HINTON, G. Deep learning. *Nature*. Nature Publishing Group. 2015, vol. 521, no. 7553, p. 436–444.
- [85] LEE, C.-J. and WANG, S.-D. Fingerprint feature extraction using Gabor filters. *Electronics Letters*. IET. 1999, vol. 35, no. 4, p. 288–290.
- [86] LEE, J., HARALICK, R. and SHAPIRO, L. Morphologic edge detection. *IEEE Journal on Robotics and Automation*. IEEE. 1987, vol. 3, no. 2, p. 142–156.
- [87] LI, S. Z. and JAIN, A., ed. In: LI, S. Z. and JAIN, A., ed. *Encyclopedia of Biometrics*. Springer US, 2009, p. 43–43. Available at: https://doi.org/10.1007/978-0-387-73003-5_968. ISBN 978-0-387-73003-5.
- [88] LIM, E., TOH, K.-A., SUGANTHAN, P., JIANG, X. and YAU, W.-Y. Fingerprint image quality analysis. In: IEEE. *2004 International Conference on Image Processing, 2004. ICIP'04*. 2004, p. 1241–1244.
- [89] LIU, C.-L., KOGA, M. and FUJISAWA, H. Gabor feature extraction for character recognition: comparison with gradient feature. In: *Eighth International Conference on Document Analysis and Recognition (ICDAR'05)*. 2005, p. 121–125 Vol. 1. ISBN 0-7695-2420-6.
- [90] LIU, H. and MOTODA, H. *Feature Extraction, Construction and Selection: A Data Mining Perspective*. USA: Kluwer Academic Publishers, 1998. ISBN 0792381963.
- [91] MALLAT, S. A theory for multiresolution signal decomposition: the wavelet representation. *IEEE Transactions on Pattern Analysis and Machine Intelligence*. 1989, vol. 11, no. 7, p. 674–693.
- [92] MALTONI, D., MAIO, D., JAIN, A. and PRABHAKAR, S. *Handbook of Fingerprint Recognition*. Springer London, 2009. Springer Professional Computing. ISBN 9781848822542.
- [93] MALTONI, D. Fingerprint Recognition, Overview. In: LI, S. Z. and JAIN, A., ed. *Encyclopedia of Biometrics*. Boston, MA: Springer US, 2009, p. 510–513. ISBN 978-0-387-73003-5.
- [94] MARCEL, S., NIXON, M. S. and LI, S. Z. *Handbook of biometric anti-spoofing*. Springer, 2014. ISBN 978-3-319-92627-8.

- [95] MATHER, P. and TSO, B. *Classification methods for remotely sensed data*. CRC press, 2016. ISBN 9780429192029.
- [96] MEYER BAESE, A. and SCHMID, V. Chapter 4 - The Wavelet Transform in Medical Imaging. In: MEYER BAESE, A. and SCHMID, V., ed. *Pattern Recognition and Signal Analysis in Medical Imaging (Second Edition)*. Second Editionth ed. Oxford: Academic Press, 2014, p. 113–134. Available at: <https://www.sciencedirect.com/science/article/pii/B9780124095458000042>. ISBN 978-0-12-409545-8.
- [97] MOUNTRAKIS, G., IM, J. and OGOLE, C. Support vector machines in remote sensing: A review. *ISPRS Journal of Photogrammetry and Remote Sensing*. Elsevier. 2011, vol. 66, no. 3, p. 247–259.
- [98] MURPHY, K., TORRALBA, A., EATON, D. and FREEMAN, W. Object Detection and Localization Using Local and Global Features. In: PONCE, J., HEBERT, M., SCHMID, C. and ZISSERMAN, A., ed. *Toward Category-Level Object Recognition*. Berlin, Heidelberg: Springer Berlin Heidelberg, 2006, p. 382–400. Available at: https://doi.org/10.1007/11957959_20. ISBN 978-3-540-68795-5.
- [99] NEUROTECHNOLOGY. *Verifinger SDK*. Dec 2022. Available at: <https://www.neurotechnology.com/verifinger.html>.
- [100] NIXON, M. and AGUADO, A. *Feature extraction and image processing for computer vision*. Academic press, 2019.
- [101] NUSSBAUMER, H. J. The Fast Fourier Transform. In: *Fast Fourier Transform and Convolution Algorithms*. Berlin, Heidelberg: Springer Berlin Heidelberg, 1981, p. 80–111. Available at: https://doi.org/10.1007/978-3-662-00551-4_4. ISBN 978-3-662-00551-4.
- [102] OJALA, T., PIETIKAINEN, M. and MAENPAA, T. Multiresolution gray-scale and rotation invariant texture classification with local binary patterns. *IEEE Transactions on Pattern Analysis and Machine Intelligence*. 2002, vol. 24, no. 7, p. 971–987.
- [103] ORAVEC, T. Methodology of Fingerprint Image Quality Measurement. *Master's thesis FIT BUT*. 2018.
- [104] PHILLIPS, P. J., MARTIN, A., WILSON, C. L. and PRZYBOCKI, M. An introduction evaluating biometric systems. *Computer*. IEEE. 2000, vol. 33, no. 2, p. 56–63.
- [105] PISANO, E. D., ZONG, S., HEMMINGER, M., B., JOHNSTON, R. et al. Contrast limited adaptive histogram equalization image processing to improve the detection of simulated spiculations in dense mammograms. *Journal of Digital Imaging*. 1998, vol. 11, p. 193–200.
- [106] PIZER, S. M., AMBURN, E. P., AUSTIN, J. D., CROMARTIE, R., GESELOWITZ, A. et al. Adaptive histogram equalization and its variations. *Computer Vision, Graphics, and Image Processing*. 1987, vol. 39, no. 3, p. 355–368. ISSN 0734-189X.
- [107] PRABHAKAR, S. and JAIN, A. K. Fingerprint Matching. In: RATHA, N. and BOLLE, R., ed. *Automatic Fingerprint Recognition Systems*. New York, NY: Springer New York, 2004, p. 229–248.
- [108] PRATT, W. K. *Digital image processing: PIKS Scientific inside*. Wiley Online Library, 2007.

- [109] QUINLAN, J. R. Induction of decision trees. *Machine learning*. Springer. 1986, vol. 1, p. 81–106.
- [110] RATHA, N. K., CHEN, S. and JAIN, A. K. Adaptive flow orientation-based feature extraction in fingerprint images. *Pattern Recognition*. 1995, vol. 28, no. 11, p. 1657–1672. Available at: <https://www.sciencedirect.com/science/article/pii/0031320395000393>. ISSN 0031-3203.
- [111] ROSS, A. A., NANDAKUMAR, K. and JAIN, A. K. *Handbook of multibiometrics*. Springer Science & Business Media, 2006.
- [112] ROUSHDY, M. Comparative study of edge detection algorithms applying on the grayscale noisy image using morphological filter. *GVIP journal*. 2006, vol. 6, no. 4, p. 17–23.
- [113] SAPARUDIN, S. and SULONG, G. Segmentation of fingerprint image based on gradient magnitude and coherence. *International Journal of Electrical and Computer Engineering*. IAES Institute of Advanced Engineering and Science. 2015, vol. 5, no. 5.
- [114] SARITAS, M. M. and YASAR, A. Performance analysis of ANN and Naive Bayes classification algorithm for data classification. *International journal of intelligent systems and applications in engineering*. 2019, vol. 7, no. 2, p. 88–91.
- [115] SCHNEIDER, J. K. Ultrasonic Fingerprint Sensors. In: RATHA, N. K. and GOVINDARAJU, V., ed. *Advances in Biometrics: Sensors, Algorithms and Systems*. London: Springer London, 2008, p. 63–74. ISBN 978-1-84628-921-7.
- [116] SHAN, C. and GRITTI, T. Learning Discriminative LBP-Histogram Bins for Facial Expression Recognition. In: *BMVC*. 2008.
- [117] SHRIVAKSHAN, G. and CHANDRASEKAR, C. A comparison of various edge detection techniques used in image processing. *International Journal of Computer Science Issues (IJCSI)*. Citeseer. 2012, vol. 9, no. 5, p. 269.
- [118] SOH, L.-K. and TSATSOULIS, C. Texture analysis of SAR sea ice imagery using gray level co-occurrence matrices. *IEEE Transactions on Geoscience and Remote Sensing*. 1999, vol. 37, no. 2, p. 780–795.
- [119] TABASSI, E. *NIST fingerprint image quality (NFIQ) compliance test*. Citeseer, 2005. Available at: <https://www.govinfo.gov/app/details/GOVPUB-C13-c81eb345eab7562fac3a45e27fba2b81>.
- [120] TICO, M., IMMONEN, E., RAMO, P., KUOSMANEN, P. and SAARINEN, J. Fingerprint recognition using wavelet features. In: *ISCAS 2001. The 2001 IEEE International Symposium on Circuits and Systems (Cat. No.01CH37196)*. 2001, p. 21–24 vol. 2.
- [121] TORRENCE, C. and COMPO, G. P. A practical guide to wavelet analysis. *Bulletin of the American Meteorological society*. American Meteorological Society. 1998, vol. 79, no. 1, p. 61–78.
- [122] VASEGHI, S. V. *Advanced digital signal processing and noise reduction*. John Wiley & Sons, 2008. ISBN 9780470754061.

- [123] WANI, N. and RAZA, K. Chapter 3 - Multiple Kernel-Learning Approach for Medical Image Analysis. In: DEY, N., ASHOUR, A. S., SHI, F. and BALAS, V. E., ed. *Soft Computing Based Medical Image Analysis*. Academic Press, 2018, p. 31–47. Available at: <https://www.sciencedirect.com/science/article/pii/B9780128130872000026>. ISBN 978-0-12-813087-2.
- [124] WAYMAN, J., JAIN, A., MALTONI, D. and MAIO, D. *Biometric Systems: Technology, Design and Performance Evaluation*. Springer London, 2005. Available at: <https://books.google.cz/books?id=LkHHDZtQwG0C>. ISBN 9781846280641.
- [125] WU, C., TULYAKOV, S. and GOVINDARAJU, V. Robust point-based feature fingerprint segmentation algorithm. In: Springer. *International Conference on Biometrics*. 2007, p. 1095–1103.
- [126] XIE, X., SU, F. and CAI, A. Ridge-Based Fingerprint Recognition. In: ZHANG, D. and JAIN, A. K., ed. *Advances in Biometrics*. Berlin, Heidelberg: Springer Berlin Heidelberg, 2005, p. 273–279.
- [127] YIN, J., ZHU, E., YANG, X., ZHANG, G. and HU, C. Two steps for fingerprint segmentation. *Image and Vision Computing*. 2007, vol. 25, no. 9, p. 1391–1403. Available at: <https://www.sciencedirect.com/science/article/pii/S0262885606003246>. ISSN 0262-8856.
- [128] YOON, S., FENG, J. and JAIN, A. K. Altered fingerprints: Analysis and detection. *IEEE transactions on pattern analysis and machine intelligence*. IEEE. 2012, vol. 34, no. 3, p. 451–464.
- [129] YU, C., XIE, M. and QI, J. An effective algorithm for low quality fingerprint segmentation. In: IEEE. *2008 3rd International Conference on Intelligent System and Knowledge Engineering*. 2008, p. 1081–1085.
- [130] ZHANG, Y. and CHEN, T. Weakly Supervised Object Recognition and Localization with Invariant High Order Features. In: *Proceedings of the British Machine Vision Conference*. BMVA Press, 2010, p. 47.1–47.11. Doi:10.5244/C.24.47. ISBN 1-901725-40-5.
- [131] ZHOU, Z.-H. Ensemble Learning. In: LI, S. Z. and JAIN, A. K., ed. *Encyclopedia of Biometrics*. Boston, MA: Springer US, 2015, p. 411–416. Available at: https://doi.org/10.1007/978-1-4899-7488-4_293. ISBN 978-1-4899-7488-4.

Appendices

Appendix A

Appendix

As an appendix to this report, the focus is to provide a brief revision of the methods employed and to present experimental results for disease detection in fingerprint images. The methods used in this study include image pre-processing techniques such as image enhancement, normalization, and segmentation, followed by feature extraction methods such as Local Binary Pattern (LBP), Gray Level Co-occurrence Matrix (GLCM) and orientation field computation. These methods aid in identifying and extracting key features in fingerprint images that are indicative of potential diseases or abnormalities.

The experimental results of this study demonstrate the effectiveness of the proposed approach in detecting diseases in fingerprint images. The accuracy of the disease detection algorithm was evaluated using metrics such as precision, recall, and F1 score. The results obtained show a high level of accuracy in disease detection, thus validating the effectiveness of the proposed approach.

In conclusion, this appendix provides a comprehensive overview of the methods and experimental results for disease detection in fingerprint images. The proposed approach is highly effective in detecting diseases in fingerprint images and has the potential to significantly improve the accuracy and reliability of disease detection systems.

As depicted in the resulting images, the main steps in disease detection in fingerprint images are chosen carefully, considering the characteristics of each disease. For instance, steps such as white spot detection and straight line detection are employed to achieve the best results. These steps aid in identifying specific features associated with different diseases, enabling the algorithm to accurately classify the fingerprint images accordingly. By incorporating various techniques and methods, disease detection in fingerprint images can be achieved with high precision and reliability, making it a valuable tool in the field of medical diagnostics.

The following pages present the experimental results, showing the steps in images from (a) to (g) respectively for disease detection in fingerprint images. To further enhance the results, additional internal steps such as morphological approaches and straight line detectors were applied to the images. These steps contribute to improving the precision of the final output and ensure that the results are more satisfactory. The main steps involved in detecting the disease characteristics, such as white spot detection and straight line detection, are shown. It begins by presenting the input image (a), followed by the detection of disease using the block orientation field (b) and the LBP approach (c). The segmented image with the extracted disease part is then shown (d), followed by the localization of the disease (e). Finally, the localization of artifacts and disease in the image is presented (f). Overall, the presented method offers a promising approach for disease detection in fingerprint images, as demonstrated by the experimental results. The percentage of the damage can be accurately evaluated using the script at the final step, making it a

valuable tool for the medical community in diagnosing diseases. These carefully chosen steps enabled the methods to achieve the best results in detecting the disease characteristics, making the presented method a promising approach for disease detection in fingerprint images.

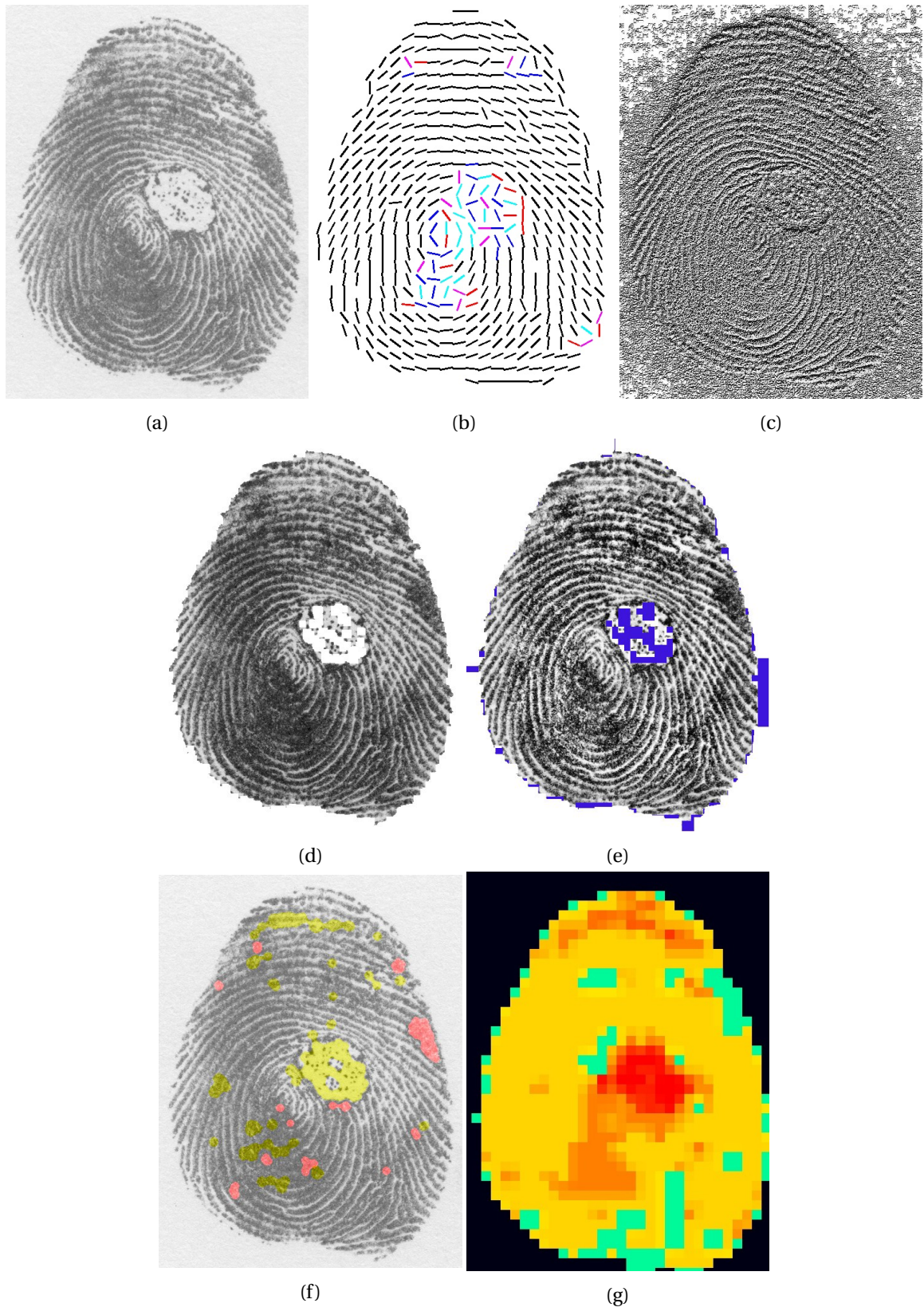


Figure A.1: Verruca vulgaris detected with 32% damage.

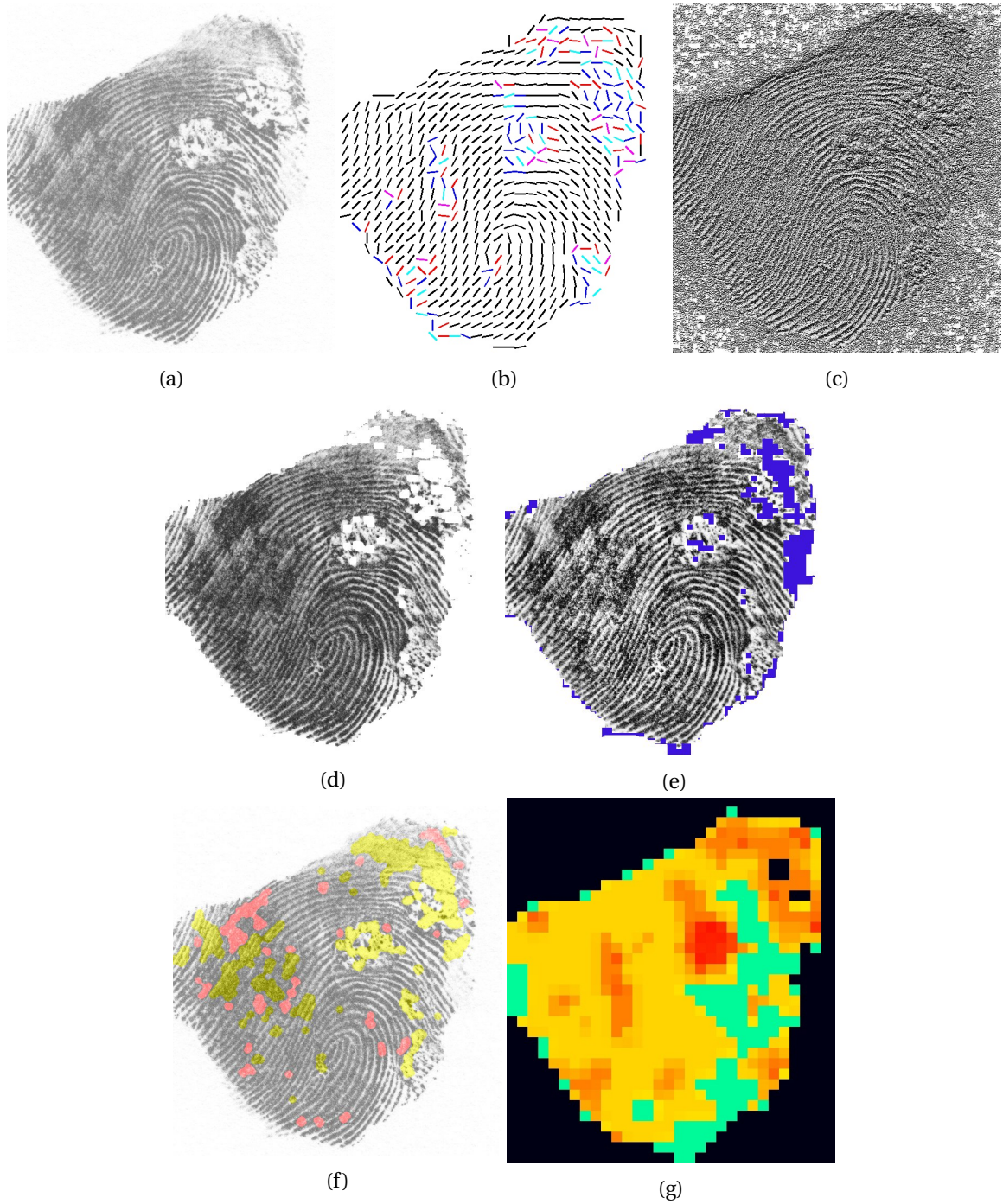
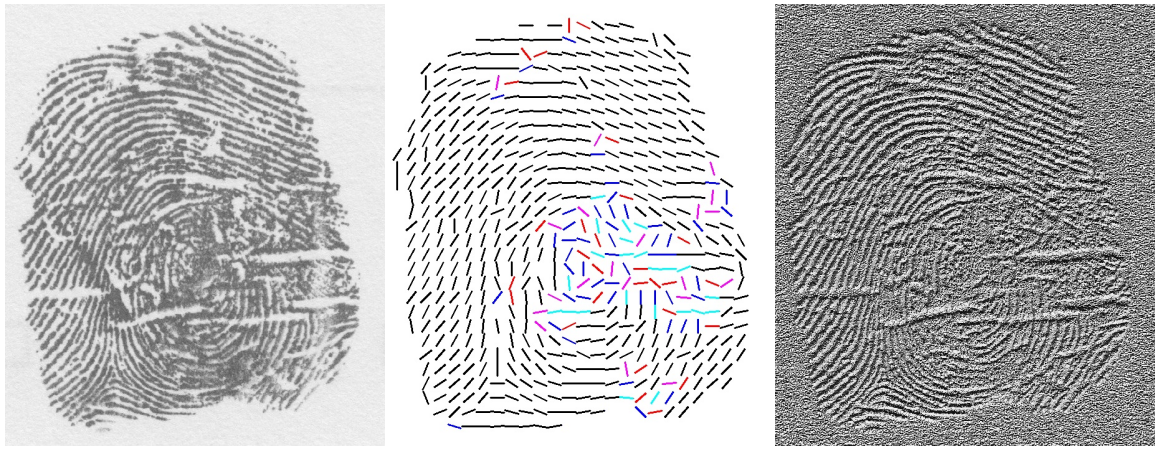


Figure A.2: Multiple verruca vulgaris detected with 34% damage.



(a)

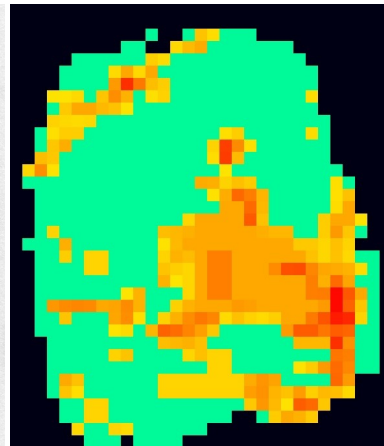
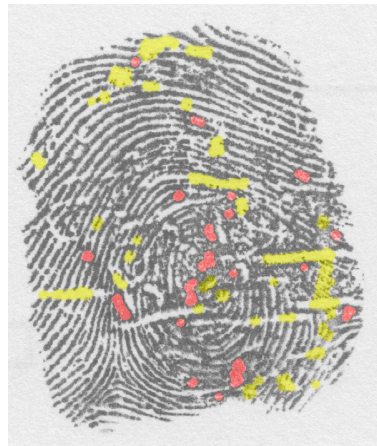
(b)

(c)



(d)

(e)



(f)

(g)

Figure A.3: Eczema detected with 24% damage.

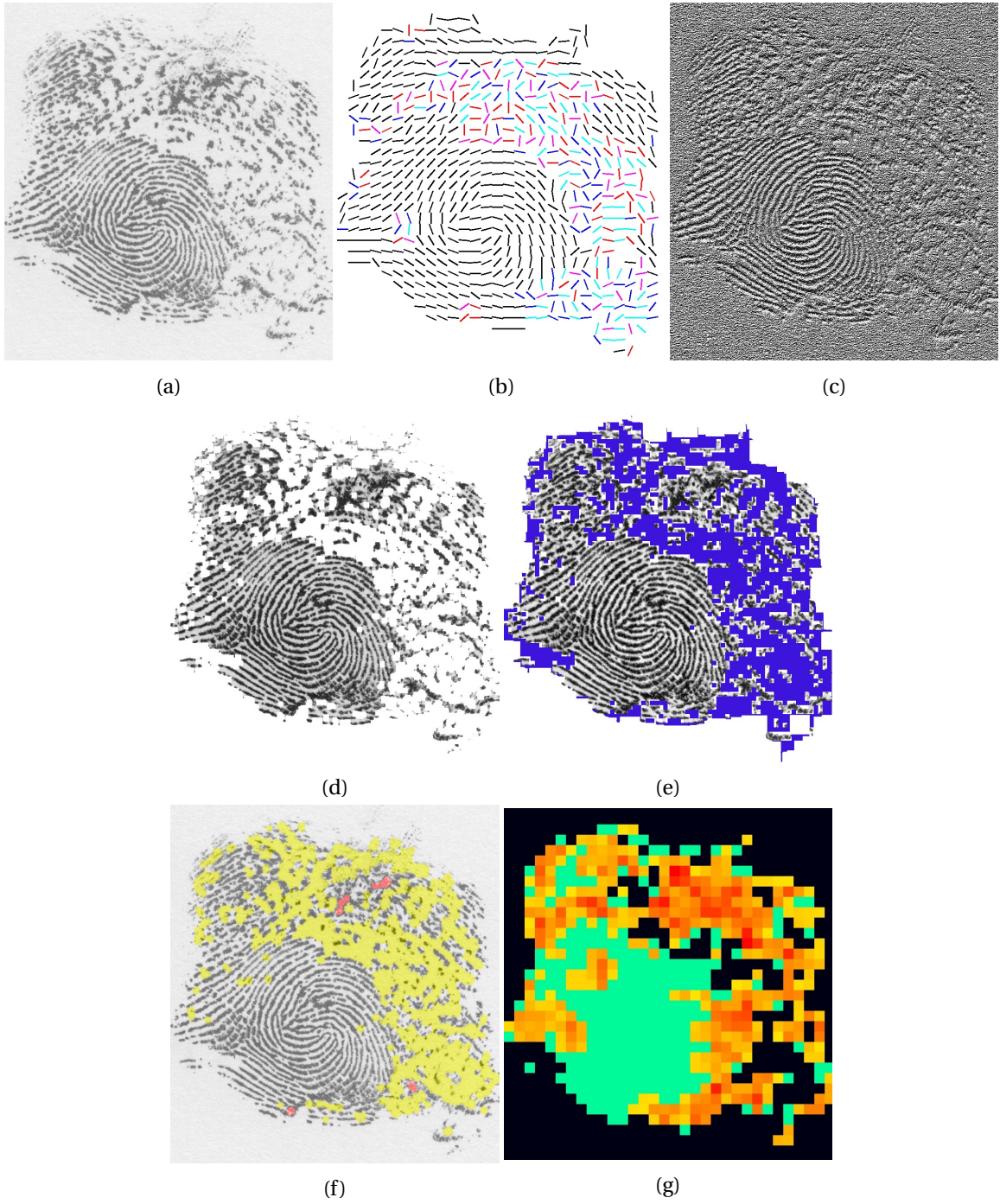


Figure A.4: Acrodermatitis detected with 39% damage.

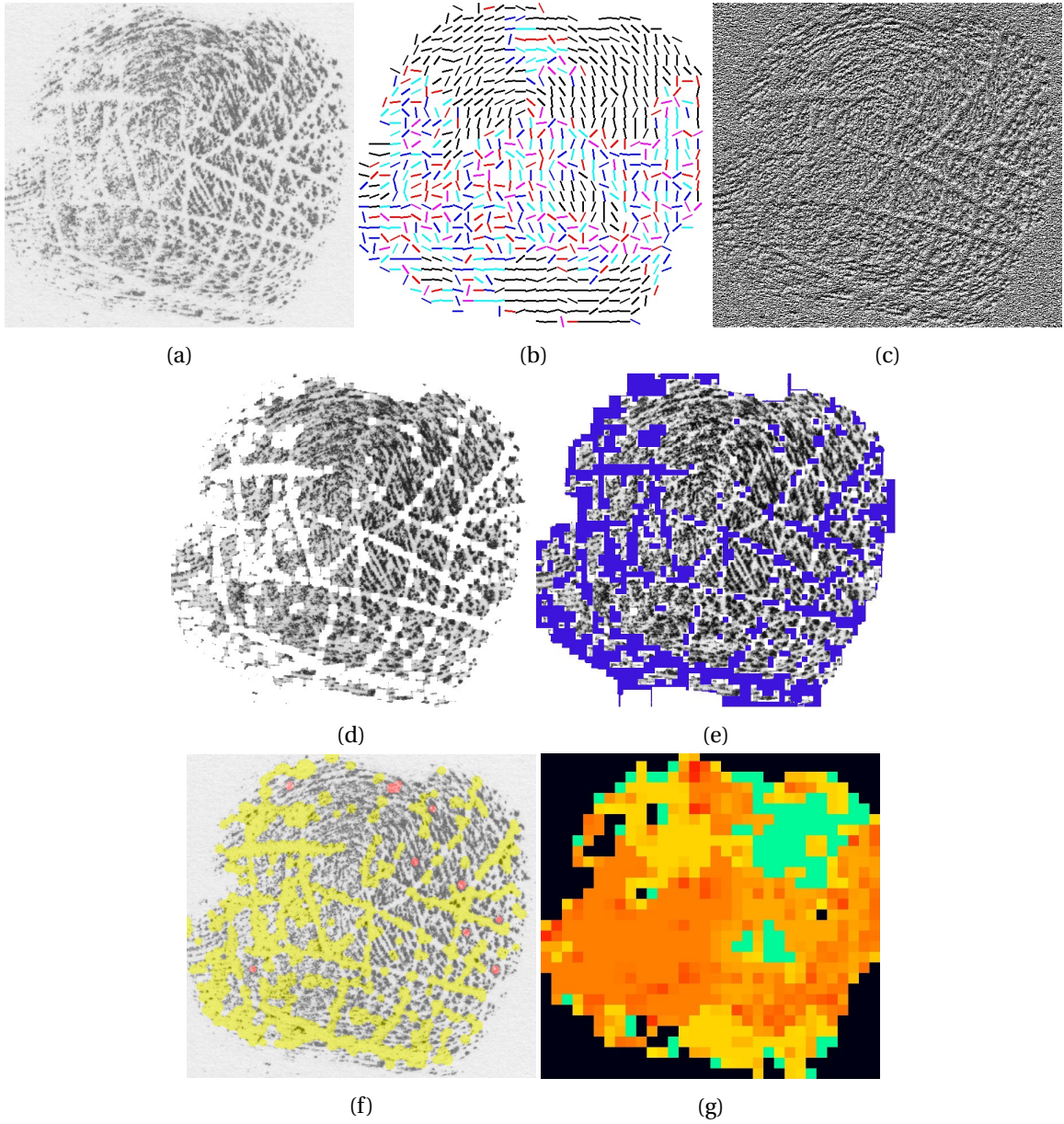


Figure A.5: Hyperkeratotic eczema detected with 66% damage.

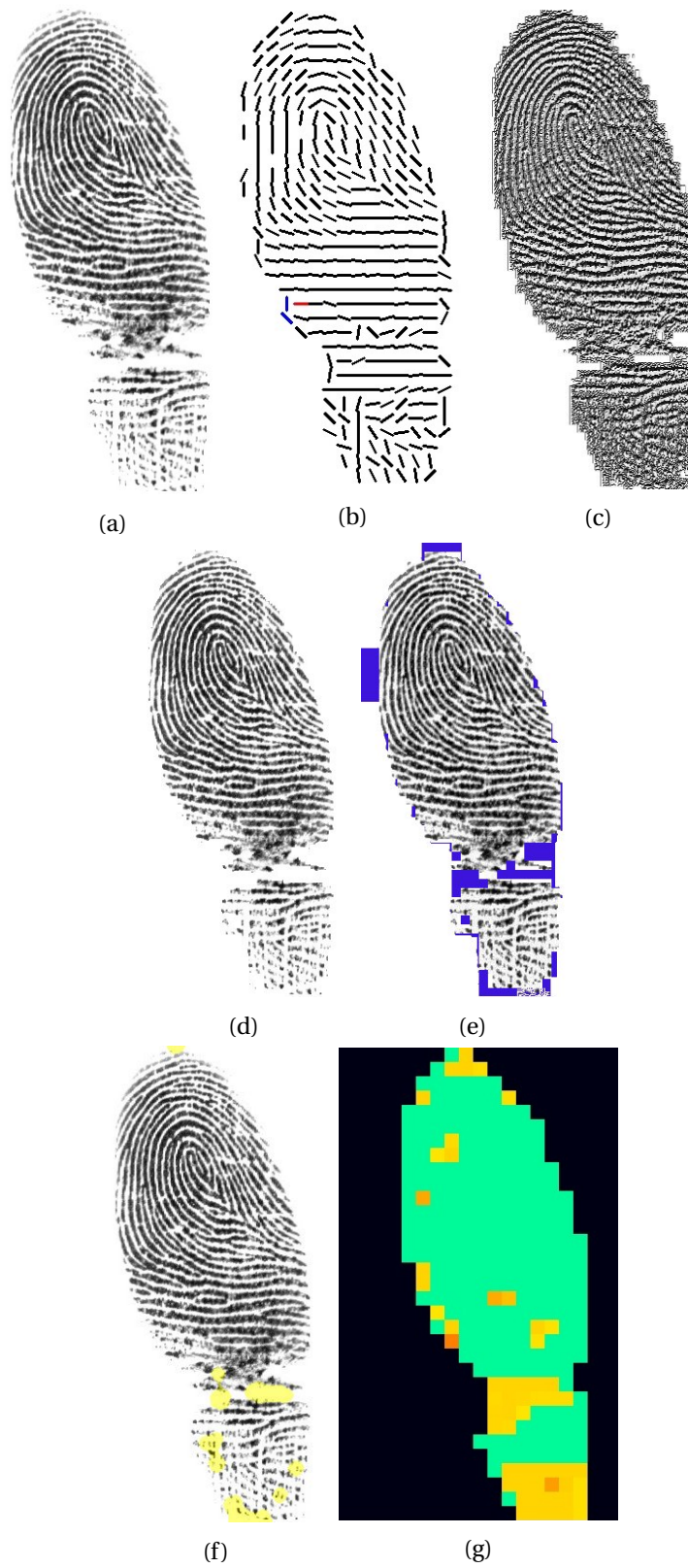


Figure A.6: Running the detection method on an almost ideal fingerprint with 5% damage.